

FORMULATION STUDY OF MULTIPARTICULATES: MICROSPHERES AND MICROPELLETS

PhD thesis

Miléna Bea Lengyel, PharmD

Doctoral School of Pharmaceutical Sciences
Semmelweis University



Supervisor: István Antal, PharmD, Ph.D

Official reviewers: Ildikó Katalin Kovácsné Bácskay, PharmD, Ph.D

Judit Kovácsné Balogh, PharmD, Ph.D

Head of the Complex Examination Committee:

Éva Szökő, PharmD, D.Sc

Members of the Complex Examination Committee:

Romána Zelkó, PharmD, D.Sc

Mária Jelinekné Nikolics, PharmD, Ph.D

Budapest

2022

TABLE OF CONTENTS

List of Abbreviations	5
1. INTRODUCTION.....	7
1.1 MULTIPARTICULATE DRUG DELIVERY SYSTEMS' UNITS	9
1.1.1 Microspheres and Microcapsules	11
1.1.1.1 Microencapsulation by Extrusion/Dripping and Coacervation Process with Alginate-based Microspheres	13
1.1.1.2 Microencapsulation by Freeze-drying	14
1.1.1.3 Emulsion Process with Solvent Evaporation	15
1.1.1.4 Spray Drying.....	15
1.1.2 Pellets	16
1.1.2.1 Air Suspension Method/Fluid-Bed Coating.....	16
1.1.3 Effect of Excipients used in the Formulation of Microparticles	17
1.1.3.1 Interactions of Excipients Within Microcapsules: Interpenetrating and Semi-Interpenetrating Polymer Networks (IPN)	17
1.1.3.2 Role of Alginic acid and Alginates in Microencapsulation	20
1.1.4 The Behavior of Microparticles in the Body	26
1.1.5 Mechanisms of Drug Release from Multiparticulate Preparations	27
1.1.6 Formulation Concepts for Sodium Bicarbonate	28
1.1.6.1 General Use of Sodium Bicarbonate.....	28
1.1.6.2 Role and Application Fields of Sodium Bicarbonate in Therapy	29
1.1.6.3 Bicarbonate-Carbon Dioxide Physiological Buffer System	33
1.1.6.4 The Acid-Base Balance of the Intestines	36
1.1.7 Challenges of Sodium Bicarbonate Delivery	40
2. OBJECTIVES	42
2.1 Investigation of Hydrogel-based Solid Microsphere Formulation.....	42

2.2 Study on Multiparticulate Pellets Coated with Multilayered Polymer Systems.....	42
3. MATERIALS AND METHODS.....	43
3.1 Materials.....	43
3.2 Pharmaceutical Technological Processing Methods of Sample Formulations.....	47
3.2.1 Preparation of Microspheres.....	47
3.2.1.1 Coacervation of Microspheres	47
3.2.1.2 Freeze-drying	48
3.2.2 Preparation of Micropellets	48
3.2.2.1 Pelletizing of Bicarbonate-containing Cores	48
3.2.2.2 Coating Process.....	50
3.3 Methods for Characterization.....	55
3.3.1 Particle Size Analysis with Laser Diffraction	55
3.3.2 Particle Analysis with Microscopic Image Analysis.....	55
3.3.3 Reconstitution.....	56
3.3.4 Micro-Computed Tomography.....	56
3.3.5 Scanning Electron Microscopy (SEM).....	56
3.3.6 Microgel Hardness Test by Texture Analyzer.....	57
3.3.7 In vitro Drug Release- Sodium Release from Sodium Bicarbonate Pellets .	58
3.3.8 Fourier Transformation Infrared Spectroscopy (FT-IR)	58
4. RESULTS.....	59
4.1 Multiparticulate Microsphere System: Investigation of Process Parameters of Microsphere Particle Formation by Vibration-Extrusion	59
4.1.1 The Effect of Surface-Active Agent on the Formation of Microspheres	59
4.1.2 Effect of Isomalt on the Formation of Microspheres	64
4.1.3 Effect of Freeze-drying on Microgel Particles	65

4.1.3.1	Structure and Morphology	65
4.1.3.2	Reconstitution	69
4.1.4	Effect of Divalent and Trivalent Ions on Particle Characteristics	70
4.2	Bicarbonate Containing Pellet Formulation.....	73
4.2.1	Composition of Matrix Core	73
4.2.2	Size and Morphology of Pellets	73
4.2.3	Dissolution Study based on Sodium Release	74
4.3	Bicarbonate Release from Pellet Preparation.....	80
4.4	Miscibility of Polymers.....	82
5.	DISCUSSION	84
5.1	Personalized, Individual Composition and Therapy	85
6.	CONCLUSIONS	87
	Conclusions Regarding Microspheres.....	87
	Conclusions Regarding Micropellet Formulation	88
7.	SUMMARY	89
8.	REFERENCES	90
9.	BIBLIOGRAPHY OF THE CANDIDATE’S PUBLICATIONS.....	103
9.1	Publications Closely Related to the Thesis	103
9.2	Publications Related to Other Works	105
9.3	Presentations, Proceedings of Conferences.....	106
10.	ACKNOWLEDGEMENTS	109

LIST OF ABBREVIATIONS

%w/v:	Percent Weight/Volume (g solute/100 mL solution)
μCT, micro-CT:	microcomputed tomography
Al(OH) ₃ :	aluminium hydroxide
API:	active pharmaceutical ingredient
AR:	aspect ratio
Bi(NO ₃) ₃ :	bismuth nitrate
BW:	body weight
CaCl ₂ :	calcium chloride
CAGR:	compound annual growth rate
CKD:	chronic kidney disease
CMC-Na:	carboxymethyl cellulose sodium
DOPC:	1,2-dioleoyl- <i>sn</i> -glycero-3-phosphocholine
DPPA:	1-{(phosphonoxy)methyl}-1,2-ethanediyl ester
DPPC:	(R)-4-hydroxy-N,N,N trimethyl-10-oxo-7- {(1-oxohexadecyl)oxy}-3,4,9-trioxa-4-phosphapentacosan-1- aminium, 4-oxide
DPPG:	1,2-dipalmitoyl- <i>sn</i> -glycero-3-phospho-rac-(1-glycerol)
DSPC:	distearoyl- <i>sn</i> -glycero-3-phosphocholine
EC:	ethylcellulose
EDTA:	ethylenediaminetetraacetate
Fe ₂ (SO ₄) ₃ :	iron (III) sulphate
FeSO ₄ :	iron (II) sulphate
FoNo:	Formulae Normales
FT-IR:	Fourier Transform Infrared Spectroscopy
G (as in G-block):	L-guluronic acid
GFR:	glomerular filtration rate
GIT:	gastrointestinal tract
H ⁺ :	proton
HCO ₃ ⁻ :	carboxyl ion
HPC:	hydroxypropylcellulose

HPMCP:	hydroxypropylmethylcellulose phtalate
IPC:	in process control
LBG:	locust bean gum
M (as in M-block):	D-mannuronic acid
MA:	metabolic acidosis
mEq/l:	milliequivalents per litre
MC:	microcapsule
MCC:	microcrystalline cellulose
MP:	micropellet
mPEG5000-DPPE:	N-(methoxypolyethylene glycol 5000 carbamoyl)- 1,2-dipalmitoyl-sn-glycero-3-phosphatidylethanolamine
MS:	microsphere
NaHCO ₃ :	sodium bicarbonate
NIR:	near-infrared (spectroscopy)
NSAID:	non-steroid anti-inflammatory drug
ODT:	orally disintegrating tablets
OTC:	over the counter
pCO ₂ :	partial pressure of carbon dioxide
PEG:	polyethylene glycol
PLA:	polylactic acid
PLGA:	poly-D, L-lactid-co-glycolide
PMMA:	poly (methyl methacrylate)
PVA:	poly (vinyl alcohol)
SEM:	scanning electron microscopy
SDS:	sodium lauryl sulfate
TEC:	triethyl citrate
ZnSO ₄ :	zinc sulphate
ZOK:	zero order kinetics

1. INTRODUCTION

Multiparticulate drug delivery systems are pharmaceutical preparations where the dose is present in many small separate subunits (micro particulates, microcapsules, and micropellets), which carry and liberate a part of the dose. Depending on the formulation, microparticles and micropellets can be incorporated into different pharmaceutical dosage forms such as solids (capsules, tablets), semisolids (gels, creams, pastes), or liquids (solutions, suspensions, emulsions). They offer numerous advantages to experts and patients (both physiologically and technologically), based on their structural and functional abilities (1), such as:

- selection of dosage form for the desired drug delivery route (peroral tablets, parenteral injections, buccal, topical, pulmonary, nasal, otic preparations);
- modified or targeted (site-specific) drug release;
- expectable pharmacokinetics with diminished intra- or inter-subject variability in bioavailability;
- more homogenous distribution in the physiological environment;
- stable fixed-dose combinations of drugs;
- the failure of function of one individual subunit does not cause the malfunction of the whole dosage;
- possibility to separate incompatible APIs;
- dose titration and less dose-dumping;
- particles under the size of 1-2 mm can pass through the pyloric sphincter even in the fed state, and in this respect, they behave like a liquid in terms of gastric emptying (2-4);
- reduction in local irritations;
- patient centric therapy through better compliance (e.g., patients with dysphagia) and adherence;
- individual therapy (e.g., for pediatric or geriatric population);
- improving the stability of the medicinal preparations;
- isolating the constituents to ensure better compatibility;
- innovative products with prolonged life-cycle through patent protection.

The global microencapsulation market values an estimated 8.5 billion USD in 2020 and

is projected to reach 15.5 billion USD by 2025, at a CAGR of 12.9% from 2020 to 2025. The pharmaceutical and healthcare industry takes up the highest segment besides the agricultural, food, printing industries (5).

Contrary to nanoparticles under 100 nm, microcarriers do not traverse into the interstitium and are not transported by the lymph, thus potentiating a local action (6). Microencapsulation in a gel matrix or shell provides further advantages as oxidizable chemicals, oil components, or possibly toxic substances can be dosed encapsulated, and liquids can be handled as solids in the form of dried microparticles.

From the viewpoint of technology, microencapsulation presents several advantages: microparticles are formulated in order to protect the core from the environment; protecting the body from the side effects; separating incompatible substances; masking an unpleasant taste; preserving volatiles or the viability of the cells; and optimizing, prolonging, or targeting the impact of a drug.

Microparticles are formulated with the aid of different polymers as auxiliary materials. The advantages are numerous:

- the excipients protect the active pharmaceutical ingredient (API) from the environment (oxidation, temperature, pH)
- protects the organ from the irritative or mucosa-damaging effect of the drug substance.
- the lesion (e.g., bisection) of the multiparticulate solid dosage form (i.e., micropellets in spansule or compressed) cause a failure in only a small number of units that does not result in a significant change of the blood level.
- prolongs the biological half-life of specific active ingredients
- adhesion, cumulation, immune-reaction depends on the shape, size, and surface charge of the particle (6).

However, there are some limitations to the use of multiparticulate drug delivery:

- higher product costs due to the more expensive excipients in the formulations
- the need for more sophisticated equipment and processes,
- stricter quality control,
- some constituents doubt to meet the requirements for biocompatibility and biodegradation.

Various dosage forms utilize the numerous advantageous properties of the microcarriers (Fig. 1, Table I). However, the structure and technology behind the microparticles in these dosage forms differ, thus determining drug delivery function.

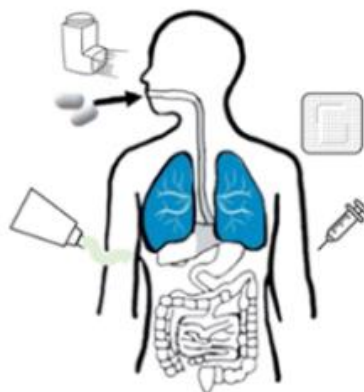


Figure 1. Most significant administration routes of multiparticulate dosage forms

1.1 MULTIPARTICULATE DRUG DELIVERY SYSTEMS' UNITS

Multiparticulate drug delivery systems usually involve coated pellets, microcapsules, or micro tablets to ensure gastric resistance (e.g., for acid-labile proton pump inhibitor compounds), prolong the duration of action, and optimize the pharmacokinetic profile. Intelligent carrier systems may react to changing pH, electric impulse, magnetic field, or temperature and developed in many forms (pellets, micro granules, microspheres). Patient-centric medication includes developing patient-friendly devices (e.g., DPI – Dry Powder Inhaler) and administration routes. Inhalatives, ODTs, and nasal routes could be an option to provoke a systemic effect. Extended-release injectable depot systems can form a reservoir at the administration site and release the API over a more extended period. This property is an advantage in treating psychotic patients or in the medication of children with acute diseases.

However, broad research is driven on this field, and there is a growing number of preparations approved by the authorities. Table I. shows the wide range of applications of the different microparticle-containing worldwide marketed products.

Table I. Examples of marketed drug products with multiparticulate carriers in the micron size range (7)

<i>Type</i>	<i>Dosage Form</i>	<i>Key Excipient</i>	<i>Drug</i>	<i>Indication</i>	<i>Product Example</i>
Micropellets	Peroral pellets in a capsule	HPC	Lansoprazole	Proton pump inhibitor	Lansoprazole [®]
Enteric-coated micro granules	Delayed-release orally disintegrating tablets	Methacrylic acid, polyacrylate	Lansoprazole	Proton pump inhibitor	Prevacid [®] SoluTab [™]
Coated pellets	Pellets compressed into extended-release tablet	HPC, EC	Metoprolol succinate	Cardioselective beta-blockers	Betaloc [®] ZOK
Microtablets	Peroral minitablets in capsule	Methacrylic acid-ethyl acrylate, MCC	Lipase, amylase	Enzyme supply	Pangrol [®]
Dry powder (Technospheres[®])	Inhalation	Fumaryl diketopiperazine	Insulin	Diabetes	Afrezza [™]
Microspheres	In suspension injection	PLGA	Risperidone	Schizophrenia	Risperdal [®] consta
Microspheres	Powder for injection	PLGA	Bromocriptine	Acromegaly, parkinsonism	Parlodel [®] LAR
Microspheres	Powder and solvent for suspension and injection	PLGA	Octreotide	pancreatic tumors	Sandostatin LAR [®]
Microspheres	Prolonged-release suspension for injection	PLGA	Exenatide	Diabetes type 2	Bydureon [®]
Lyophilized microspheres	Suspension depot injection	PLGA	Leuprolide acetate	Endometriosis	Lupron [®] depot
Liposomes	Liposome inhalation suspension	Cholesterol, DPPC	Amikacin	Antibacterial	Arikayce [®]
Liposomes (DepoFoam[™])	Powder for suspension for injection	Cholesterol, DOPC, DPPG	Cytarabine	Neoplastic meningitis	Depocyte [®]
Liposomes (DepoFoam[™])	Powder for suspension for injection	Cholesterol, DOPC, DPPG, tricaprilyn, triolein	Morphine	Epidural analgesia	DepoDur [®]
Microbubbles	Intravenous injection	Albumin	Perflutren	Ultrasound contrast agent	Albunex [®]
Microbubbles	Intravenous injection	PEG 4000, DSFC, DPPG-Na, palmitic acid	Sulfur hexafluoride	Ultrasound contrast agent	Lumason [®] / SonoVue [®]
Microbubbles	Intravenous injection	DPPA, DPPC, mPEG5000-DPPE	Perflutren	Ultrasound contrast agent	Definity [®]
Microsponge	Topical gel	Methyl methacrylate/glycol dimethacrylate crosspolymer	Tretinoin	Acne vulgaris	Retin-A micro [®] gel
Microsponge	Topical cream	Methyl methacrylate glycol dimethacrylate crosspolymer	5-fluorouracil	Multiple acne/solar keratoses	Carac [®] cream 0.5%

1.1.1 MICROSPHERES AND MICROCAPSULES

Microspheres are monolithic matrix drug carriers carrying the active ingredient either in the solid (suspended) or liquid form. The homogenous distribution of the active in the excipient matrix offers a platform for various release procedures and kinetics and different application routes (peroral, parenteral).

Microcapsules are core-shell reservoir systems, where the drug-loaded liquid or solid reservoir is embraced by a functional, inert, or possibly drug-loaded coating shell. The latter represents a limitation and plays a function in the drug release mechanisms.

Table II. Microencapsulation processes (based on (8))

<i>CHEMICAL</i>	<i>PHYSICO-CHEMICAL</i>	<i>PHYSICO-MECHANICAL</i>
<i>PROCESSES</i>		
<i>Interfacial Polymerization</i>	Emulsions techniques (Polymerization, Solvent extraction/evaporation)	Spray techniques: drying and congealing
<i>In situ Polymerization</i>	Phase separation (Single/multiple coacervation, Sol-gel encapsulation)	Dripping, Extrusion (Vibration, Electrochemical, Cutting wire)
<i>Polycondensation</i>	<i>Supercritical CO₂-microencapsulation</i>	Coating (Fluidization, Pan coating)
		<i>Microfluidic microfabrication (hydrodynamic flow-focusing), Lithography</i>

Microencapsulation Market, published in September 2020 (Report Code: FB 5546), presents the most effective techniques for microencapsulation in marketed products (Table II.). These are spray technologies, emulsion, dripping technologies, followed by other technologies, respectively, which are of lower significance (*marked in italics*) (5).

Along with the conventional manners of production, microfabrication and lithography offer a new route in the preparation of microparticles. Microfabrication processes produce particles with different structures and forms (elliptic, rod, bullet, star) (9).

The shape has a role in the performance of the particles during operation. Spherical solid particles perform higher flowability and better homogeneity in fluidization processes (10), yet have worse mixing ability than non-spherical particles during drum

drug coating (11). Spherical particles' surface area-volume ratio is low, which influences further processing and in vivo performance (wetting, drug release).

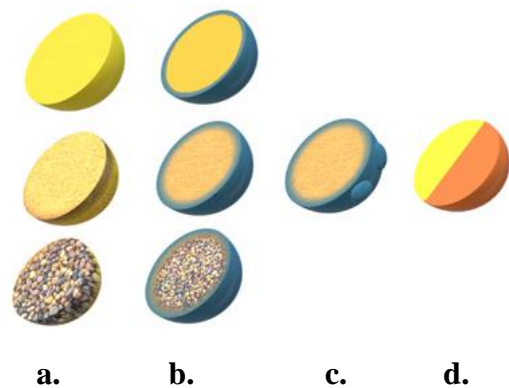


Figure 2. Schematic presentation of microparticles of various structures

- a.) Microsphere matrices of different porosity/ heterogeneity
- b.) Core-shell microcapsules of different heterogeneity in the core
- c.) Patchy particle d.) Janus particle (*own scheme*)

Fig. 2 and Fig. 3 illustrates some common structures: the fundamental monolithic matrix or the core-shell structures combined with dispersed solid or liquid particles, oil-containing cores, and solid sponges, anisotropic Janus particles are represented among microparticles.

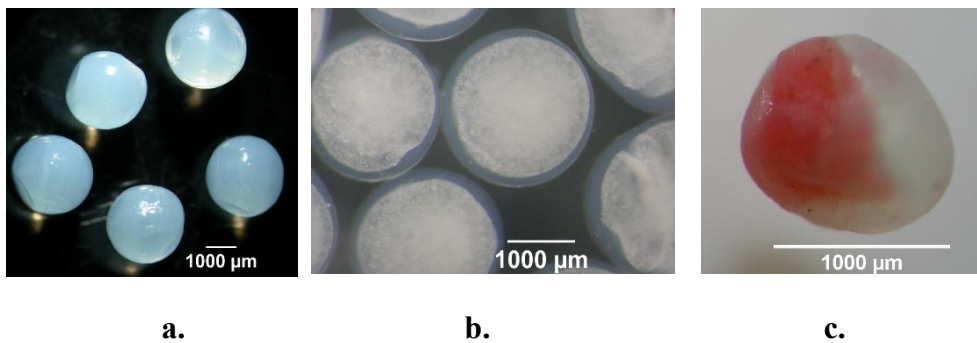


Figure 3. Structures of calcium alginate microparticle spheres

The particles were prepared by Büchi B-390 Microencapsulator, Stereomicroscopic images: Nikon SMZ 1000, own experiments (7)

- a.) Microspheres
- b.) Microcapsules W/O/W emulsion in core surrounded by calcium alginate shell
- c.) “Janus particle”

1.1.1.1 MICROENCAPSULATION BY EXTRUSION/DRIPPING AND COACERVATION PROCESS WITH ALGINATE-BASED MICROSPHERES

Extrusion and dripping techniques followed by either simple or complex coacervation are established methods of microencapsulation.

The extrusion through a nozzle with a determined orifice is followed by internal or external gelation during the procedure. The resulting particle size and shape are highly dependent on droplet formation. Many factors influence this process: density, temperature, viscosity, surface tension of the liquid and the size and material of the orifice from which it drops. The drop falls from the tip as soon as its weight overcomes the adhesion to the orifice. Thick, viscous liquids form large drops, while a decrease in density or surface tension leads to a decrease in drop size. The formation of satellite droplets depends on the rheological character of the liquid (12).

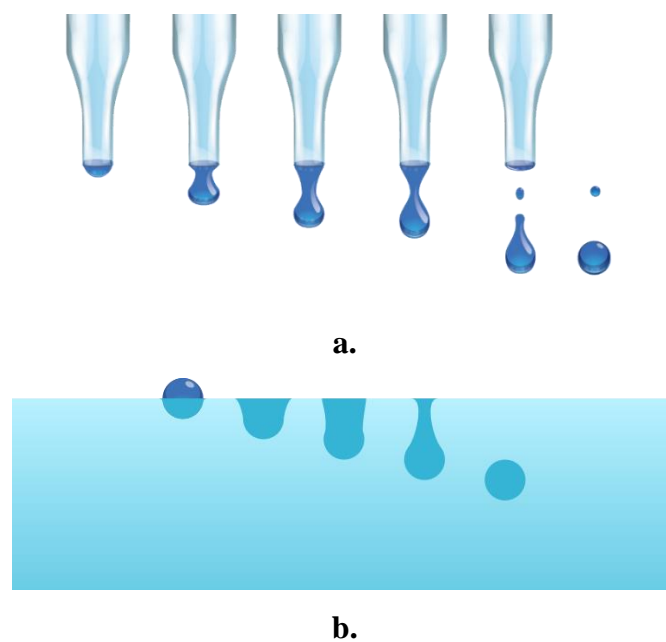


Figure 4. Steps of droplet formation

a.) at nozzle tip (*scheme by Artishus*)

b.) and droplet formation with coacervation within the solidifying bath (*scheme by Farkas Dóra*)

Earlier studies drew empirical conclusions, sometimes contradictory, in complex numerical relationships between all the process parameters. The collecting distance apparently affects particles' shape (13). Whelehan et al. (14) examined the influential parameters in the course of the vibrating nozzle method. Since one droplet is generated by each hertz of vibration, the drop diameter, d_d , can be calculated by the following simple mass balance equation (15):

$$d_d = \sqrt[3]{6 \cdot \frac{F}{\pi \cdot f}} \quad (1)$$

where F is the flow rate of the extruded liquid, f is the frequency vibration. However, the influence of the viscosity, nozzle diameter and interfacial tension is not defined in this relation, although all are fundamental in determining the particle size.

The feeding rate, frequency, and voltage are critical parameters in influencing the size during the vibration-extrusion process (16). Upon landing in the agitated bath, the alginate droplets harden by ionotropic gelation to form microspheres. The drop penetration into the cross-linking medium, CaCl_2 , e.g., with a high surface tension, may cause the spheres' deformation. Surface active agents (Tween 20 and Tween 80), considering the risk of the possible drug-excipient interaction, can be used to decrease the interfacial tension of the gelation bath. The size of droplets and coacervated beads is generally different, and so can be the shape. The frequency and feeding rate influences the formed hydrogel microsphere size (14).

1.1.1.2 MICROENCAPSULATION BY FREEZE-DRYING

The freeze-drying method for microencapsulation is generally used for protein-containing compositions and heat-sensitive molecules per se or following another physicochemical process, e.g., coacervation. The process starts with freezing the sample, whereby the eutectic point of the components must be concerned. As a result of the sublimation of ice and subsequent primary and secondary drying, a highly porous sample can be reached, where lyoprotectants and cryoprotectants can stabilize the active ingredient by creating a glassy matrix on replacing the water and preserve the original structure. During the process, the mobility of the molecules is reduced due to the formation of hydrogen bonds and van der Waals bonds between the molecules. This method solidifies the particles,

forming a highly porous structure; therefore, the particles can be quickly reconstituted in an aqueous medium. The method is simple; however, the relatively higher cost limits its application.

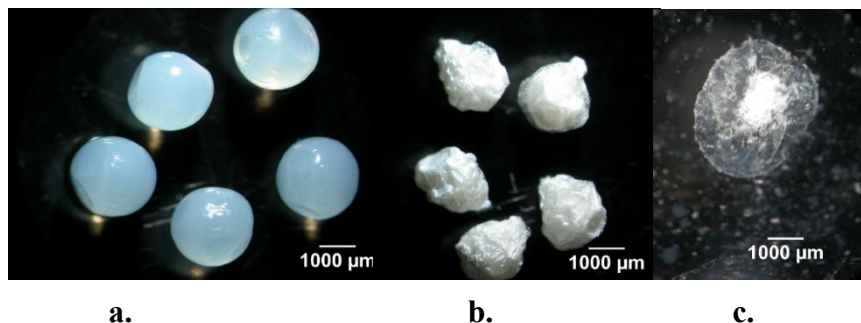


Figure 5. Calcium alginate microparticles: **a.)** initial (prepared by simple coacervation using a Büchi B-390 Microencapsulator),
b.) freeze-dried
c.) reconstituted in a pH 6.8 phosphate buffer (60 min) -*own work* (7)

1.1.1.3 EMULSION PROCESS WITH SOLVENT EVAPORATION

This process is particularly suitable for embedding hydrophobic active ingredients, generally in biodegradable polymers, such as polylactide microspheres. The biodegradable polymer is dissolved with a volatile, organic solvent to create an emulsion. In the case of polylactide (PLA), for example, dichloromethane is used. The substance to be incorporated into the microspheres is dissolved or dispersed, and then the mixture is emulsified in an aqueous medium using detergents to stabilize the O/W emulsion. Microcapsules are formed by evaporating the solvent from the microdroplets either gradually or by continuous stirring. In the case of hydrophilic active ingredients, a double emulsion process must be followed.

1.1.1.4 SPRAY DRYING

Spray drying is widely used in the industry for microencapsulation of volatiles, probiotics, and viable cells. Besides the obvious drawback (high loss, low yield), the numerous advantages make this technology very popular (uniform particle size, all steps carried out in one apparatus, use of organic solvents, and the capability to encapsulate heat-labile materials). The solution or emulsion of the active ingredient is sprayed into a chamber, where warm air dries the particles, and as a result, regular shaped, micron-sized, uniform

particles are created.

Extruded wax particles can be solidified using congealing, which offers a solution for embedding hydrophilic components to perform sustained-release via the slow erosion of the wall in the biological medium.

1.1.2 PELLETS

Pellets are free-flowing, compact, spherical units of a narrow particle size range. They are either filled into sachets or capsules (Harvoni[®] or Solvadi[®] oral pellets, Kreon[®] capsule, Kaldyum[®] retard capsule) or compressed into tablets with proper cushioning filler excipient systems to protect and guarantee the multi-particulates' excellent character (Betaloc[®] ZOK). The agglomeration techniques, through which fine powder is transformed into compact globules, are diverse:

- Solvent/Melt Extrusion-Spheronisation
- High-Shear Pelletization- Spheronisation
- Spray Congealing
- Spray Drying
- Air Suspension Coating/ Drug Layering
 - Dry Powder Layering
 - Solution and Suspension Layering on Inert Cores

The active ingredient is either integrated inside the pellet matrix's core or layered onto the inert pellets' surface. The application of different starter pellet cores (MCC, saccharose, isomalt, or dibasic calcium phosphate) can significantly influence the drug release process (17). The global market of pharmaceutical pellets' usage is in augmentation; the first four processes are most significant in the production, according to the 2019 financial report of Market Intellica (18).

1.1.2.1 AIR SUSPENSION METHOD/FLUID-BED COATING

Wurster (19) has administered fluidization in macroencapsulation for the coating of solid particles usually in a higher size range, in 1959. It was, however, also administered to encapsulate small particles in size range of 74–250 μm by Hinkes et al. (20). The particles are suspended in an air (or inert gas) stream during the process, being mixed constantly

and relatively independent from each other, while the wall material solution or dispersion is sprayed on their surface and dried inside the coating chamber. The following process parameters take part in the control of the particle size: properties of the core (density, hygroscopicity, surface area, particle size and shape, melting point, wettability, solubility, volatility, compressibility, crystallinity, hardness, cohesiveness, adsorption, friability and flowability of the core material). The critical process parameters are wall material concentration and quantity, inlet, outlet air temperature, and spray settings.

1.1.3 EFFECT OF EXCIPIENTS USED IN THE FORMULATION OF MICROPARTICLES

1.1.3.1 INTERACTIONS OF EXCIPIENTS WITHIN MICROCAPSULES: INTERPENETRATING AND SEMI-INTERPENETRATING POLYMER NETWORKS (IPN)

The formation of microparticles is often attributed to the creation of interpenetrating polymer networks (IPN), where the linear or branched polymer chains penetrate at a molecular scale of at least one of the networks by at least some of the linear or branched macromolecules; and the network is due to non-covalent interactions. Semi-interpenetrating networks (SIPN) consist of one linear (non-crosslinked) polymer that can create a network with ionic interactions (21). SIPN is distinguished from an IPN because the constituent linear or branched macromolecules can, in principle, be separated from the constituent polymer network(s) without breaking chemical bonds. Semi-interpenetrating networks can generally be formulated by ionic interactions between the polymers (Fig. 6, examples shown in Table III.).

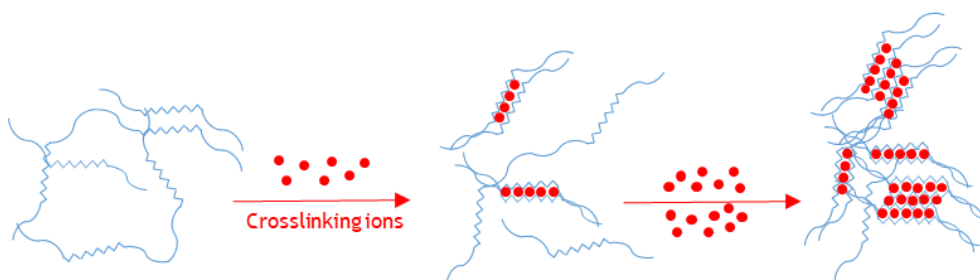


Figure 6. Effect of crosslinking ions in the formation of hydrogel structure (*own scheme*)

Polyelectrolyte complexes are formed by ionic interactions between two oppositely charged polyelectrolytes in an aqueous solution, characterized by a hydrophilic microenvironment with high water content and electrical charge density. An example of

a polycation is the synthetically produced poly-L-lysine. The resulting polyelectrolyte complex called alginate-poly-lysine-alginate (APA) is used for biomedical purposes. The problem, however, is that polylysine has poor biocompatibility and can induce immunogenicity so it is not of sufficient clinical relevance.

Due to the opposite charges, the combination of alginate and chitosan form a polyelectrolyte complex at an acidic pH, which reduces the porosity of the polymer network and further delays the release of the active ingredient. This combination of alginate and chitosan has a high mechanical force. Chitin is isolated mainly from the shells of crustaceans, lobsters, crabs and is considered a biocompatible, biodegradable, non-toxic polysaccharide. It is bioadhesive and binds to negatively charged mucosal cell surfaces. As it also occurs in the human body, the residence time is increased, which is positive for the mode of action of the microcapsules, increasing adsorption. In addition to all these favorable properties, chitosan is also very cost-effective.

Table III. a, b Synergistic polymer combinations and preparation processes (7)

<i>Polymer</i>	<i>Active Ingredient</i>	<i>Particle Size (μm)</i>	<i>Physicochemical Mechanisms</i>	<i>Ref</i>
<i>a. Carbohydrate-Carbohydrate</i>				
Chitosan-alginate	Leydig cells	230–370	Complex coacervation	(22)
Agarose-alginate (CaCl₂)	Sertoli cells	250	Microfluidics ionic gelation	(23)
Gelatin + gum arabic	Raspberry anthocyanins	150	Emulsification, coacervation	(24)
CMC-Na + xanthan gum	Diclofenac sodium	1000–1500	Emulsification, ionic gelation, Interpenetrating network	(25)
LBG + PVA	Buflomedil hydrochloride (BH)	350–750	Emulsification, Interpenetrating network	(26)
Chitosan + pectin	Insulin	0.24–2	Electrostatic self-assembly	(27)

<i>Polymer</i>	<i>Active Ingredient</i>	<i>Particle Size (μm)</i>	<i>Physicochemical Mechanisms</i>	<i>Ref</i>
<i>b. Carbohydrate-Protein</i>				
Gelatin + gum arabic	Aspartame	100	Double emulsion/complex coacervation	(28)
Gelatin + chitosan	Citronella oil	100	Coacervation	(29)
Whey protein + alginate	Flaxseed oil	<10	Double layer emulsification spray drying	(30)
Alginate + gelatin	Whey peptides (antihypertensive)	1000	Dripping, coacervation	(31)
Alginate + zein	Bifidobacterium bifidum	1200–1700	Extrusion coacervation shell-core	(32)
Chitosan+zein	Oral gene delivery	10	Zein-sodium tripolyphosphate, W/O emuls.	(33)
Poly (L-ornithine) + alginate + PLA, PLGA	Superoxide dismutase, ketoprofen	500	W/O/W, O/W, solvent evaporation	(34)
Poly (L-ornithine) + ursodeoxycholic acid, Polystyrene sulfonate, polyallilamine	Pancreatic β -cells	700	Complex coacervation, vibrational jet	(35)
Poly (ethylene glycol) (PEG)-anthracene alginate	Coomassie blue	no data	Coacervation	(36)
Vinyl-sulfone terminated PEG + alginate	Human foreskin fibroblast	550	Simple coacervation	(37)
Alginate + Poly-ϵ-caprolactone	Theophylline	800	Complex coacervation	(38)
Polypropylene + PMMA + ethylcellulose	Verapamil	150–200	O/W solvent evaporation	(39)
PLGA-alginate	Rifampicin	15–50	Microfluidics	(40)

1.1.3.2 ROLE OF ALGINIC ACID AND ALGINATES IN MICROENCAPSULATION

Alginate is a naturally occurring anionic polymer typically obtained from brown seaweed. It is bio-inert and naturally hydrophilic, allowing covalent functionalization via interaction with extracellular matrix proteins, peptides, and growth factors (41). With its high biocompatibility, alginate is ideal as a gelling agent. In addition, it counteracts the development of peptic ulcers, which gives an additional positive effect in the case of the encapsulation of NSAIDs. Microencapsulation technology is beneficial in inflammatory bowel disease, as the patients must ingest anti-inflammatory drugs and other substances. These can cause undesirable side effects due to their rapid absorption and long application time, which puts additional strain on the gastrointestinal tract of these patients. Since the oral intake of medication is an option often desired by patients, medication based on alginate microcapsules can be used. The polymer alginate can form pH-sensitive hydrogels under mild conditions. With microparticles that react to the pH value in the respective area of the gastrointestinal tract, it is possible to achieve a biomimetic approach and small intestine or colon-targeted delivery (42).

Alginate is a linear anionic polysaccharide and consists of D-mannuronic acid and L-guluronic acid, glycosidically linked in position 1,4. The D-mannuronic acid (M-blocks) and L-guluronic acid (G-blocks) residues vary along the polymer (Fig.7).

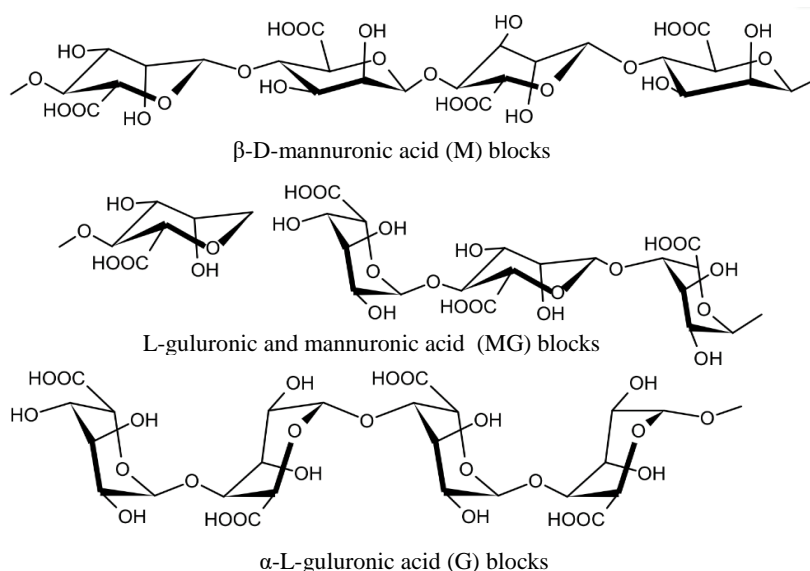


Figure 7. Main components of alginic acid: β -D-mannuronic acid (M) and α -L-guluronic acid (G) and their combination

The unique property of sodium alginate is the conversion of sol to hydrogel with more than 95% of the water molecules physically held inside, which is necessary for maintaining bioactivity by providing an aqueous environment for the entrapped substances. When a guluronic acid residue meets bivalent cations such as calcium, an elastic hydrogel is formed by means of an ionotropic bond, provided that the conditions are optimal (43). These guluronic acid residues of sodium alginate are folded and stacked when bound. This leads to the structural transformation of the alginate chains from a random structure to an ordered, calcium-bound, ribbon-like structure. This interweaving or linking of the alginate chains results in the three-dimensional network structure of the hydrogel. This structure is also known as the *eggbox structure* (Fig. 8). In the microencapsulation with sodium alginate, the desired alginate hydrogel beads are created through the above-described ionotropic bonding and subsequent structural transformation.

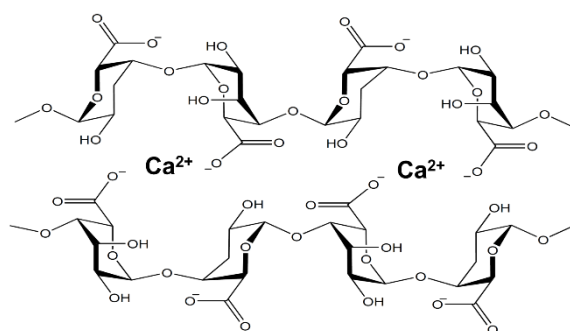


Figure 8. Representation of the interaction between calcium ions and alginate and the concomitant formation of an eggbox structure

In addition to calcium ions, other ions can bind to the alginate structure and thereby form a gel. Barium and strontium ions preferentially bind to the G-blocks. Alginate has the highest affinity for lead, copper, and in descending order, cadmium, barium, strontium, calcium, cobalt, nickel, zinc, and manganese. The cross-linking properties of the ions play a role in the rearrangement and different block structure-forming along with the different types of alginate. Calcium, in particular, is used to facilitate gelling, but calcium alginate beads are sensitive to chelating agents such as EDTA, citrates, lactates, phosphates, and non-gelling ions such as sodium and magnesium. Under physiological conditions, this ion exchange can lead to osmotic swelling of the particles and thus increase the pore size and destabilize the gel, which leads to the beads' bursting. To prevent this and stabilize them,

a polycation layer can be added to the alginate core. However, most polycations are toxic. Poly-L-Lysine is the most widely used polycation, but this can lead to a fibrotic overgrowth in implanted microcapsules. Newer methods, therefore, try to omit the use of polycations. Epimerized alginate or covalently crosslinked alginate can be used as the core material. Covalent networks by biofunctional crosslinkers such as glutaraldehyde and epichlorohydrin enable a more robust and more stable structure. The toxic residue of these excipients limits their use. Barium and strontium increase the stability of the microcapsules using alginate with a high guluronic acid content, with a lower permeability compared to calcium alginate beads. Barium, however, has the property of inhibiting the potassium channels of biological membranes (44), so the lowest possible concentration of this ion needs to be administrated. In the case of alginates with a high proportion of mannuronic acid, no effect was found with these ions in terms of gelling ability.

Alginates with a high proportion of guluronic acid are considered rigid and mechanically stable; however, a higher degree of brittleness occurs.

There are various compositions of polymers to stabilize the structure and influence the release. Methylcellulose can stabilize the emulsion, and aluminum ions crosslink sodium alginate in a single water-in-water emulsion gelling process. The spherical microbeads with the amorphously distributed drug make it possible to reduce the release, thus reducing the side effects of oral intake (45).

The stretchability of the pure hydrogel networks can be increased by the combination of the advantageous characteristics of polymers. The calcium alginate/ polyacrylamide hydrogel is up to 20 times more stretchable than the constituting hydrogels. It reaches fracture energy of up to $\sim 9000 \text{ J m}^{-2}$ (46). In addition to its mechanical properties, it also has excellent biocompatibility. The polyacrylamide reinforces the calcium alginate, and under stress, the loosely cross-linked polyacrylamide polymer chains stretch, while alginate opens from the ionic binding sites like a zipper, enabling an energy dissipation mechanism. During the stretching and “unzipping” of the ionic crosslinking, the number of polymer chains increases, which can then withstand stress again, and the stretchable polyacrylamide polymer chains stabilize the deformation after the ionic crosslinking is opened. The gel can be produced by a two-step method. In the first step, all components

except the ionic crosslinker are dissolved, then transferred to a mold and heated up to 50 degrees Celsius for three hours, creating a sodium alginate/ polyacrylamide hydrogel. In the second step, the hydrogel is placed in an aqueous solution with polyvalent cations for three hours to crosslink the hydrogel and polyvalent cations. Divalent and trivalent cations can modify the mechanical properties of this two-component hydrogel.

Alginate hydrogels can be used as a matrix for three-dimensional cell immobilization. Calcium, barium and strontium are the main crosslinkers. Calcium binds to GG and GM blocks, barium binds to GG and MM blocks, and strontium uniquely binds to GG blocks. Alginates that have been crosslinked with barium or aluminum have exceptionally high stability compared to calcium. Di- and trivalent cations increase the rigidity and strength of the alginate/polyacrylamide hydrogels. Aluminum and iron provide high stiffness and strength, while monovalent sodium has low strength and a low modulus of elasticity.

The hydrogels with di- and trivalent cations are less stretchable, are nevertheless stretchable to ten times their original position, which is sufficient for most applications. Above all, the ion charge of the multivalent cations influences the interactions with the hydrogel, the ion radius plays a subordinate role. The divalent cations bind with the alginate blocks in a two-dimensional planar form, resulting in the egg carton shape. The higher the ionic radius in the case of divalent cations, the less strong the bond. Trivalent cations can bind three carboxyl groups of alginate chains, creating a three-dimensional, compact structure. Therefore, hydrogels with trivalent cations have better mechanical properties. It should be mentioned that trivalent iron has a higher stiffness than aluminum. Hydrogels with trivalent cations have a higher elastic limit than divalent cations. The reason for this is, again, presumably the different bonding. The divalent and trivalent crosslinked hydrogels show energy dissipation that can be characterized by a hysteresis. The reason for this is probably the zipper-like opening of the ion-bound network (47). Zinc ions can also form a network by binding the negatively charged alginate chains. In addition, zinc can form insoluble complexes with most proteins and peptides and stabilize them in a complex. Zinc-alginate microparticles can be administered via the pulmonary route (48). Avoidance of the first-pass effect and representing a further non-invasive therapy option carries a great advantage in therapy. The biocompatibility of alginate is preferred to PLA and PLGA. The latter polymers are soluble in organic solvents, thus can

only be carefully administered in the formulation of protein molecules and could also lead to organic solvent residues. In addition, the more extended degradation of PLA/ PLGA would lead to an accumulation in the lung tissue. The aim in production is to obtain highly porous microparticles with a high geometric diameter but a small aerodynamic diameter. The microparticles having a hydrophilic smooth surface swelling in the lungs make opsonization and phagocytosis of the particles less likely (49).

Barium, a bivalent cation, has valuable properties in microencapsulation and can form a hydrogel with alginate. In Type 1 diabetes mellitus patients, transplanting tissue from islet cells of Langerhans to prevent pathological changes such as neuropathy, nephropathy, and retinopathy is an excellent option. However, previous transplants can be rejected due to immune reactions. The immunosuppressive therapy preventing this can drastically increase the risk of infection and damage the transplanted tissue. Microparticulate drug delivery systems can circumvent these problems. Smooth, spherical microcapsules, in particular, are suitable because they have a large surface/ volume ratio and no irregular surface, which could more likely trigger an immune response. In addition, the surface can be crosslinked with a polycationic polymer and covered by an outer alginate layer. The second outer layer may prevent or delay immune reactions by electrostatic repulsion of the negatively charged immune cells and the polyanionic alginate.

Barium has a higher affinity to alginate than calcium, which makes a more robust hydrogel. Because of this high level of binding, the microparticles are also more resistant to osmosis than calcium alginate. High barium concentration can negatively affect the encapsulated cells' metabolism, and the low nutrient supply causes the death of inner cells. It is also important that the microcapsules remain free from erosion, barium residues can dissociate from the alginate through osmotic pressure.

The strontium cations have similar properties to calcium, promote the differentiation of pre-osteoblasts to osteoblasts, and inhibit bone resorption by directly inhibiting resorption activity and apoptosis of the osteoblasts in diseases like osteoporosis or osteopenia. In treating bone defects after osteoporotic bone fractures, it is a minimally invasive technique by injecting ceramic materials containing microparticles or nanoparticles suspended in a suitable carrier (50). Microparticles with a spherical shape are preferred due to their better adaptation to irregular implantation sites, and over their favorable biopharmaceutical characters they also have a more predictable flow behavior.

Strontium causes an improvement in the mechanical properties (breaking strength, indirect tensile strength and hardness) of an injectable microsphere preparation. The crosslinking time of strontium (having a larger ionic radius than calcium) was shorter as opposed to calcium. The introduction of strontium into microparticles enables strontium to act locally and as a significant advantage over the systemically used active ingredient strontium ranelate, not to cause any undesirable side effects such as myocardial infarction in patients with ischemic heart disease and peripheral arterial diseases (51).

1.1.4 THE BEHAVIOR OF MICROPARTICLES IN THE BODY

Microparticles' dosage forms administered in the peroral route carry many advantages summarized in the introduction. The parenteral application route, however, also has great significance. In the parenteral pathway, the nonspherical microparticles show higher targeting efficiency than spherical particles, and elongated particles show more resistance to phagocytosis (52). Decuzzi et al. stated that compared to spherical particles, “discoidal particles” travel laterally toward the blood vessel wall and can exhibit a stronger affinity toward the blood vessel wall (53). Most similar experiments tended to use nanoparticles. However, experiments now also involve the geometry of microparticles and how they influence the in vivo behavior (54).

The wide variety of polymers used for microencapsulation open different routes for the trigger of drug release. Single or multiple stimuli lead to fine-tuning of the release process (Fig. 9).

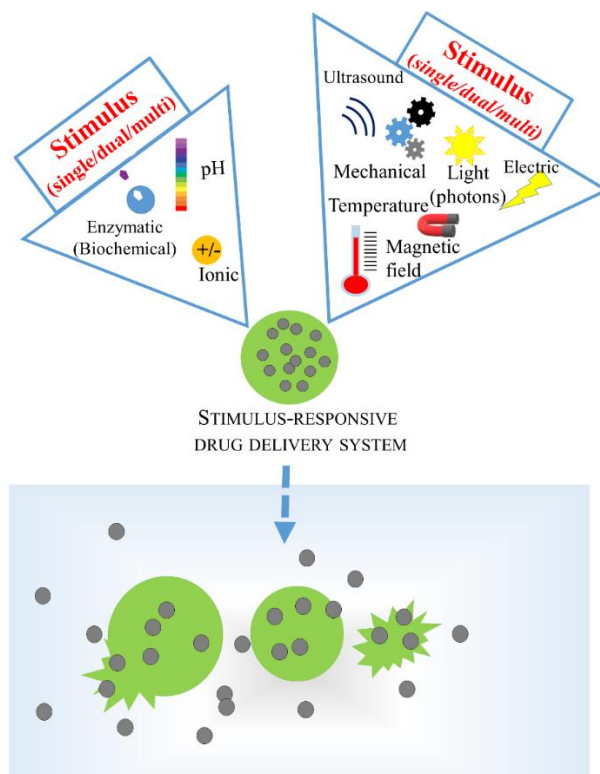


Figure 9. The external signals and corresponding release of microparticulates (modified figure based on (7))

1.1.5 MECHANISMS OF DRUG RELEASE FROM MULTIPARTICULATE PREPARATIONS

Three main processes and their combinations commonly progress the drug release from multi-particulate preparations (Fig. 10):

- diffusion (through the swollen layer or via pores)
- erosion (bulk or surface erosion)
- osmosis (permeable or semipermeable shell layer)

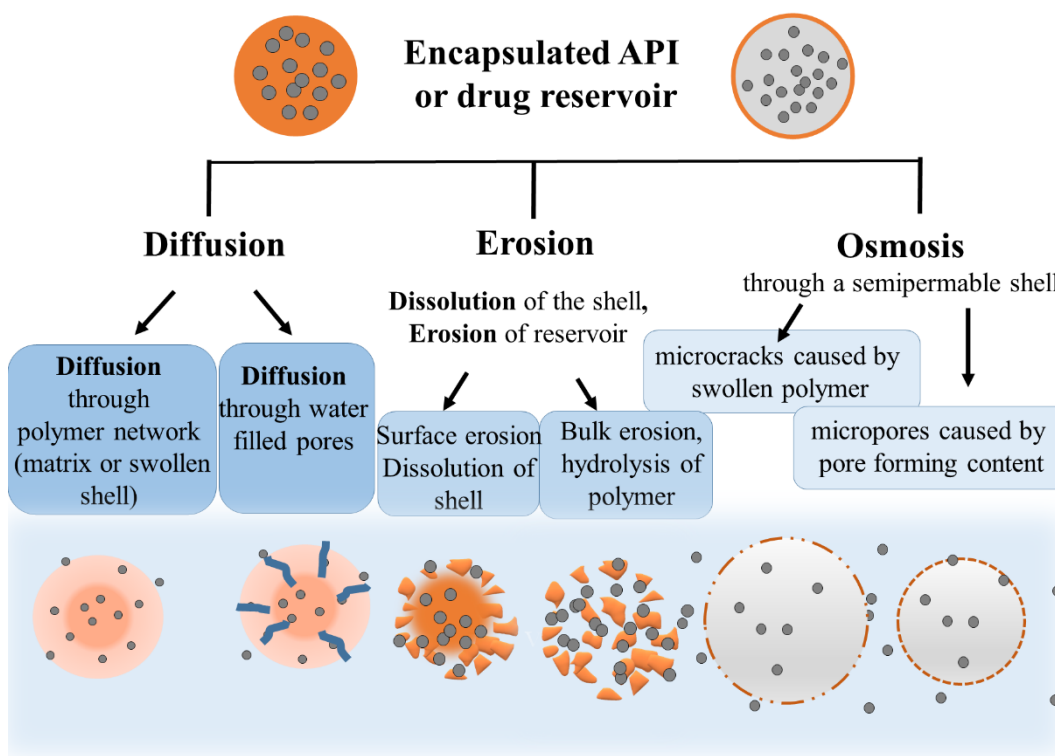


Figure 10. The primary drug release mechanisms of the multiparticulate preparations (modified figure based on (7))

The kinetics of drug release depends on many factors, such as the type, structure, and composition of the particles, follows different mechanisms and can be described by versatile models (zero-order kinetics, first-order kinetics, Higuchi, Hixson-Crowell, Korsmeyer-Peppas models) (55-58).

1.1.6 FORMULATION CONCEPTS FOR SODIUM BICARBONATE

1.1.6.1 GENERAL USE OF SODIUM BICARBONATE

Sodium bicarbonate is a well-known alkaline chemical material used in the medicinal field and the household.

The mild alkalinity, along with the mild abrasiveness, makes sodium bicarbonate a versatile substance. It is also recognized as a “generally safe food product” worldwide (59).

It is used as a baking powder component, creating an aerated, loose dough consistency (its synonym name is baking soda), and as a mildly abrasive, non-corroding cleaning agent in stain-removal, especially in the non-scratching cleaning of metal surfaces (dentistry and implantation).

In pharmaceutical formulation, it is commonly used as a *chemical disintegrant* excipient of tablets, granules, effervescent tablets, or *buoyant preparations*. Formerly it was a common technique in prescription pharmacy to dispense powders by formulating a pill to facilitate swallowing. Pulvis coffeini FoNo VII., the composite powder can be dispensed in the form of pills to the patient. In this case, the composition has to be implemented with Polyvinylpyrrolidon as a binder (15%) and sodium bicarbonate as a disintegrant (7.6%) to precipitate the disintegration of the preparation.

In parenteral solutions, sodium bicarbonate is also used as an alkalic buffer component. It is isotonic at the concentration of 1.26% solution.

Sodium bicarbonate is relatively abundant in nature. The natural minerals Nahcolite and Trona consisting of NaHCO_3 (nahcolite > 90%, trona approx. 36%) are very efficient for SO_2 reduction in dry injection systems used in air cleaning processes. This is due to the immense reactive surface area created as sodium bicarbonate decomposes to sodium carbonate prior to the reaction with SO_2 , which has a tremendous role in the mitigation of SO_2 (60).

1.1.6.2 ROLE AND APPLICATION FIELDS OF SODIUM BICARBONATE IN THERAPY

Table IV. Registered preparations in Hungary containing sodium hydrogen carbonate (based on OGYEI Database (25))

<i>Medicinal preparation</i>	<i>Active ingredient</i>
ALKALIGEN <i>solution for infusion</i>	sodium hydrogen carbonate
BIPHOZYL <i>solution for haemodialysis or haemofiltration</i>	magnesium chloride hexahydrate, sodium chloride, disodium phosphate dihydrate, sodium hydrogen carbonate, potassium chloride
GAVISCON <i>chewable tablet</i>	sodium hydrogen carbonate, calcium carbonate, sodium alginate
GAVISCON FORTE <i>internal suspension in sachet</i>	sodium alginate, sodium hydrogen carbonate, calcium carbonate
GAVISCON <i>internal suspension</i>	sodium hydrogen carbonate, sodium alginate, calcium carbonate
LECICARBON <i>rectal suppository</i>	sodium hydrogen carbonate, sodium dihydrogen phosphate dihydrate
MOXALOLE <i>powder for internal powder</i>	sodium hydrogen carbonate, Macrogols (type 3350), potassium chloride, sodium chloride
NÁTRIUM-HIDROGÉNKARBONÁT B. BRAUN <i>8,4% injection</i>	sodium hydrogen carbonate
NATRIUM-HYDROGEN-CARBONICUM PHARMAMAGIST <i>42 mg/ml injection; 84 mg/ml injection</i>	sodium hydrogen carbonate
NEFROSOL <i>2 mmol/l; 4 mmol/l potassium solution for haemofiltration</i>	sodium hydrogen carbonate, calcium chloride dihydrate, magnesium chloride hexahydrate, glucose monohydrate, potassium chloride
PHYSIONEAL 35 CLEAR-FLEX GLUCOSE <i>13,6 mg/ml; 22,7 mg/ml; 38,6 mg/ml solution for peritoneal dialysis</i>	glucose monohydrate, sodium chloride, calcium chloride dihydrate, magnesium chloride hexahydrate, sodium hydrogen carbonate, sodium lactate solution
PHYSIONEAL 40 CLEAR-FLEX GLUCOSE <i>13,6 mg/ml; 22,7 mg/ml; 38,6 mg/ml solution for peritoneal dialysis</i>	glucose monohydrate, sodium chloride, calcium chloride dihydrate, magnesium chloride hexahydrate, sodium hydrogen carbonate, sodium lactate solution

Many therapeutical effects of this substance are utilized in magistral preparations (62-63).

MUCOLYTIC AGENT

As being a Ca^{2+} chelator, sodium bicarbonate also works as a mucolytic agent as calcium ions have a tremendous role in transport through the mucus layer of humans. In expectorant preparations, NaHCO_3 was proved to alter the viscosity of mucin aggregates and dispersion of mucin fibers (64).

Severe impairment of Na^+ , Cl^- and HCO_3^- secretion as a reason for mutations in the gene encoding cystic fibrosis transmembrane conductance regulator (CFTR) follows to abnormal viscosity and function in many organs (lungs, intestines, salivary glands, sweat glands, reproductive organs). For cleaning the secretions of the inner cannula of tracheotomy tubes, the use of 2% sodium bicarbonate for direct tracheal irrigation or as a spray has been reported (65). The magistral expectorant composition is advised for increasing bronchial mucus secretion.

Pulvis expectorans FoNo VIII.

for 10 divided powders

<i>Terpinum</i>	<i>1.0 g</i>
<i>Natrii hydrogenocarbonas</i>	<i>2.0 g</i>
<i>Saccharosum</i>	
	<i>vel</i>
<i>Sorbitolum</i>	<i>2.0 g</i>
<i>Anisi aetheroleum</i>	<i>gtt I.</i>

LAXATIVE COMPONENT

On its reaction with acids, carbon dioxide release occurs, which acts both physically and through a reflex mechanism in the defecation process.

Suppositorium laxans FoNo VIII.

<i>Natrii hydrogenocarbonas</i>	<i>6.0 g</i>
<i>Kalii hydrogenotartras</i>	<i>9.0 g</i>
<i>Adeps solidus 50</i>	<i>qu. sat.</i>

The ear drop *Otogutta hydrogencarbonatis FoNo VIII.* softens the cerumen, thus helps the leaning of the blocked auditory duct.

Otogutta hydrogencarbonatis FoNo VIII.

<i>Natrii hydrogenocarbonas</i>	1.0 g
<i>Aqua purificata</i>	9.5 g
<i>Glycerolum 85 per centum</i>	ad 20.0 g

PERORAL ADMINISTRATION, GASTRIC TARGET- ANTACID INGREDIENT

Sodium bicarbonate is a crucial component in antacid preparations. It binds the proton, forms carbonic acid, which decomposes into carbon dioxide and water, soothes reflux symptoms, heartburn and gastric discomfort.



Numerous OTC (over the counter) preparations, such as Tums[®], Gaviscon[®], as well as magistral preparations contain sodium hydrogencarbonate as an active antacid ingredient. The following antacid *Pulvis antacidus FoNo VIII.* contains magnesium salt, which is a laxative salt and can influence the absorption of drugs's absorption and can only be carefully administered in reduced renal function.

Pulvis antacidus FoNo VIII.

<i>Natrii hydrogenocarbonas</i>	20.0 g
<i>Magnesii subcarbonas levis</i>	40.0 g

or

Pulvis ad pyrosim FoNo VIII.

<i>Dinatrii phosphas dodecahydricus</i>	2.0 g
<i>Calcii carbonas</i>	20.0 g
<i>Natrii hydrogenocarbonas</i>	18.0 g
<i>Magnesii subcarbonas levis</i>	ad 100.0 g

The administration and dosing of bicarbonates and carbonates as antacids should be taken with care and only within a short period, as during the neutralization process in the stomach a high volume of gas (CO₂) is released, which causes flatulence and inconvenience.

ORAL ADMINISTRATION, TARGET IN THE MOUTH CAVITY

Fermentation of carbohydrates in the mouth produces acids and, as a consequence, decreases the pH. This increased concentration of H⁺ is neutralized by salivary HCO₃⁻ to form water and carbon dioxide. A hypotonic, 1% (w/v) solution used as a mouthwash neutralizes the pH, moisturizes, acts against halitosis, and decreases the microbial load of the oral cavity. As a chewing gum component, it promotes saliva secretion, increasing the saliva flow to flush away debris and set up optimal mouth hygiene.

On behalf of its solubility and low intrinsic hardness, sodium bicarbonate is versatilely used in dental fields. Air polishing with bicarbonate polish powder (particle size of 74 µm)- was safe and effective in removing plaque and subgingival biofilm even around titanium surfaces (66).

A hypertonic solution of sodium bicarbonate can promote the osmotic movement of water from bacterial cells, resulting in shrinkage, plasmolysis, and finally the bacterial cell death (67). Periodontal disease can be effectively reduced by the aid of sodium hydrogencarbonate in mouthwash or subgingival irrigation. 2.5%–5% of sodium bicarbonate was proved bactericide against major periodontal pathogens (*Prevotella intermedia*, *Porphyromonas gingivalis*, *Aggregatibacter actinomycetemcomitans* Gram-negative anaerobic organisms) (68). Acting not only as a physicochemical whitening and disinfecting component of toothpaste, but its bactericidal property also makes it a patient-friendly mouthwash and can be used on a long-term basis as it is practically free of any side effects (69).

The anti-inflammatory action of sodium bicarbonate lays on the fact that this substance can neutralize the inflammatory chemicals such as proteases, lipopolysaccharides, hydrogen sulfide, ammonia, and short-chain fatty acids such as butyric acid and propionic acid, which oral pathogens release and that could induce both micro- and macro-level tissue destruction (70).

ALKALINE BUFFER COMPONENT

Sodium bicarbonate is a standard buffer component in liquid dosage forms, in eyedrops (Oculogutta antidota FoNo VII., Oculogutta fluoresceini FoNo VIII.). However, it can also be used as a buffering agent in solid preparations.

As a buffer excipient, sodium bicarbonate can protect acid-sensitive active ingredients. A clinical study successfully administered 1100 mg sodium bicarbonate in combination with the proton-pump inhibitor omeprazole (40 mg) to increase the stomach's pH, thus providing the API in healthy male volunteers and reaching similar pharmacodynamic performance and safety profile as a delayed-release proton pump inhibitor preparation (Losec[®]) (71).

In 2004 the U.S. Food and Drug Administration approved the immediate-release formulation (Zegerid[®]) of the proton-pump inhibitor omeprazole combined with the antacid buffer (sodium bicarbonate), which neutralizes gastric acid and protects omeprazole from gastric acid degradation.

The neutralizing effect of sodium hydrogencarbonate plays a role in the neutralization of the odoriferous fatty acids produced by bacteria's action on sweat; therefore, it is used in deodorant preparations.

1.1.6.3 BICARBONATE-CARBON DIOXIDE PHYSIOLOGICAL BUFFER SYSTEM

The role of bicarbonate ions in physiological regulation is crucial. Besides hemoglobin and plasma proteins, bicarbonate ion is an essential component of a pH buffer system of the extracellular fluid (plasma and interstitial fluid) (72). It is secreted at numerous places within the body (renal tubules, lungs, hemoglobin cells, mouth cavity, intestine). Epithelial cells in pancreatic ducts are the source of the bicarbonate and water secreted by the pancreas. Bicarbonate is critical in neutralizing the acid getting into the small intestine from the stomach.

On dissolving in water, sodium bicarbonate ionizes and forms HCO_3^- ions, which then react with H^+ ions of the acids, followed by the release of carbon dioxide.

Carbon dioxide diffuses rapidly from the tissues into red blood cells, where it is hydrated with water to form carbonic acid. This reaction is facilitated by carbonic anhydrase, an enzyme that exists in high concentrations in red blood cells. The carbonic acid dissociates into bicarbonate- and hydrogen ions. Most of the bicarbonate ions diffuse into the plasma. Since the ratio of H_2CO_3 to dissolved CO_2 is constant at equilibrium, pH may be expressed in terms of bicarbonate ion concentration and partial pressure of CO_2 summarized by the Henderson-Hasselbach equation:

$$\text{pH} = \text{pK} + \log \left(\frac{[\text{HCO}_3^-]}{0.03 \cdot \text{pCO}_2} \right) \quad (3)$$

The human blood plasma has a pH of 7.4 (7.35-7.45). A pH fall below 7.0 or rise above 7.8 would lead to irreversible processes. Compensatory mechanisms for acid-base disturbances function to change the ratio of HCO_3^- ; to pCO_2 returning the pH of the blood to normal. Metabolic acidosis might be compensated by hyperventilation and increased renal reabsorption of HCO_3^- . Metabolic alkalosis –a less common symptom- may be compensated by hypoventilation and the excretion of excess HCO_3^- in the urine.

Metabolic acidosis (when the arterial blood pH decreases below the normal range of 7.35-7.45) is a complex disorder showing symptoms like fatigue, nausea or hypotonia, breathing deficiency (profound and quick breathing). Kidneys and lungs are capable of blood pH correction via complex mechanisms, e.g., excreting the excess H^+ in urine or exhaling in the form of CO_2 . The condition is commonly encountered in both chronic renal failure and end-stage renal disease. Many adverse effects are associated with metabolic acidosis: increased protein decomposition, negative nitrogen balance, bone lesions, impaired function of the cardiovascular system, impaired function of the gastrointestinal system, anorexia, hormonal disturbances, fatigue, insulin resistance, hyperkalemia, altered gluconeogenesis, and triglyceride metabolism, increased progression of chronic renal failure, and growth retardation in children. Even metabolic acidosis's minor degrees are deleterious. 'High' dialysate bicarbonate (40– 42 mmol/l) is a safe, well-tolerated, and valuable tool for better correction of metabolic acidosis and must become a standard of hemodialysis treatment.

Metabolic acidosis of end-stage renal patients could be successfully corrected with bicarbonate hemodialysis and with peroral bicarbonate containing phosphate binders, i.e., calcium carbonate (73). Bicarbonate powder, compared with bicarbonate solutions, has

some advantages and enables a stable composition of electrolytes.

The administration of sodium bicarbonate perorally can improve the tolerance for exercises, and the gradual intake enhances high-intensity intermittent exercise performance in young trained males by promoting the acid-base buffer capacity in the blood and muscles during training (74). Sodium bicarbonate is among the leading *ergogenic aids*. Athletes participating in strenuous exercise use it to delay muscle fatigue and improve performance. Both short-term and long-term high-intensity exercise can benefit from the *ergogenic effects* of this buffer component (75).

An acidic extracellular pH ranging from 6.5 to 6.9 is developed in the microenvironment of various *malignant tumors*. Metabolic activity and oxygen supply influence tumor acidosis through various mechanisms. In severe hypoxia, the cancer cells produce mainly lactate and H^+ ions via glycolysis. In the regions where oxygen is moderately available, cells with enhanced glycolysis produce a variety of substrates, including glutamine, fatty acid, as well as lactate, from cells with enhanced glycolysis. As a result of oxidative phosphorylation, which serves energy generation, CO_2 diffuses out of the cells. Near the blood vessels, where there is a sufficient amount of oxygen, the tumor cells still tend to generate ATP (adenosine triphosphate) due to enhanced glycolysis, known as the Warburg effect. Due to the acidic substrates (lactate, H^+ , and hydrolysis of CO_2), the tumor microenvironment becomes acidic. Bicarbonate ions have a prominent role in maintaining the homeostasis of the cells by neutralizing the H^+ of the acidic microenvironment. It contributes to the immunosuppressive effect of cancerous cells. Several studies revealed the potential anticancer effects of sodium bicarbonate alone or in combination with other therapies (76).

1.1.6.4 THE ACID-BASE BALANCE OF THE INTESTINES

The acid-base balance of the body is a critical factor in the adequate regulation of metabolic processes. This balance is frequently jeopardized by diseases, as well as lifestyle habits of our age, for example, stress, inappropriate nutrition, and addictions.

Mucous cells secrete sodium bicarbonate, creating the mucus bicarbonate barrier, providing a near-neutral chemical environment on the luminal surface, thus protecting gastric and duodenal mucosa against acid load as a pre-epithelial defensive factor (77-78).

The gastric emptying is regulated by the pH of the duodenal lumen or its change since the prolonged acid-load of the duodenum delays emptying the chymus (i.e., the food that is partly digested in the stomach and converted into pulp) into the duodenum. The luminal pancreatic digestive enzymes are secreted into the duodenal lumen and present in the upper third of the small intestine. Their pH optimum is in the pH range of 6.5 to 8.7. Orally supplemented digestive enzymes also need this optimal chemical environment. The inactivation of pepsin - required to protect the small intestinal mucosa and the luminal pancreatic digestive enzymes - also takes place in the duodenal lumen at this pH. Thanks to the carbon dioxide/bicarbonate cycle, the alkaline environment, which is present in the mucin layer adhered to the intestinal mucosa, facilitates intestinal digestion, the emulsification of the lipid aggregates, and micelle-forming. Duodenal luminal pH can fluctuate rapidly between pH 2 and 7 depending on the mixing of secreted bicarbonate and gastric acid (79). The mucosa of the duodenum reacts on the acid-load by a unique luminal chemosensing capacity. After duodenal luminal acidification, a number of compounds stimulate bicarbonate secretion from the liver, pancreas, and duodenum including secretin, vagally produced acetylcholine, vasoactive intestinal polypeptide (VIP), pituitary adenylate cyclase-activating polypeptide (PACAP), melatonin, and motilin. The principal components contributing to duodenal mucosal defense involve HCO_3^- secretion from the epithelium (80).

The neutral or slightly alkaline pH promotes the luminal phase digestion, which may help avoid the harmful effects caused by the improperly digested food that remains in the small intestine and colon lumen. Inadequate luminal digestion may contribute to the following clinical scenarios:

- Absorption disorders, deficiency diseases (vitamins, trace elements), and, as a consequence, decline in the resistance of the organism,
- Osmotic pressure increases within the lumen of the small intestine and the colon,
- Allergic, cellular, and humoral immunoreactions due to improperly digested food fragments (peptides, hydrocarbons),
- Gastrointestinal dysbacteriosis and absorption of toxic products caused by the condition,
- Increased intestine mucosal permeability, promoting the absorption of toxic byproducts as well as immunoreactions,
- Irritation of the intestinal mucosa,
- Disturbances of the enterohepatic circulation of bile acids,
- Abdominal complaints caused by prolonged transit time and increased gas formation (discomfort, distention, pains, defecation complaints).

These disturbances are traditionally treated, for example, by orally administered sodium bicarbonate by delivering it directly into the gastric lumen. However, it is important to note that the adverse effects (e.g., hypernatraemia, rarely metabolic and respiratory alkalosis, and respiratory acidosis) are negligible compared to the scope of the indication field of bicarbonate.

Bicarbonate and its metabolites (carbonic acid or carbon dioxide and water) within wide physiological ranges are not toxic elements in the vital processes.

In humans, bicarbonate is secreted by the pancreas, liver, and intestinal wall and is responsible for neutralizing gastric acid. However, neutralization occurs primarily in the duodenum and the upper part of the small intestine rather than in the gastric lumen under physiological circumstances. Due to the absolute or relative bicarbonate deficit developed in the duodenal lumen (as a consequence of transient or permanent deviations from a healthy lifestyle or functional disorders, gastrointestinal tract-related diseases, parenchymal injuries), the duodenum is subjected to an increased acid-load.

Oral bicarbonate intake in chronic kidney disease (CKD) patients with metabolic acidosis (not yet put on dialysis) slowed down the progression of GFR decline over five years, where a mechanism attributed to a decrease in endothelin-mediated renal injury is assumed. There was a link between low bicarbonate and increased endothelin and

aldosterone levels, which are considered to be pro-inflammatory mediators. It was revealed that the oral bicarbonate correction of the metabolic acidosis was associated with the reduction in the secretion of IL-10, which cytokine is a negative mediator in cancer immunity (81). In hypertensive nephropathy, daily sodium bicarbonate is an effective kidney protective adjunct to blood pressure control along with angiotensin-converting enzyme inhibition (82).

After peroral bicarbonate application, the nutritional status was significantly ameliorated to treat metabolic acidosis in peritoneal dialyzed patients (73).

Bases can have adverse effects, and the optimal serum bicarbonate concentration should be set between 22-24 mEq/L. The apparent volume of distribution of the administered bicarbonate is 50% of the body weight (in kilograms). The bicarbonate requirement can be calculated by the desired serum bicarbonate minus the actual serum bicarbonate concentration and the result being multiplied by half of the body weight (kg). The necessary base quantity can be administered over 3 to 4 days to treat metabolic acidosis; monitoring is required. Once the serum bicarbonate concentration reaches the desired level (24 mEq/L), the daily base quantity should be titrated to maintain the target (83). In moderate metabolic acidosis, it means 325 to 2000 mg orally 1 to 4 times a day for adults (over 18 years). One gram provides 11.9 mEq (mmol) each of sodium and bicarbonate.

The peroral rehydration solution for children can be prepared according to the following prescription (Sal ad rehydrationem cum natrio hydrogencarbonico pro parvulo).

Sal ad rehydrationem cum natrio hydrogencarbonico pro parvulo *FoNo VIII.*

<i>Natrii chloridum</i>	<i>0.9 g</i>
<i>Kalii chloridum</i>	<i>1.9 g</i>
<i>Natrii hydrogenocarbonas</i>	<i>2.5 g</i>
<i>Glucosum anhydricum</i>	<i>25.0 g</i>

The salts should be dissolved in 1000 mL water, and 50 mL/kg BW can be administered within 4 hours (in the case of a 5% kg BW decrease) perorally.

The base replacement needs to be more aggressive in chronic kidney disease patients suffering from disorders associated with base loss (e.g., profuse diarrhea) or generation of large acid loads (e.g., ketoacidosis). Sodium bicarbonate can be used with caution and a close monitoring of this patient's plasma electrolytes and bicarbonate is recommended in cases of the patient's renal dysfunction due to the risk of hypernatremia, electrolyte shifts, and systemic pH changes.

Bicarbonate ions are basically absorbed from the small intestines. The absorption mechanism is partially saturable (84).

A possible therapeutical requirement of bicarbonate is also warranted in other serious cases:

- chronic pancreatitis,
- extensive malignant and benign pancreatic tumors,
- autoimmune disorders of the pancreas or the liver, e.g., Sjögren syndrome,
- partial external (e.g., by malignant/benign tumorous compression, scars) or partial internal (e.g., stones, inflammation, parasites, mucus) occlusions of the efferent duct systems of the pancreas or liver
- abdominal surgical interventions (stomach, small intestine, pancreas, liver, or bile),
- hereditary pancreatic diseases (pancreatic cystic fibrosis)

1.1.7 CHALLENGES OF SODIUM BICARBONATE DELIVERY

The importance of bicarbonate in therapy is apparent; however, the dosage regimen of the active ingredient needs to be optimized. By the peroral use of sodium bicarbonate per se, the hydrochloric acid in the stomach immediately neutralizes the bicarbonate, carbon dioxide gas develops, causing tonicity and distension in the gastric wall. Along with an excess intake or an incorrect dosing regimen, over the flatulence and abdominal discomfort can occur in many cases, severe side effects (e.g., gastric wall rupture) were observed in the case of a tense stomach or higher doses (85). Using bicarbonate in a high dose in the stomach is contraindicated.

The gradual intake of bicarbonate can avoid the harmful side effects, which underlines the importance of formulating gradual release preparations.

From the pharmaceutical technology point of view, the per os formulation of sodium bicarbonate is challenging, as its dissolution in the gastric fluid needs to be controlled, the instant dissolution of bicarbonate be avoided.

To control the release of sodium bicarbonate or avoid side effects, various enterosolvent bicarbonate-containing compositions were developed. As a result, several preparations are on the market: Pancrecarb[®] *enteric-coated tablet*, (Digestive Care Inc., Pennsylvania USA) or Pertzye[®] *delayed-release capsules* with microspheres (Chiesi Inc., Cary, NC, USA) where bicarbonate serves as a buffer besides pancreatic enzymes.

Some preparations solely contain sodium bicarbonate: in the form of *enteric-coated tablets* (BicaNorm[®] tablets (Fresenius Medical Care Deutschland GmbH, Homburg, DE); and *oil-based soft gelatine capsules* (Nephrotrans[®], Medice Arzneimittel Pütter GmbH & Co. KG, Iserlohn, DE).

In vitro dissolution models of the release of the active agent from these compositions and other compositions were studied by Breitzkreutz et al. (86). Nephrotrans[®] is a hypromellose phthalate enteric-coated *soft gelatine capsule* containing bicarbonate in triglycerides, lecithin, sugar alcohols (sorbitol and mannitol). BicaNorm[®] tablets, where bicarbonate is formulated in a starch, microcrystalline cellulose, macrogol, polyvinylpyrrolidone core, a hypromellose subcoat, and Eudragit[®] L as an enteric layer. According to patients' complaints, the latter shows more adverse effects due to possible dose dumping.

The presently known compositions formulated with enterosolvent coatings (for example,

cellulose acetate, hydroxypropyl methylcellulose phthalate, carboxymethyl ethylcellulose, polyvinyl acetate phthalate, and polymethacrylate) resist the gastric acidic environment and start to release the active agent at near-neutral or higher pH values ($\text{pH} > 6$). Some of the pharmaceutical compositions presented in the literature release the active agent gradually when moving along in the increasing pH environment of the intestines. However, these compositions also reach their effect above pH 6. Accordingly, they cannot treat or prevent the harmful effects appearing in the duodenum and the initial region of the jejunum ($\text{pH} < 6$), such as digestive, functional, dyspeptic troubles, motility disorders, and mucosal irritation.

Studies have proved that enteric polymers, which in many cases carry acidic groups, may induce the instability of acid-sensitive drugs (omeprazole, bicarbonate) themselves when moisture is present (86).

2. OBJECTIVES

2.1 INVESTIGATION OF HYDROGEL-BASED SOLID MICROSPHERE FORMULATION

The research work focused on creating alginate hydrogel microparticles formed by electrostatic-vibration extrusion method and coacervation with different di- and trivalent cations. The hydrogels' morphology in relation to their production and the effect of surface-active tensides on the formulation process was of interest. The efficiency of the different di- and trivalent cations (Ca, Zn, Fe(II), Fe(III), Al, Bi-ions) was examined based on the determination of shape, size, and strength of the cation-alginate coacervate particles. Isomalt, a sugar-alcohol with a taste-masking effect, served as a structure-forming excipient in the freeze-drying process to solidify the particles. The aim was to observe the dried particles' morphology, porosity, reconstitution, and the swelling behavior of the particles at various media (difference in pH and osmotic pressure). The scope was to formulate microparticles with a pH-dependent swelling ability and drug release to formulate micron range particles capable of reconstituting as gel particles of different gel strength.

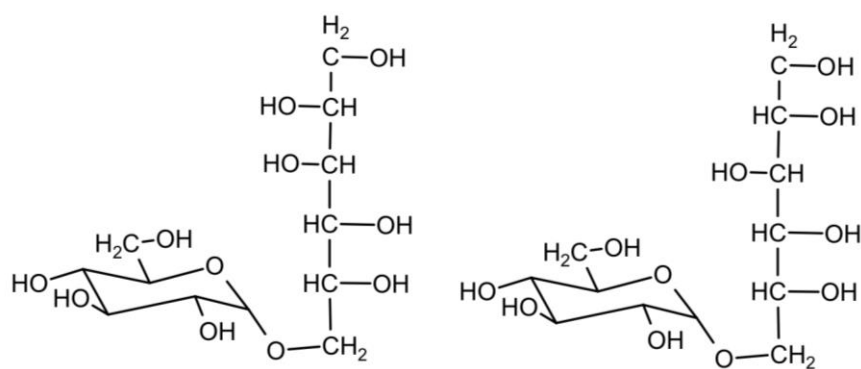
2.2 STUDY ON MULTIPARTICULATE PELLETS COATED WITH MULTILAYERED POLYMER SYSTEMS

The goal of the development concerns a pH-dependent gradual, sustained release multiparticulate pharmaceutical composition that resists the highly acidic environment of the stomach; however, it increases the pH in the upper part of the small intestine. The release of bicarbonate is planned a gradual and sustained release in an acidic environment while moving on mixed with the intestinal content, increasing the pH of the acidified parts of the intestines. The multilayer polymer coating of a specific structure on the surface of the particles ensures the gradual release of the active agent in the range of pH 4.5 to 5.5. The aim of the special coating is to prevent the excess alkali load in the stomach, and thus, the active ingredient can exert its gastric acid neutralizing activity in the duodenum. The bicarbonate deficit can be alleviated right in the duodenal lumen. The release of sodium bicarbonate mimicking ideal physiological conditions can be an advantage in treating several health disorders.

3. MATERIALS AND METHODS

3.1 MATERIALS

Alginic acid sodium salt, medium viscosity (Merck[®] Life Science KGaA, Darmstadt, Germany-previously Sigma-Aldrich[®]), galenIQ[™] 800 isomalt (Beneo Palatinit GmbH, Mannheim, Germany) (Fig. 11),



α -D-glucopyranosil-mannitol

α -D-glucopyranosil-sorbitol

Figure 11. Chemical structure of Isomaltose units

Calcium chloride, Polysorbate 80, Potassium dihydrogenphosphate, Sodium hydroxide, Sodium Chloride, Zinc sulphate, Hydrochloric acid, Bismuth subnitrate, Sodium hydroxide, Magnesium chloride, Iron (II) chloride tetrahydrate, Iron (III) chloride, Aluminium chloride, Glucose were purchased from Molar Chemicals and were of analytical grade. Microcrystalline cellulose (Comprecel[®] M101, Mingtai Chemical Co., Taoyuan City, Taiwan) is of fine particles (45-75 μ m particle diameter) and is suitable for direct compression and for wet granulation and spheronisation with a relatively low flowability. The polymers used for coating of the particles are listed in Table V. and were provided by Evonik Industries AG, (previously Röhm-Degussa GmbH), Darmstadt, Germany and Shin-Etsu Chemical Co., Tokyo, Japan. The excipients applied for the coating procedures are listed below (Table VI.)

Table V. Polymers used in micropellet coating process (own schemes based on (87))

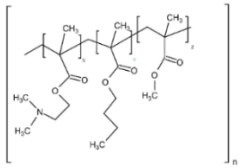
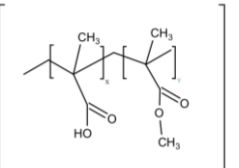
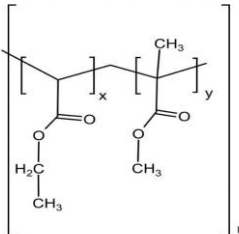
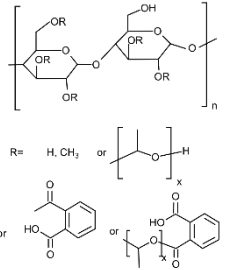
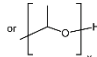
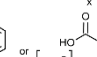
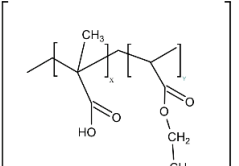
<i>Polymer</i>	<i>Chemical name (Ph. Eur.)</i>	<i>Formula</i>	<i>Solubility</i>	<i>MFT (°C)</i>
Eudragit® E (Evonik GmbH)	Amino Methacrylate Copolymer Aminoalkyl Methacrylate Copolymer E	 <p>x:y:z=2:1:1 (molar ratio)</p>	pH<5	45
Eudragit® L (Evonik GmbH)	Methacrylic Acid and Methacrylate Copolymer	 <p>x:y =1:1 (molar ratio)</p>	pH>6.0	25
Eudragit® NE 30D (Evonik GmbH)	Ethyl Acrylate Methyl Methacrylate Copolymer	 <p>x:y=2:1 (molar ratio)</p>	not soluble, but permeable	5
HPMCP-50 (Shin-Etsu Chemical Co.)	Hydroxypropylmethylcellulose phthalate	 <p>R= H, CH₃ or  or </p>	pH>5 (4.5)	143 (88)
Eudragit® L 100-55 (Evonik GmbH)	Methacrylic Acid and Ethylacrylate Copolymer	 <p>x:y =1:1 (molar ratio)</p>	pH>5.5	111

Table VI. Additives used in polymer coating dispersions and solutions

<i>Excipient</i>	<i>Function</i>	<i>Distributor</i>
Triethyl citrate	plasticizer	Fluka [®] Chemicals
Sodium lauryl sulfate	emulsifier	Molar Chemicals Ltd.
Dimethicone	anti-foaming agent	Sigma-Aldrich [®] (Merck Life Science)
Ammonia solution	pH-correction	Molar Chemicals Ltd.
Micronized talc (<10 μm)	anti-tacking agent	Sigma-Aldrich [®] (Merck Life Science)
Stearic acid	anti-tacking agent, emulsifier	Molar Chemicals Ltd.

SODIUM HYDROGEN CARBONATE

(Sodium bicarbonate, Natrii hydrogencarbonas Ph. Hg. VIII.), E 500

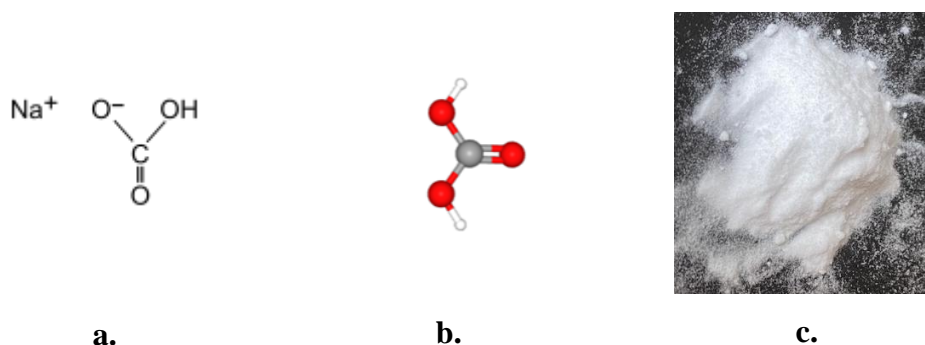


Figure 12. a.) 2D, b.) 3D structure of NaHCO₃ c.) physical appearance (90)

Sodium bicarbonate ($M_w = 84.007$ g/Mol) is a white, crystalline, odorless powder with a slightly salty alkaline taste and high water solubility (10.3 g/100 g) at 25 °C, and practically no solubility in alcohol (89). Freshly prepared 0.1 molar aqueous solution has a pH of 8.6 at 25°C. The pH of the saturated solution is 8-9. It decomposes at approximately $\geq 50^\circ\text{C}$ and is gently abrasive (Mohs' hardness: 2.5) (90). In nature, it occurs in saliferous soil or some alkaline lake's water (in Hungary Fertő-tó, Velencei-tó, Fehér-tó in Szeged or Szelidi-tó count to this group with a pH > 9 and of great balneological significance.

Nahcolite, the monocline crystal of NaHCO₃, is also found single or accompanied by its relative compounds: sodium carbonate (Na₂CO₃) and trona, e.g., sodium sesquicarbonate (NaHCO₃, Na₂CO₃·2H₂O) and can be mined from Eocene-age deposits from several parts of the world (Botswana, Colorado, Mexico).

However, sodium bicarbonate is usually produced by synthesis. In the *Solvay process*, ammonia and CO₂ gases are introduced into saturated sodium chloride solution (brine) under pressure. As sodium bicarbonate has a lower solubility in water than the reaction components, it precipitates and can be filtered from the solution.



In the presence of mild acids, a moist environment, or heat (≥ 50 °C), decomposition occurs, carbon dioxide is released, contributing to the multivarious use of this salt. NaHCO₃ decomposes to Na₂CO₃ gradually in both a solid form or a solution when warmed (Ph. Hg. VIII.).

3.2 PHARMACEUTICAL TECHNOLOGICAL PROCESSING METHODS OF SAMPLE FORMULATIONS

3.2.1 PREPARATION OF MICROSPHERES

3.2.1.1 COACERVATION OF MICROSPHERES

Vibrating technology on Büchi B-390 Encapsulator (Büchi Labortechnik AG, Flawil, Switzerland) apparatus was used for the production of microcapsules and microspheres. During this process, vibrational frequency breaks up the laminar jet of the polymer to form small liquid drops. These fall into the polymerization liquid (200 ml 0.1 M CaCl₂) separated thanks to the electrostatic repulsion on their surface the adjustable voltage sets.

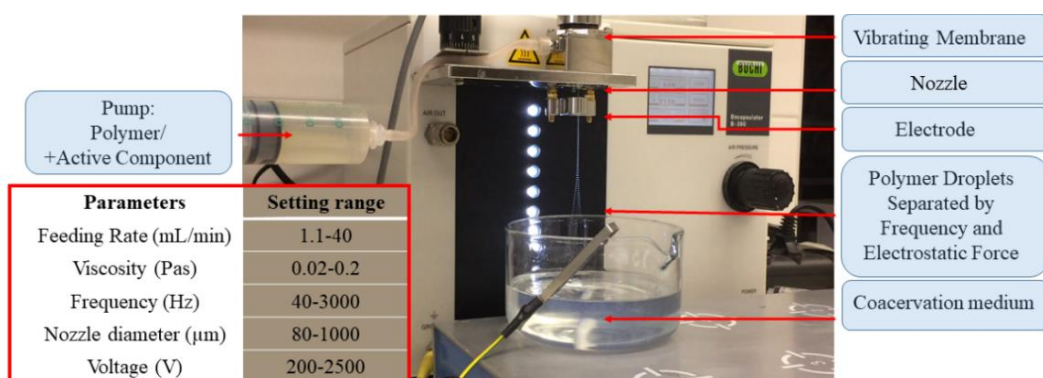


Figure 13. The influential constituents' and setting parameters of coacervation-phase separation microencapsulation process (*Büchi B-390 Encapsulator; own photo*)

Numerous parameters influence the droplet formation and the size and character of the particles: the nozzle diameter, the feeding rate of polymer, the frequency of vibration, the voltage administered, the concentration and type of excipients applied, the distance of nozzle and coacervation bath (Fig.13).

Among process parameters, feeding rate (100, 300, 450, 600 ml/min), frequency (500, 1000, 1500 Hz), voltage were studied for 0.5% and 2% alginate concentration in the preparation of alginate and alginate-isomalt microspheres using nozzle diameters (150, 300 and 450 µm). The volume of the coacervation medium and the distance of the nozzle from the liquid were kept constant at 0.12 m.

To determine the effect of surface-active ingredient use on the gel particle formation,

Polysorbate was administered in the core material of the spheres or the immersion liquid in the indicated concentrations to reach a spherical shape of the gel particles.

During the formulation studies different coacervation medium were applied: calcium chloride (CaCl_2), zincum sulphate (ZnSO_4), iron (II) sulphate (FeSO_4), iron (III) sulphate ($\text{Fe}_2(\text{SO}_4)_3$), bismuth nitrate ($\text{Bi}(\text{NO}_3)_3$), and aluminium hydroxide ($\text{Al}(\text{OH})_3$) solutions in the concentration of 0.05; 0.1; 0.15; 0.25 M for different time periods. The gel particles were produced and coacervated for the following time periods: 1 min, 5 min, 10 min, 15 min, 30 min, 45 min, 60 min, 90 min, 120 min, 180 min. The texture tests were performed directly after taking out the samples from the coacervating medium.

To study the effect of isomalt, dripping with extrusion through a nozzle with an orifice of 450 μm was used.

3.2.1.2 FREEZE-DRYING

The spherical microgel particles were solidified by lyophilization (Scanvac Coolsafe 110-04 cryosiccator LaboGene™, Lyngø, Denmark) with the following parameters: shelf temp.: -40 °C to + 40 °C, sample temp: -40 °C to + 20 °C, vacuum: 2 hPa-0.02 hPa; 24 hr process time. 20 w/w% of isomalt (GalenIQ® 800) served as a cryoprotectant.

3.2.2 PREPARATION OF MICROPELLETS

3.2.2.1 PELLETIZING OF BICARBONATE-CONTAINING CORES

The core is created by solid, granulated sodium bicarbonate matrix particles with microcrystalline cellulose (Comprecel® 101, Mingtai Chemical, Taiwan) of various ratios, of which 80% sodium bicarbonate to 20% microcrystalline cellulose was the maximum sodium bicarbonate content that proved to be successful in particle forming. The cores are provided with a gastro-resistant pH-dependent soluble coating having a layered structure.

The particles were formed with high shear aggregation and a concomitant spheronization process. As sodium bicarbonate has practically no solubility in alcohol (Ph. Hg. VIII.), beads were initially prepared with the binder Kollidon® VA64 (10% w/w) in an alcoholic solution (Ethanol 96%). The mixing and granulation processes were made in a Stephan UMC 5 electronic mixer (Stephan Machinery GmbH, Hameln, Germany). The homogenization of the 300 g batch of the sieved (0.8 mm) powder mixture took 5 minutes

at 500 rpm and the wetting process was done at 900 rpm. The binder solution (130 g) was sprayed on by using a 2-mm nozzle, an air compressor (Balma LT50, Balma International, Torino, Italy) at 1.2 bar, and a peristaltic pump (Peripump D, KUTESZ, Hungary) with a feeding rate of 12.5 g/min. After the complete wetting an additional core forming was proceeded at 1000 rpm, 15 min. The particles were dried in a drying chamber layered on trays in an approximately 1-cm-thick layer (40 °C, 24 h).

An aqueous granulation process was also developed to reduce alcohol consumption and optimize production. The mixing and granulation processes were made in a Diosna V25 (Dierks und Söhne GmbH, Osnabrück, Germany) high-shear granulator, the batch size was 2700 g. Table VII. summarizes the parameters of the aqueous granulation process.

Table VII. The process parameters of particle formation of sodium bicarbonate

<i>Process</i>	<i>Rate</i>	<i>Granulation liquid (g)</i>	<i>Process time (min)</i>
Homogenization	Mixer set I. (180 rpm)	-	10
Wetting	Mixer set I. (180 rpm)	700	10
Kneading	Mixer set II. (360 rpm)	310	20
Bead formation (chopping)	Chopper (1400 rpm)	-	5

To smoothen the surfaces, the wet particles were spheronized in a spheronizer (GSZF-AK 200 Spheronizer, Locost Kft., Hungary) in smaller sub-batches of 200 g. Spheronisation parameters: 50 Hz, 2 min (Fig. 14).



Figure 14. a.) Spheroniser disc surface b.) wet spheronised micropellet particles

Particles were settled on drying plates and dried in a drying chamber (Kutesz, Hungary) at 40 °C for 24 hours. Final moisture content was determined by Scaltec SMO01, 60°C, 0-100%. The particle size was characterized by a sieve (Retsch AS200) with the following settings: 100 g sample, amplitude: 1.5 mm, time: 10 min, 2.0; 1.4; 1.25; 1.00; 0.8; 0.63; 0.5; 0.16 mm sieves). The sodium bicarbonate content was controlled by titration with 1 M HCl with methyl orange indicator (Ph. Hg. VIII. 01/2002:0195).

3.2.2.2 COATING PROCESS

The development work was challenging and during the work, many commercially available compositions were tested, which are generally used for obtaining modified-release or protection of bicarbonate core from the acidic components of release-modifying polymers (PVA, Shellac, HPMC of different producers and compositions). The development work proved that the special needs set up concerning the particles' behavior in the GIT can be provided with a unique combination of coating layers. This section describes the compositions which finally proved to be effective in meeting the special requirements.

The modifying coating layer was added in four consecutive steps in an Aeromatic STREA-I Apparatus (Aeromatic, Niro, Germany) with a bottom-spray Wurster method, using a 0.8 mm nozzle in an air-conditioned room (20 °C). The compositions and roles of the layers are detailed below (Tables VIII-XII.); the process parameters are summarized in Table XIII.

During the coating process, the coating layer providing a unique effect was applied in multiple layers. The layers are marked 'a, A, B, C, D'. As a result, particles coated with 'aABC' and 'aABD' layer combinations were formulated.

Coating layer 'a':

The function of the layer is caused by poly [butyl methacrylate, (2-dimethylaminoethyl) methacrylate, methyl methacrylate 1:2:1] polymer (Eudragit® E PO).

Table VIII. Composition of layer 'a'

<i>Composition</i>	<i>Quantity (g)</i>
Eudragit® E PO	25.5
sodium lauryl sulfate	2.4
stearic acid	3.9
micronized talc	12.9
distilled water	255.3

Preparation of the dispersion: With the exception of micronized talc, all components were dispersed with an Art-Micra laboratory homogenizer (Falc Instruments, S.r.L.) at 19,000 rpm, then dispersed for 5 minutes after the addition of talc, made up with water and stirred for 30 minutes (magnet stirrer 50 rpm). The dispersion was passed through a 100 µm sieve before use.

Batch size: 250.0 g. Application of coating dispersion: 147 g dispersion, 5% polymer concentration, theoretical weight increase: 21.9 g.

Coating layer 'A'

The gastro-resistant function is due to enteric Poly[methacrylic acid, methyl methacrylate 1:1] polymer (Eudragit® L100). The polymer coating is soluble at or above pH 6.

Table IX. Composition of layer 'A'

<i>Composition</i>	<i>Quantity (g)</i>
Eudragit® L 100	30.0
NH₃ (1N)	16.8
triethyl citrate	15.0
micronized talc	15.0
distilled water	225.0

Preparation of the dispersion: The talc was dispersed in 50 g of water in small portions. The ammonia solution was diluted in 50 g of water, the polymer was added in a thin jet, the mixture was stirred for 15 minutes. Then the dispersion was mixed with it and stirred

for further 15 minutes. The plasticizer (TEC) was also added and stirred at least for 30 minutes. The suspension was passed through a 100 µm sieve before use.

Batch size: 250.0 g. Coating dispersion application: 251 g, 10% polymer application, theoretical weight increase: 50.2 g.

Coating layer 'B'

Poly[Ethyl Acrylate, Methyl Methacrylate 2:1] (Eudragit® NE 30D) provides the formula retard release in a pH-independent manner.

Table X. Composition of layer 'B'

<i>Composition</i>	<i>Quantity (g)</i>
Eudragit® NE 30D	90.0
micronized talc	12.0
distilled water	90.0

Preparation of the dispersion: The talc is dispersed in small portions in half the prescribed amount of water, and after the addition of the polymer dispersion filled up with distilled water and stirred up to 30 minutes. The dispersion is passed through a 100 µm sieve before use.

Batch size: 250.0 g. Consumption: 160 g dispersion, 10% polymer application, theoretical weight increase: 32.5 g.

As this layer requires a certain curing to perform its *lege artis* efficacy, but becomes very sticky at higher temperatures, 0.1 % colloidal silicon dioxide (Aerosil 200, Evonik GmbH) was added after the coating layer was dried and before 24 h curing was started.

Coating layer 'C'

The anionic polymer, hydroxypropylmethylcellulose phtalate (HPMCP-50) provides a release starting at pH 4.5-5.0 in the duodenal lumen.

Table XI. Composition of layer 'C'

<i>Composition</i>	<i>Quantity (g)</i>
HPMCP 50	14.0
triethyl citrate	6.0
Polysorbate 80	0.06
dimethicone	0.2
distilled water	ad 200.0

Preparation of dispersion: Polysorbate 80, TEC, dimethicone are added to the polymer dispersion with continuous stirring, water is added and the dispersion mixed for 30 minutes.

Batch size: 250.0 g. Coating dispersion consumption: 178.5 g dispersion, 5% polymer application, weight increase: 18.1 g.

Composition of Coating'D'

Anionic Poly[Methacrylic Acid, Ethyl Acrylate] 1:1 (Eudragit® L30D55) provides the particles a release starting at pH ≥ 5.5 in the duodenal lumen.

Table XII. Composition of layer 'D'

<i>Composition</i>	<i>Quantity (g)</i>
Eudragit® L30D55	100.0
triethyl citrate (TEC)	12.0
Polysorbate 80	0.12
dimethicone	0.4
distilled water	ad 400.0

Preparation of dispersion: Polysorbate 80, TEC, dimethicone are added to the polymer dispersion under continuous stirring (magnet stirrer 100 rpm); water is added and mixed for 15 minutes.

Batch size: 250.0 g. Quantity of dispersion applied: 330 g, 10% polymer, theoretical weight increase: 35.1 g.

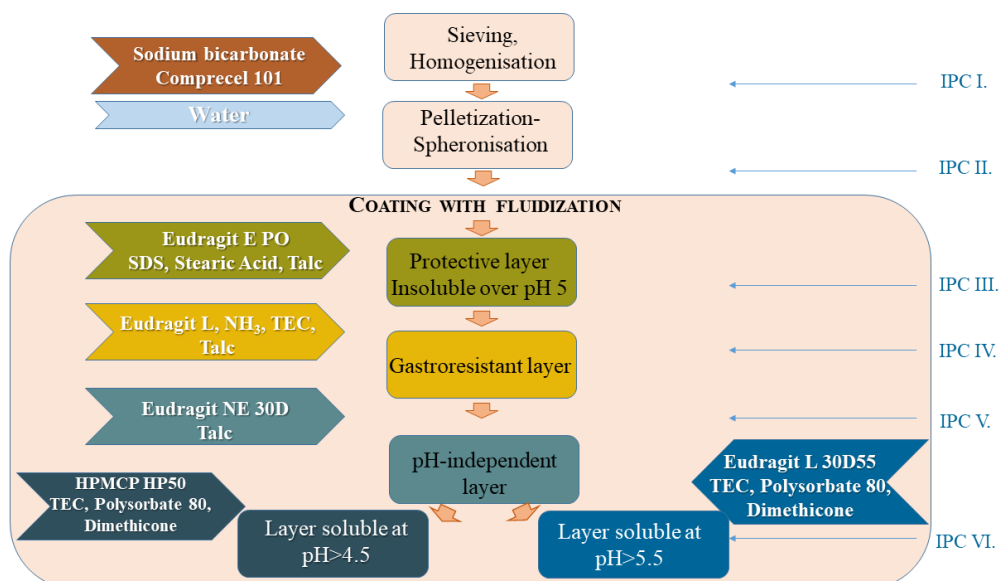


Figure 15. The process of pellet preparation and the possible steps of in-process control

There are several steps where IPC tests can be included in the production to control the quality of pellets: IPC-I.: a test of homogeneity during mixing, IPC-II. the size and loss on drying determination, IPC III-VI. test of the sufficient coating thickness. The quality controls can be maintained by classic methods or continuously by NIR or Raman spectroscopy (Fig. 15).

Table XIII. The process parameters of coating by fluidization in Aeromatic Strea-I. Apparatus.

<i>Parameters</i>	<i>Units</i>	<i>Coating 'a'</i>	<i>Coating 'A'</i>	<i>Coating 'B'</i>	<i>Coating 'C'</i>	<i>Coating 'D'</i>
Set coating temp.	(°C)	50	45	10	25	25
Inlet air	(°C)	50±2	45±2	34±2	29±2	29±2
Outlet air	(°C)	45±2	39±2	29±2	25±2	25±2
Atomizing pressure	(bar)	1	1.2	1.0	1.2	1.2
Feeding rate	(ml/min)	2.2	2.6	3	1.5-2.4	1.5-2.2
Fluid.air volume rate	(m ³ /h)	100	100	90	100	100

3.3 METHODS FOR CHARACTERIZATION

3.3.1 PARTICLE SIZE ANALYSIS WITH LASER DIFFRACTION

The size distribution of particles was measured with Mastersizer 2000 (Malvern Instruments Ltd., Malvern, England). Hydro SM 2000 Dispersion Unit (Malvern Instruments Ltd., Malvern, England) at 1500 rpm provided that the samples were homogeneously introduced to the measuring cell. Span-value and $d_{v,0.9}$ are the parameters we chose to compare the results. Span-value demonstrated the size distribution and was calculated based on the following equation:

$$\text{Span} = \frac{d_{v,0.9} - d_{v,0.1}}{d_{v,0.5}} \quad (4)$$

90% of the particles are under the diameter $d_{v,0.9}$; 10 % of the particles are under the diameter $d_{v,0.1}$, and 50% are under the diameter $d_{v,0.5}$.

3.3.2 PARTICLE ANALYSIS WITH MICROSCOPIC IMAGE ANALYSIS

Digital Image Analysis of pictures taken by Nikon Coolpix 450 camera (Nikon Imaging, Tokyo, Japan) on a Nikon SMZ 1000 microscope (Nikon Corp. Tokyo, Japan) evaluated the particle size distribution and swelling. Both wet and solid samples were tested (50 particles per batch). The shape and size were characterized by the *roundness*, *aspect ratio (AR)*, and *the Feret-diameter, d_{eq}* calculated by ImageJ software (NIH Image, USA). *Roundness (R)* was calculated as

$$R = \frac{P^2}{4\pi A} \quad (5)$$

P is the perimeter, A is the projection area

$$AR = \frac{D_{max}}{D_o} \quad (6)$$

D_o is the longest orthogonal diameter perpendicular to D_{max} . d_{eq} was calculated by the area based on the equivalent area of 2-dimensional objects and spherical particles.

3.3.3 RECONSTITUTION

The microparticles were reconstituted in relevant media: Pharmacopoeial pH 1.2 hydrochloric acid; and pH 4.5 and 6.8 phosphate buffers (Ph. Eur.) and the osmotic pressure (250 mosmol/l and 1250 mosmol/l) were made by using sodium chloride and glucose in demineralized water to observe the effect of ions or osmotic active sugars. The samples were tested in a 50-ml beaker stirred with a magnetic bar at 50 rpm for 45 min. The images of swollen particles were taken and analyzed as in Section 3.3.2. Swelling index (S%) was calculated by the swollen particle diameter (d_s) and the initial particle diameter before reconstitution (d_i) as follows

$$S(\%) = \frac{d_s - d_i}{d_i} * 100 \quad (7)$$

3.3.4 MICRO-COMPUTED TOMOGRAPHY

The freeze-dried samples were scanned using a microcomputed tomography scanner (Skyscan 1172 X-ray microtomography, Bruker μ CT, Kontich, Belgium) at a resolution of 4.86 μ m isometric voxel size (70 kV, 124 μ A). The average scan duration was 25 min. After the acquisition, raw images were reconstructed by using NRecon software (v.1.7.1.6., Bruker μ CT, Kontich, Belgium). Ring artifact correction was 10, and the beam hardening correction was 61%. The morphometric variables relevant to our study were calculated by CTAn software (v.1.17.7.2, Bruker μ CT, Kontich, Belgium).

3.3.5 SCANNING ELECTRON MICROSCOPY (SEM)

Scanning electron microscopy (SEM) makes it possible to compare the microsphere surface morphology, especially the microparticles' characteristics with and without isomalt content. Dried samples were fixed on carbon adhesive tape (Structure Probe Inc., West Chester, PA, USA), gold-coated, and examined in a Hitachi 2360 N (Hitachi Ltd., Tokyo, Japan) scanning electron microscope at 220 \times to 1500 \times magnification with 15 kV, 30 kV electron beam accelerating voltage.

3.3.6 MICROGEL HARDNESS TEST BY TEXTURE ANALYZER

Hardness is the resistance of solid materials against permanent shape changes after applying a compressing force. The production of 1.5% alginate solution in the case of all acceptor liquids was found to be: 300 μm nozzle, 330 ml/h feeding rate, 350 Hz frequency, 2350 V, 12 cm distance from the coacervation liquid (0.15 M).

The hardness of the microspheres gelled in various coacervation media (CaCl_2 , ZnSO_4 , FeSO_4 , $\text{Fe}_2(\text{SO}_4)_3$, $\text{Bi}(\text{NO}_3)_3$, $\text{Al}(\text{OH})_3$ solutions) in the indicated concentration (0.15 M) was tested by Brookfield CT3 Texture Analyzer (Brookfield Engineering Labs, AMETEK, MA, USA). The six parallel measurements were performed on wet microgel particles selected randomly from the coacervation medium and set on the analyzer plate. The test gauge (TA39) of a diameter of 2.0 mm was lowered by a rate of 0.5 mm/s to a target of 1 mm and a trigger load of 0.05 N (Fig. 16).

Compression curves were registered; hardness, compression work and fracturability were determined by the Software Texture Pro CT.

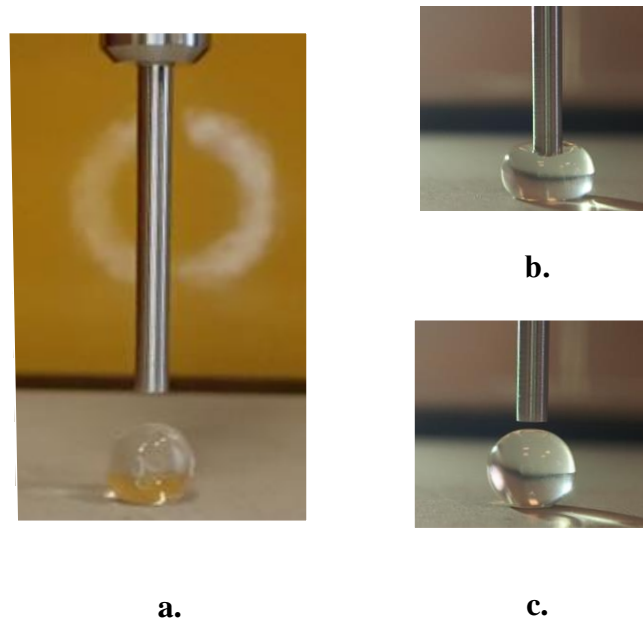


Figure 16. Compression of gel particles by Brookfield CT3 Texture Analyzer

a.) initial stage, **b.)** compression with predefined parameters

c.) gel particle post-compression

3.3.7 IN VITRO DRUG RELEASE- SODIUM RELEASE FROM SODIUM BICARBONATE PELLETS

Dissolution experiments were carried out using the standard rotating basket method according to the Hungarian Pharmacopoeia (Ph. Hg. VIII.) in 900 ml, pH 3.0 (Ph. Hg. VIII.) hydrochloric acid, and pH 4.5 and pH 5.5 phosphate buffer solutions (Ph. Hg. VIII.), on 37 ± 0.5 °C, at a mixing speed of 100 rpm. In the experiments, the sample size was determined according to the calculated expected sodium bicarbonate content of ~ 1.0 g. The pH change was registered using Microprocessor pH Meter pH 210 (Hanna Instruments, Woonsocket, US). The measuring precision of the device is ± 0.01 pH value. Test times were: 0, 5, 10, 15, 30, 45, 60, 90, 120, 150, 180, 240 minutes.

The sodium content was determined by flame photometry.

The values were plotted as an average of the measures values (number of samples, and SD was indicated in the legends.

The statistical differences among groups was performed with Student's *t-test*, significant differences are indicated in the legends.

3.3.8 FOURIER TRANSFORMATION INFRARED SPECTROSCOPY (FT-IR)

Physicochemical properties of pellet coatings were examined using Jasco FT/IR-4200 spectrophotometer (Jasco Products Company, Oklahoma City, OK, USA), which was equipped with Jasco ATR PRO470-H single reflection accessory. The measurements were performed in absorbance mode. The spectra were collected over a wavenumber range of 4000 and 500 cm^{-1} . After 50 scans, the measurements were evaluated with the Spectra Manager-II Software (Jasco).

4. RESULTS

4.1 MULTIPARTICULATE MICROSPHERE SYSTEM: INVESTIGATION OF PROCESS PARAMETERS OF MICROSPHERE PARTICLE FORMATION BY VIBRATION-EXTRUSION

4.1.1 THE EFFECT OF SURFACE-ACTIVE AGENT ON THE FORMATION OF MICROSPHERES

The observations accord with the cited studies: the right frequency, feeding rate, and voltage set enable the production of spherical particles, even at relatively low alginate concentrations. Previous studies noted that the particle size of gel beads is double of the nozzle diameter when using 1.5-2% alginate concentrations (14).

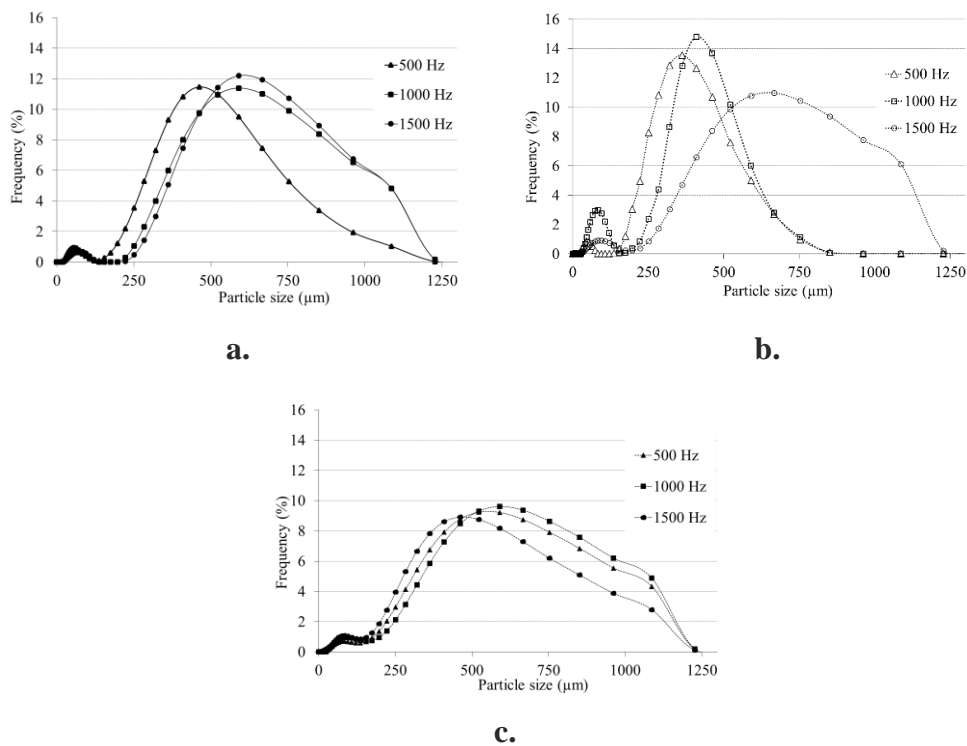


Figure 17. Effect of feeding rate and frequency change on microsphere formation, the size of microgel beads were determined by Mastersizer 2000 (Malvern Panalytical Ltd., UK) at various parameters: feeding rate **a.)** 300 ml/h; **b.)** 400 ml/h; **c.)** 600 ml/h and various Hz (300 μm nozzle, 0.5% alginate, 0.15 M CaCl₂, 1% Polysorbate 80 in alginate) (n=3, SD<0.05)

Our experiments proved that using lower alginate concentrations (0.5%), the sphere-size approximates the scale size (diameter) of the orifice with correct settings. With particular frequency settings, however, the particle size distribution proved to be broad (Fig. 17).

The effect of surface-active agents on the droplet formation of liquids is well-known, the role of the same group of excipients on the morphological characteristics of microsphere gels needs further examination.

The laser-diffractometric measurements proved that by using 0.5% sodium alginate solution the feeding rate of 400 ml/h resulted in a relatively high monodispersity (and low Span values) with the lowest particle size (distribution shown on Fig.17).

The addition of 0.25-1.00% Polysorbate 80 to the sodium alginate solution did not significantly influence the particle size and the Span value (indicating the particle size distribution), however, the frequency of vibration had a visible effect (Fig. 18).

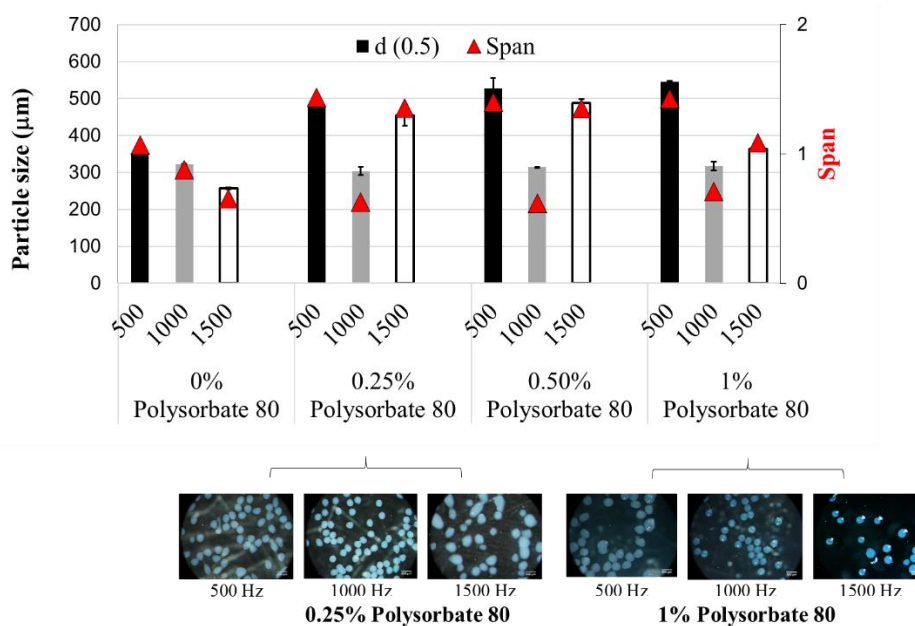


Figure 18. Effect of Polysorbate (Tween) 80 addition and process parameters on microsphere size(columns) and size distribution (indicated by markers-Span values) by vibrational nozzle method by Image analysis (0.5% alginate, 300 µm nozzle, 400 ml/h feeding rate, CaCl₂ medium, tenside added to microsphere base material) (n=50)

The results of laser diffractometric size determination were explained by image analysis. (Images on Fig 18.) The acquired data confirmed that the feeding rate and the applied frequency observably affect the shape and size of processed microspheres (*Table XIV*).

Table XIV. Morphological parameters of microspheres constructed from 0.5% alginate solution with 1% Polysorbate 80 in 0.1 M CaCl₂ and 1% Polysorbate 80 in 0.5 % alginate solution (n=50)

		<i>Process parameters</i>		<i>Shape and Size Parameters</i>			
		<i>Feed. rate (ml/h)</i>	<i>Vibration frequency (Hz)</i>	<i>Roundness</i>		<i>AR</i>	<i>Span</i>
			<i>Mean</i>	<i>SD</i>	<i>Mean</i>	<i>SD</i>	
1% Polysorbate 80 in 0.1 M CaCl₂	300	500	0.91	0.06	1.10	0.09	0.73
		1000	0.93	0.02	1.08	0.04	1.01
		1500	0.92	0.05	1.09	0.06	1.09
	400	500	0.82	0.07	1.23	0.10	0.78
		1000	0.91	0.07	1.11	0.10	1.22
		1500	0.93	0.04	1.08	0.05	1.25
	600	500	0.79	0.11	1.29	0.21	1.06
		1000	0.80	0.11	1.29	0.30	1.57
		1500	0.83	0.08	1.22	0.12	1.47
1% Polysorbate 80 in 0.5 % alginate solution	300	500	0.84	0.15	1.23	0.31	1.28
		1000	0.83	0.16	1.26	0.32	0.90
		1500	0.97	0.01	0.90	0.08	1.16
	400	500	0.85	0.06	1.18	0.09	1.50
		1000	0.93	0.03	1.08	0.04	0.94
		1500	0.91	0.06	1.11	0.07	1.23
	600	500	0.78	0.09	1.28	0.13	1.38
		1000	0.82	0.10	1.24	0.82	1.57
		1500	0.90	0.07	1.12	0.09	1.47

The roundness data made it evident that the particles' shape is deformed, impacting particle size measured by the laser diffraction method. At high feeding rate, the improper separation of the liquid flow may lead to elongated particles. The incorrect frequency setting may result in a wide particle size distribution due to the formation of satellite drops. The combination of low feeding rate with high-frequency results in particle size increase because of particles' aggregates thanks to the improper droplet forming, i.e., post-droplet-forming and coalescence. High feeding rate and low frequency cause dumbbell-shaped particles with a high aspect ratio (AR), as the low frequency cannot separate the alginate flow into isolated droplets.

The application of Polysorbate (Tween) 80 in the coacervation medium or in the alginate solution can influence the particle formation and the shape of the gel particles. (Table XIV).

In concordance with the literature: at low frequency, surface tension decrease causes the production of different size droplets, where small satellites tear down from the tip of the nozzle at low feeding rate and formation of doublets due to coalescence at higher feeding rates can be observed (15). However, at a 1% concentration of Polysorbate the influence of higher frequency on the size character has a lower impact. Chan et al. [14] present the shape-forming effects in the extrusion-dripping method in detail. They established that the surface tension of alginate solutions decreases with elevating concentration, while the viscosity increases. These factors play an essential role in the shape of coacervated gel drops. It was pointed out that critical viscosity is 60-150 cP; below this, no spherical particles can be formed (91) as low viscosity droplets are less able to retain their spherical shape in the coacervation bath due to the more significant disrupting effect of the CaCl_2 solution at the collision. The surface-active role of Polysorbate 80 and the higher viscosity of the 1% solution are antagonistic in creating particles. The addition of 0.25; 0.5; 1% Polysorbate 80 to the 0.5% sodium alginate solution decreases the initial 52.33 mN/m surface activity to 38.29; 37.41; 36.77 mN/m, respectively. The low viscosity of the 0.5% sodium alginate solution (0.0167 Pas), however, increases to 0.082; 0.099; 0.1045 Pas, by the addition of 0.25; 0.5; 1% Polysorbate 80, respectively.

However, the beads take an irregular shape at higher flow rates (600 ml/h). The image

analysis results confirm that roundness showed the highest difference from 1.0 for the samples produced with 600 ml/min and 1000 Hz. The aspect ratio, in this case, was higher, indicating ellipsoid-like particles. The feeding rate of 600 ml/h was too high for a solution of such a high viscosity to build up uniform, separated droplets with a low frequency. The increase in vibration frequency can help this difficulty. The frequency increase was propitious even at the same feeding rate for creating more spherical particles (increase in roundness and decrease in AR). Decreasing Span values confirms the more balanced generation of particles. In combination with a high feeding rate, the elevated frequency leads to broader size distribution due to the generation of smaller satellite drops.

4.1.2 EFFECT OF ISOMALT ON THE FORMATION OF MICROSPHERES

Considering the particle shape parameters (roundness, Feret diameter, the aspect ratio, and the particle size and distribution, the feeding rate of 400 ml/h with 1000 Hz and 1% Polysorbate 80 in addition to the coacervation medium was found optimal. These parameters were used to create microspheres with isomalt. The application of isomalt aims to increase the sphericity of the solid particles (thus ameliorating the flow characteristics of the solid spheres without a significant effect on the swelling ability of the particles). The addition of 1% Polysorbatum 80 did not cause size reduction and an increase in the roundness of the gel particles, either (Fig. 19).

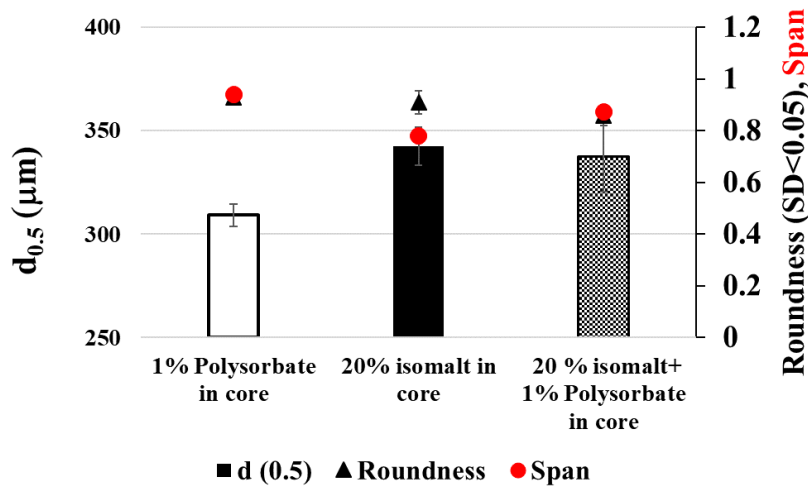


Figure 19. Isomalt and Polysorbate effect on the size (columns- $d_{0.5}$), size distribution (red dashed line-Span) and shape (black line- Roundness) of 0.5% alginate microspheres (300 μm nozzle, 400 ml/h feeding rate, 1000 Hz $n=50$, $SD < 0.05$)

4.1.3 EFFECT OF FREEZE-DRYING ON MICROGEL PARTICLES

4.1.3.1 STRUCTURE AND MORPHOLOGY

The size decrease of calcium alginate microbeads due to drying depends on the drying method (92). Due to the slow evaporation of water, the shrinking in air-dried particles proved to be greater than in freeze-dried ones, and the structure change is significant. Shrinking affects the shape, size, internal and surface texture, and integrity of particles. The shrinkage is more significant in the case of air-dried particles and also depends on the alginate concentration. 52.2 % shrinkage was detected in the case of 2 % alginate due to cryosiccation.

The freeze-dried samples' structure was most porous; the greater surface presumes a quicker reconstitution and faster drug release. The drying process causes a loss in the sphericity due to strain-relaxation processes upon drying (93).

The sphericity in dried particles with low alginate concentrations is lower than in the case of spheres prepared from more concentrated alginate solutions, but the sphericity can be further ameliorated by the addition of cryoprotectants (Fig. 20). A study presents the effect of different grades of isomalt in freeze-drying (94). Crystalline isomalt transformed into an amorphous form during freeze-drying and was found to maintain good physicochemical stability in stabilizing proteins at various temperatures and relative humidity by Koskinen et al. (95).

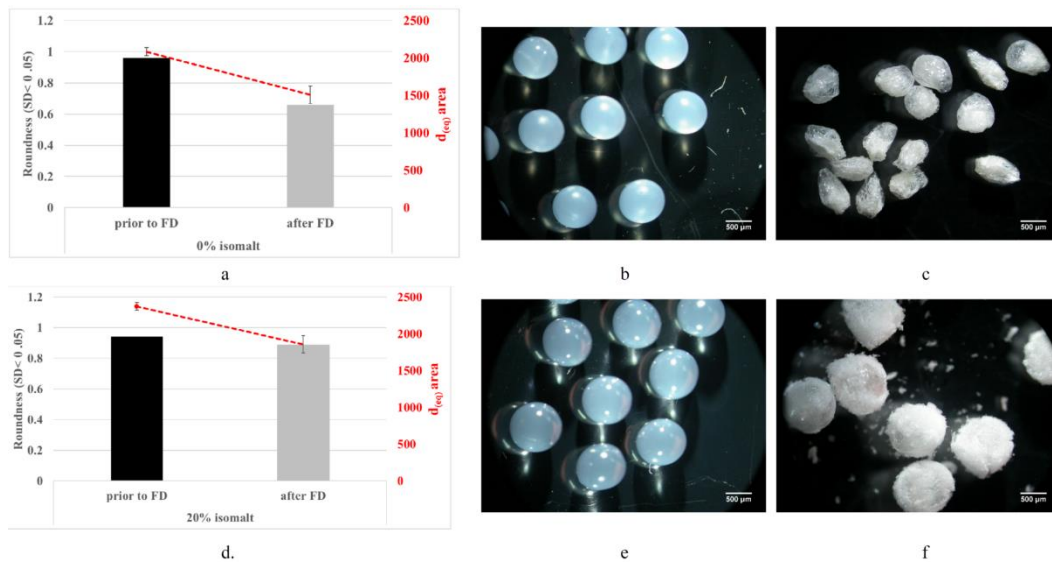


Figure 20. Morphological characteristics of microspheres

a.) decrease in roundness (columns) and $d_{0.5}$ size concomitant freeze-drying in 2% alginate hydrogel spheres; **b.)** microscopic image of original alginate spheres before drying; **c.)** microscopic image of freeze-dried alginate spheres; **d.)** change in roundness (column) and $d_{0.5}$ size concomitant freeze-drying in 2% alginate hydrogel spheres containing 20% isomalt; **e.)** microscopic image of alginate-isomalt spheres before drying; **f.)** microscopic image of freeze-dried alginate-isomalt spheres) ($d_{eq,area}$ expressed in μm²)

Without isomalt, the difference in roundness is significant before and after lyophilization of 2 % alginate microspheres. Isomalt administered in 20% produced relatively round particles ($R > 0.94$, $SD < 0.05$).

Scanning electron microscopic pictures showed a denser calcium-alginate network on the surface when the cores contained isomalt (Fig. 21).

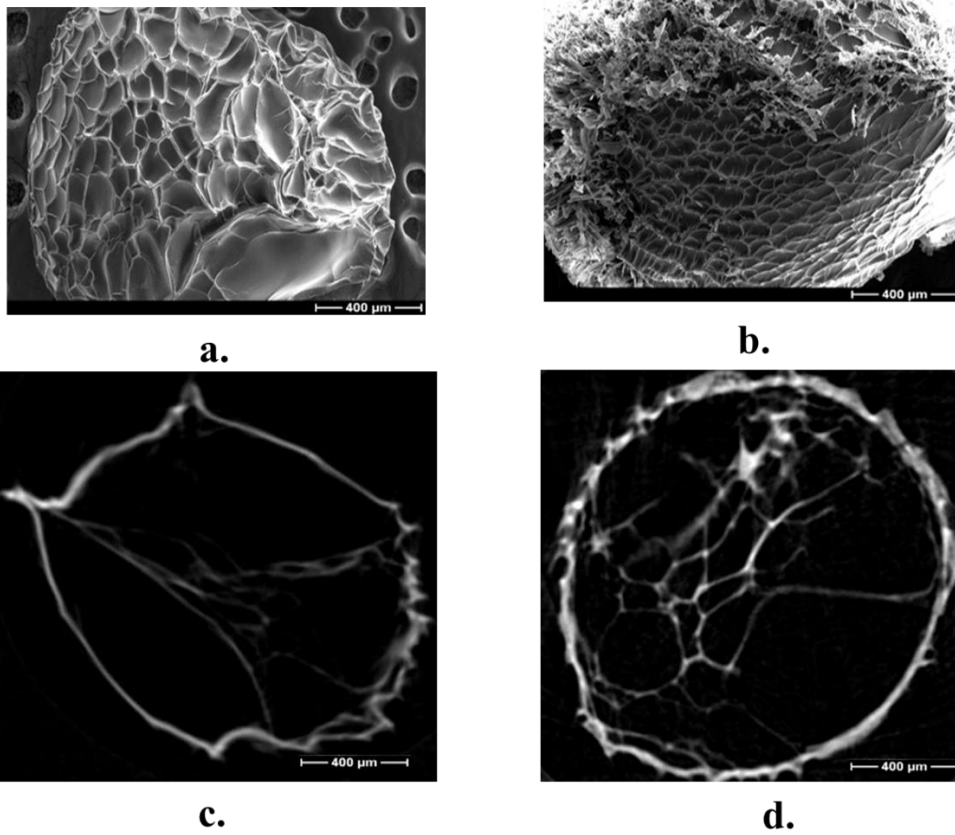


Figure 21. Structure of of 2% calcium alginate microspheres

Surface by SEM photographs: **a.)** 0% isomalt, **b.)** 20% isomalt)

Internal structure by micro-CT images **c.)** 0% isomalt, **d.)** 20% isomalt)

Micro-CT was used to detect the internal structure of the particles. It is a non-invasive 3D-analysis of calcified bone tissue morphometry analyzing cross-sectional- X-ray images by mathematical techniques of back-projection and convolution used in osteoporosis (96). It was also successfully used to detect scaffolds' porous design in bone tissue engineering. In vivo calcification of alginate beads was followed by micro-CT (97). Micro-CTs calcium-alginate chains show X-ray positivity, the structure of Ca-induced coacervated microparticles can be evaluated by μ -CT (97).

The freeze-dried samples subjected to micro-CT scans show a defined internal calcium-alginate network within the beads. (Fig. 21. c-d) Trabecular separation means the thickness of the spaces essentially as defined by binarisation within the volume of interest. The porosity is measured by 2D slice-by-slice analysis of closed pores, and as it is based on voxel counting, an accurate 3D porosity can be obtained.

The structural differences between the alginate particles and the isomalt-containing microparticles after freeze-drying can be evaluated based on the trabecular separation, total porosity, and total volume of pores (Table XV).

Table XV. Analysis of reconstructed micro-CT scans (98)

	<i>Trabecular number</i>		<i>Trabecular separation (μm)</i>		<i>Number of closed pores</i>		<i>The total volume of pore space (μm^3)</i>		<i>Total porosity (%)</i>
	<i>average</i>	<i>S.D.</i>	<i>average</i>	<i>S.D.</i>	<i>average</i>	<i>S.D.</i>	<i>average</i>	<i>S.D.</i>	<i>average</i>
20% isomalt	0.004090	0.000	326.5	40.3	212.3	84.3	$4.94 \cdot 10^9$	$1.74 \cdot 10^9$	79.7
0% isomalt	0.004147	0.001	224.8	21.9	64.3	17.8	$1.87 \cdot 10^9$	$6.58 \cdot 10^8$	78.2
Evaluation	<i>not significant</i>		<i>significant</i>		<i>significant</i>		<i>significant</i>		<i>not significant</i>

Data comparison was made by t-tests ($p \leq 0.05$)

Comparing the pure alginate and the 20 w/w% isomalt-containing samples, the number of trabeculas (i.e., calcium-alginate chains) was the same, so was the porosity. The total volume of pores and trabecular separation in the case of isomalt administration and pure alginate microparticles showed a difference, indicating a spongy matrix facilitating the formation of more regularly shaped microparticles ensured by isomalt (Fig. 22).

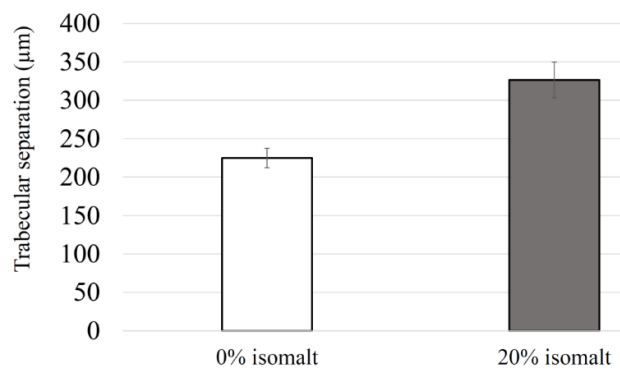


Figure 22. Trabecular separation in freeze-dried pure calcium alginate microsphere and calcium alginate microsphere with 20% isomalt.

4.1.3.2 RECONSTITUTION

Swelling is due to polymer chain relaxation; the electrostatic complexes of calcium and alginate are highly sensitive to pH and ionic strength since these parameters emphasize the electrostatic attraction (99). Various stimuli have been studied to change the swelling behavior of calcium alginate hydrogels. The hydrogel is pH-responsive (Fig. 23), poor swelling ability or shrinking is performed at low pH thanks to the attachment of anionic groups and H⁺-ions.

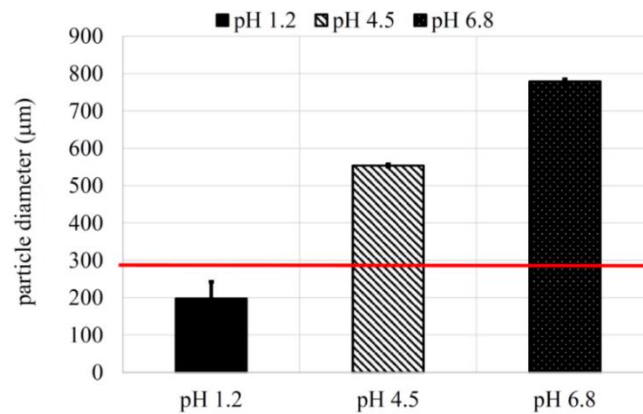


Figure 23. Alterations in size of calcium alginate in different pH media (red line indicates the initial size of gel microspheres).

The recovery of the original structure during reconstitution among different osmotic environments showed a tremendous difference depending on the osmotic active material being ionic or nonionic (Fig. 24).

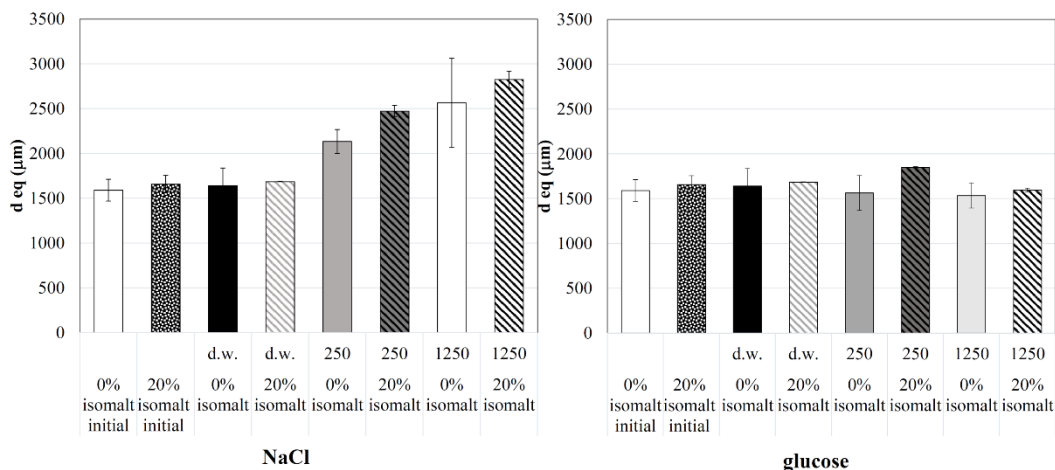


Figure 24. Reconstitution of calcium alginate and isomalt-calcium alginate microspheres in distilled water (d.w.) and at 250 and 1250 mosmol/l concentration media (t=60 min).

In NaCl solutions, the particles were swollen more than their original size in 60 min, and swelling proceeded until the particles were dissolved entirely (in 4 hours). The glucose solution and distilled water, on the contrary, did not cause rapid swelling. The reason for the electrolyte effect lies in the structure destabilizing effect of Na^+ -ions by binding to the guluronic acid COO^- groups replacing Ca^{2+} ions. Isomalt did not change the swelling process.

4.1.4 EFFECT OF DIVALENT AND TRIVALENT IONS ON PARTICLE CHARACTERISTICS

The effect of di- and trivalent ions as crosslinking agents in the formation of alginate gel microparticles was shown in terms of size and hardness.

The type and concentration of administered coacervation medium and the time the gel particles spent in those for gelling significantly affect the cross-linking, thus the shape and hardness of particles (Fig. 25).

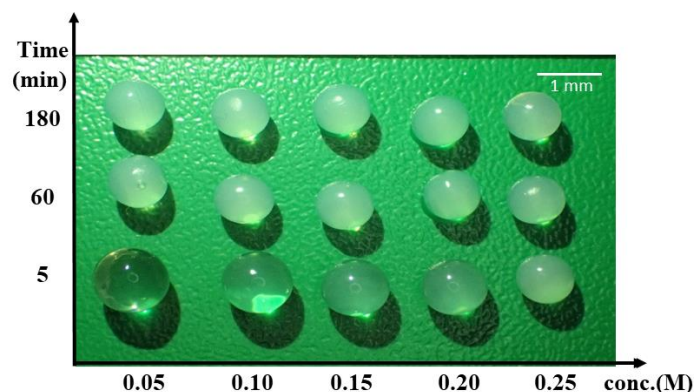


Figure 25. Particles' organoleptic character is influenced by the coacervation time (y-axis) and concentration of the medium (2% sodium alginate and CaCl_2 solution was used)

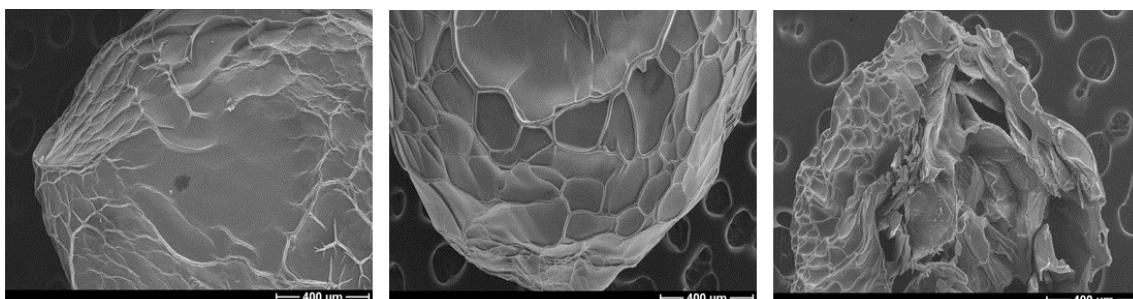


Figure 26. SEM of 2% sodium alginate crosslinked in CaCl_2 of different concentration (0.05M, 0.15M, 0.25M) for 60 min

The surface shows an observable difference according to the concentration of the coacervation medium: a higher concentration of crosslinking ions lead to more segmented structure (Fig. 26). The same observations are made for all di- and trivalent cations examined. However, there is a difference in the crosslinking ability of the different ions and as a result of faster or slower coacervation, different internal structure with different porosity is built up.

The force-displacement diagram (Fig. 27) is used to register the total work administered to compress the gel particles with a certain force at a predefined distance, which can be used to calculate the gel particles' hardness, after coacervation (Fig. 28).

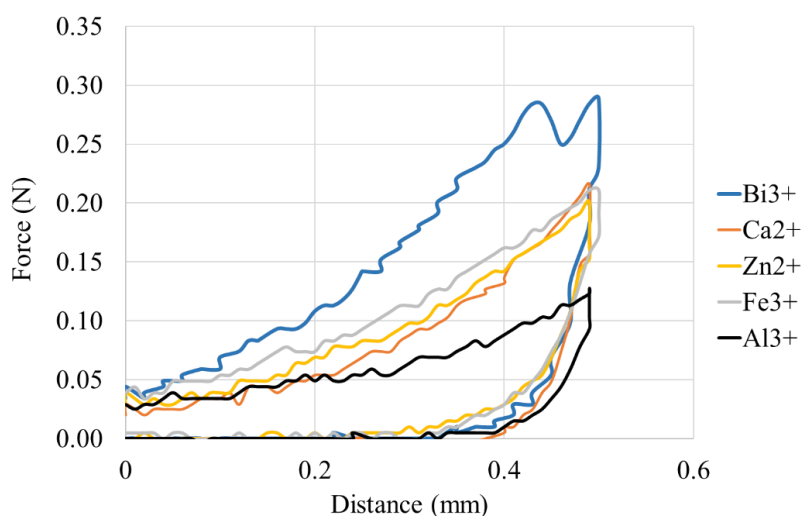


Figure 27. Force-distance curves registered on compression of gel particles formed with different di- and trivalent ions. (1.5% sodium alginate dropped into 0.15 M coacervation medium)

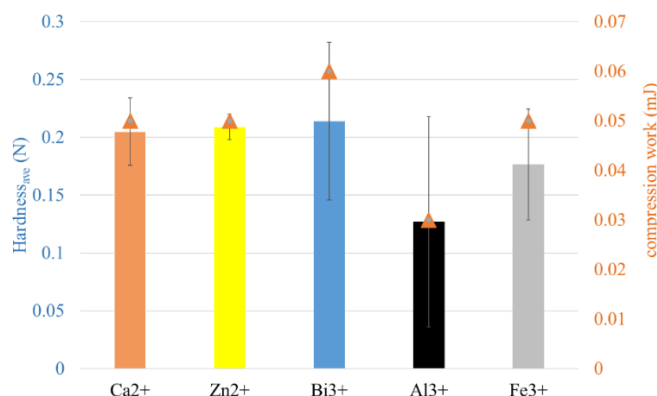


Figure 28. Total work (marked) calculated based on the force-displacement curve and hardness of the gel particles (columns) (1.5% sodium alginate in 0.15 M coacervation medium)

The texture analysis of the gel particles shows an elastic character in all cases, based on five concomitant compressions, the hardness, and the size depend on the character of the ions (Fig. 29).

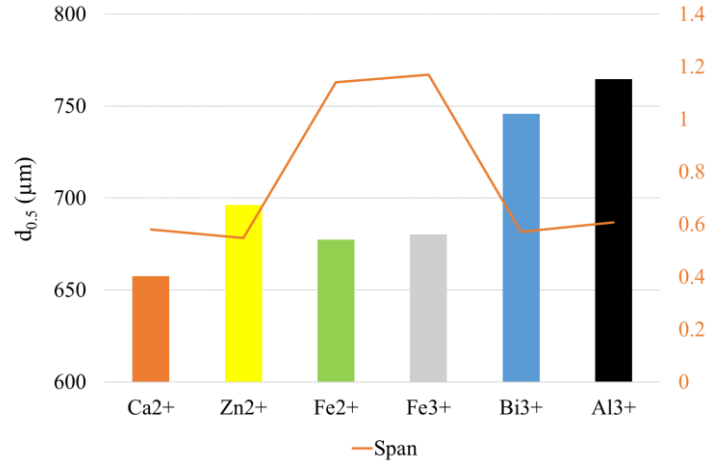


Figure 29. Alterations in average particle size ($d_{0.5}$) and Span value as a result of the application of different multivalent cations as coacervation medium (1.5% sodium alginate, 300 μm nozzle)

The observations concerning particle size of alginate spheres accord with the literature. However, the hydrogel spheres' formation by Fe^{2+} or Bi^{3+} has only been partly described (100). The cross-linking effect of the ions depends on both the ion radius and electronegativity.

4.2 BICARBONATE CONTAINING PELLET FORMULATION

4.2.1 COMPOSITION OF MATRIX CORE

The sodium bicarbonate-microcrystalline cellulose ratio of 70:30 and 40% w/w added water resulted in the highest percentage of pellet size (0.85-1.0 mm), with sphericity > 0.90. The dried pellets contained 66.2% w/w sodium bicarbonate prior to the coating process. The loss on drying was 3.5%± 0.5% w/w.

4.2.2 SIZE AND MORPHOLOGY OF PELLETS

The size distribution of the uncoated pellets was determined by a sieve analysis (Ph. Eur.) (Fig. 30) For an optimal coating process with fluidized-bed apparatus, the particles in the range of 630-1250 µm were chosen. Based on the results of 6 batches, 83.5% of the particles are in this range.

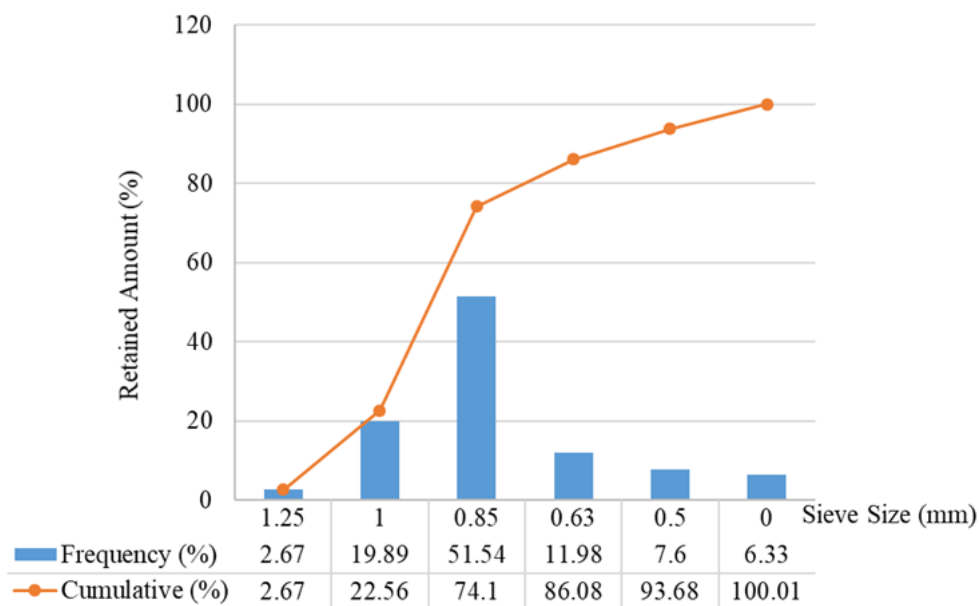


Figure 30. Particle size distribution of uncoated particles (*Retsch AS 200 vibration sieve, Retsch GmbH, Haan, Germany*) Columns indicate frequency, marked values indicate the cumulative retained amount.

The surface of the processed pellets was compared to a marketed bicarbonate core (Fig.31). The application 5% coating layer visibly smoothens the surface roughness of the pellet core.

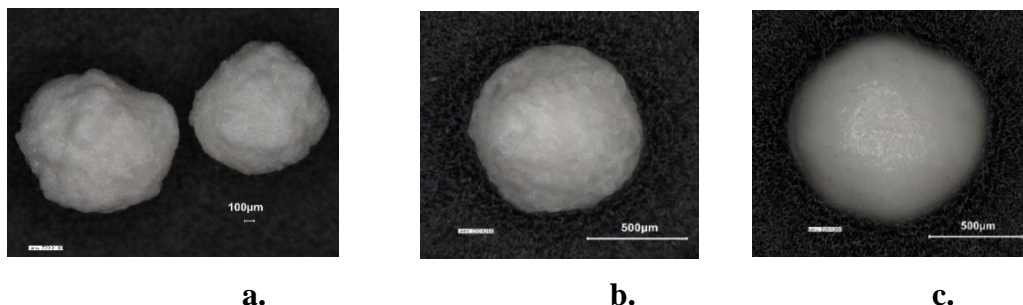


Figure 31. Surface morphology of NaHCO_3 pellets uncoated **a.)** marketed ready-to-use pellet cores (Umang Pharmatech Ltd., India) **b.)** our product and **c.)** our product coated with 5% Eudragit® E (*Keyence VHX 970 digital microscope, Keyence International, Mechelen, Belgium*)

4.2.3 DISSOLUTION STUDY BASED ON SODIUM RELEASE

Direct application of anionic polymers – which would regularly provide a good gastro-resistance and adequate drug release performance by numerous active ingredients- when applied on alkaline bicarbonate cores caused loss of their gastro-resistant property and leaking of bicarbonate at low pH (Fig. 32).

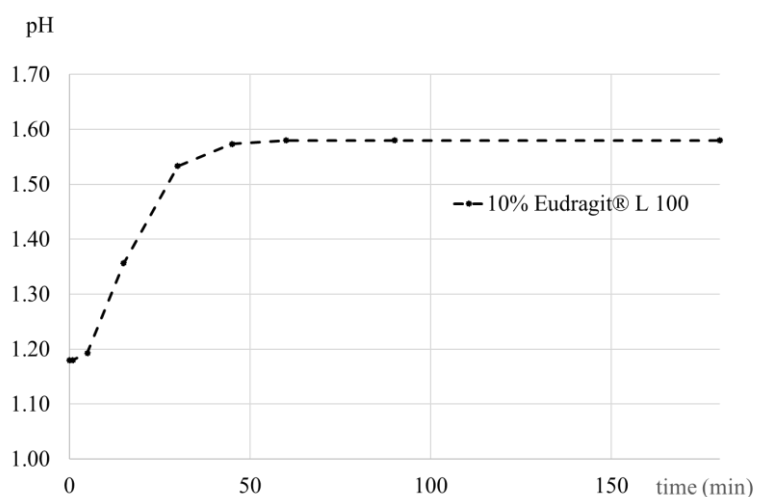


Figure 32. pH change caused by sodium bicarbonate containing pellet core having coated with Eudragit® L100 (10 w/w% weight gain) in *in vitro* gastric model medium (0.1 N HCl) (n=3, SD<0.05)

Several enterosolvent and gastrosolvent polymers of different chemical structure (Kollicoat[®] SR, MarCoat[™]125 shellac aqueous solution, Opadry[®] II white, Kollicoat[®] Protect, Eudragit[®] L, Eudragit[®] S, Eudragit[®] L100-55) and their combinations have been tested on the bicarbonate cores in different thicknesses and pH values. Some applied polymers proved to decrease the release rate (containing Eudragit NE 5% to 10%). However, this effect was pH-independent. It means that the aimed pH-gradient-dependent bicarbonate release can not be reached.

A particular combination of enterosolvent and non-pH-dependent polymers is required to protect the API from the strong acidic medium of the empty stomach.

After several trials, the combination of Eudragit[®] NE and Eudragit[®] L100 or L100-55 was found to help govern the gradual release administered on top of the Eudragit[®] NE coating layer. The application of HPMCP was also leading to a good result, the lag time at pH 3 was still shorter than planned, but the drug release rate was lower than in the case of pH 4.5; pH 5.5 phosphate buffer media.

With a certain combination of Eudragit[®] L, Eudragit[®] NE and Eudragit[®] L100-55 (ABD) or HPMCP (ABC), bicarbonate release starts at pH 3 from ABC pellets, and a lag time in the release can be observed for ABD pellets. However, the release of the two pellet components (1:1) does not differ in the dissolution significantly, because dissolution starts at lower pH (Fig. 33).

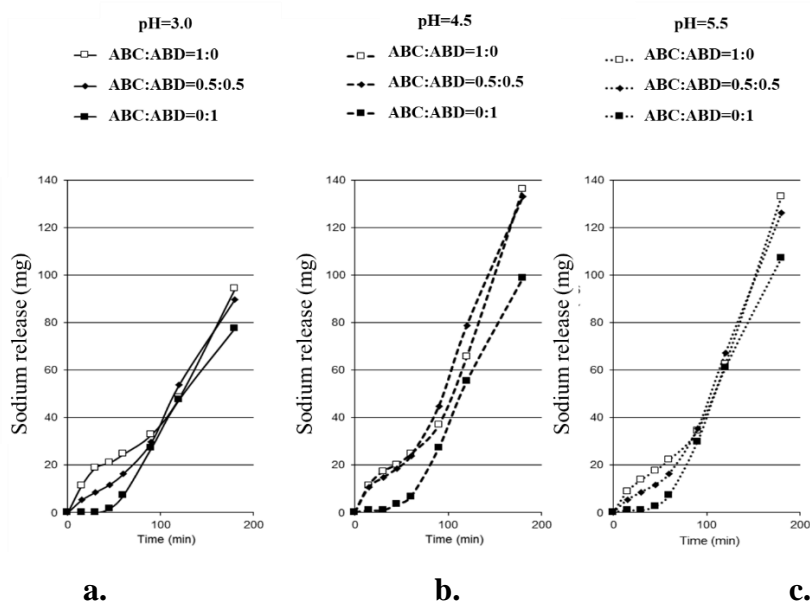


Figure 33. Sodium release at different pH media determined by flame photometry of ABC and ABD coated micropellets

The explanation for the start of the release is that the dissolving sodium bicarbonate led to a local alkalization of the inner enterosolvent layer, which became dissolvable due to this local effect.

Further development overcame the previous problem. The protection of the enterosolvent layer from the inner erosive effect of the dissolved alkaline core can be reached with an additional coating layer. The novelty of the application of polymer layer combination focuses on the use of more than three polymer layers, where the first layer ('a') involves the cationic polymer (Eudragit® E) to protect the anionic polymer layer (Eudragit® L) from the solid surface of the bicarbonate compound. These polymers are significantly different from Eudragit® NE since they show various solubility in a given pH range compared to Eudragit® NE, which polymer is insoluble in an aqueous medium.

The application layer 'a' avoided the release of NaHCO₃ from excessive release at low pH medium (Fig. 34).

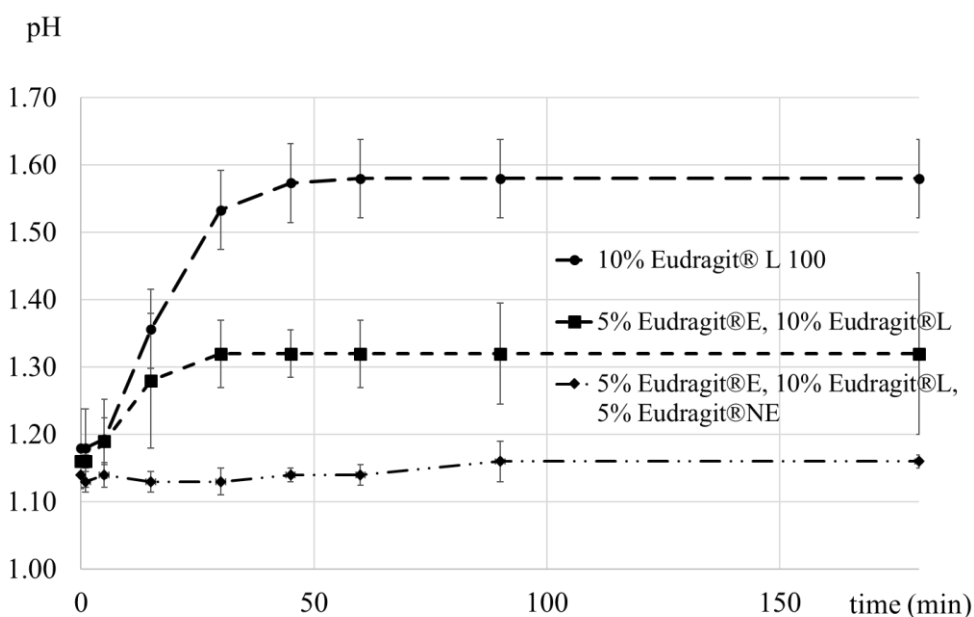
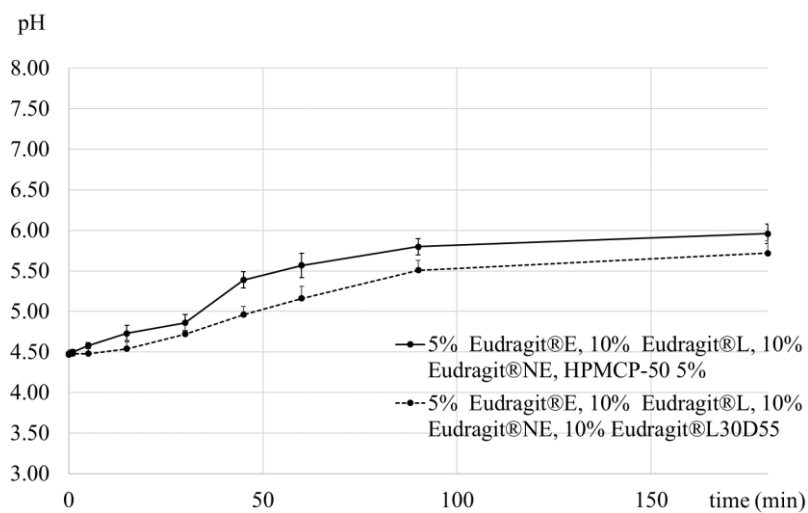


Figure 34. The application of Eudragit® E prevented the excessive release of NaHCO₃ at low pH (pH 1.2± 0.5)

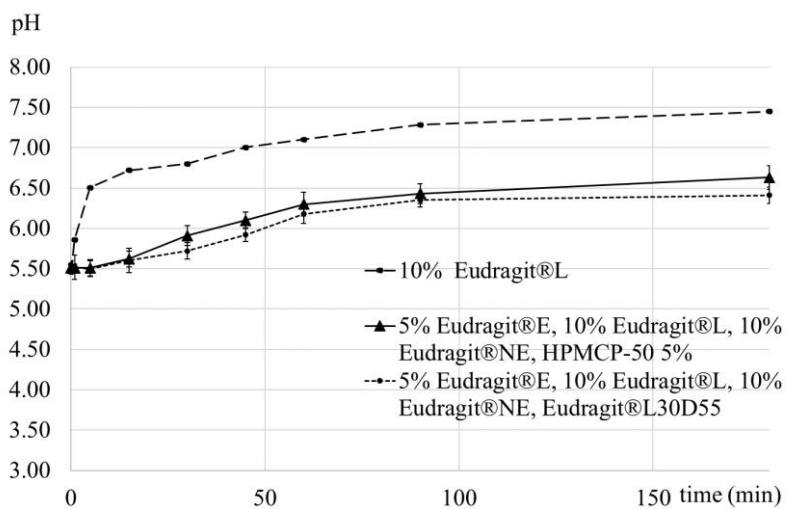
The combination of these polymer layers is unique due to their particular order: a cationic first layer was applied in order to prevent the sodium bicarbonate from degradation due to the application of the anionic layer, which in a solution has an acidic pH value (~pH 5.25-5.5) and would degrade sodium bicarbonate within a short period of time. Due to

this coating combination the sodium release starts slowly above pH 3 as the application of “a” layer slows down the release at lower pH, however, at pH 5.5 a higher release rate is reached.

Thus the order of polymers follows: cationic first layer, an anionic second layer, and then another water-insoluble third polymer layer is used to slow down the release of bicarbonate. Finally, the fourth polymer layer is selected from a polymer soluble above pH=4.5 or above pH=5.5 (Fig. 35. a, b).



a.



b.

Figure 35. a.) and b.) aABC and aABD coated micropellets pH change performance at pH=4.5 and pH=5.5.

The pellets have a complex structure with several functional layers (Fig. 36).

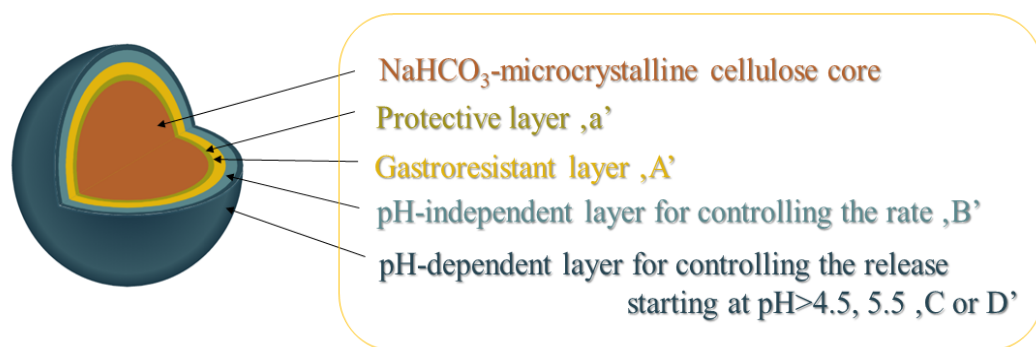


Figure 36. Schematic representation of functional coating layers of the surface of pellets

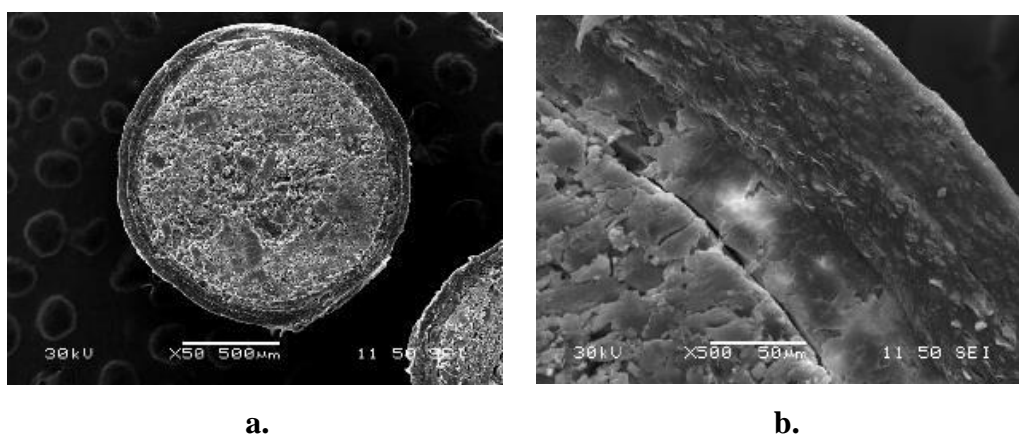
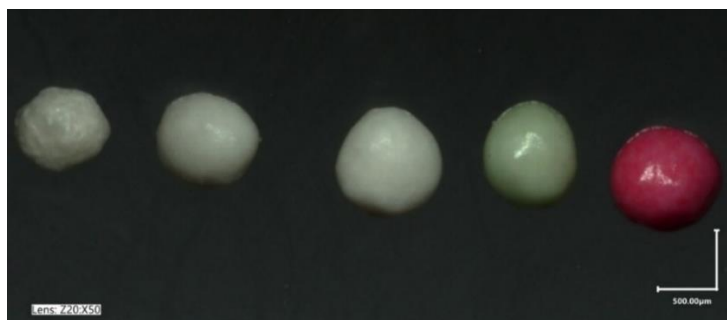
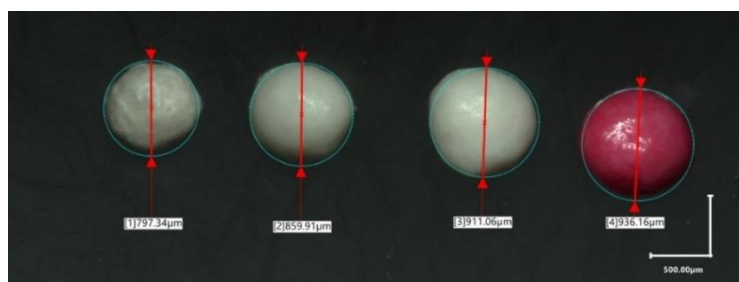


Figure 37. Scanning electron microscopic pictures of the coated (aABC) particles

The first coating layer smoothens the surface roughness of the cores. The thickness of different layers can be controlled at-line or online by in situ NIR probes (101) or at-line by a high-speed camera and dynamic image analysis (102)(103). The coating thickness causes the increase in the average diameter of the pellets, which can be followed by image analysis (104) (Fig. 37, 38). In addition, dissolution tests can examine the performance of the layer.



a.



b.

Figure 38. Different stages of coating of sodium bicarbonate-MCC matrix cores. **a.)** From left to right: pellet core; pellet core coated with layer 'a'; pellet core coated with layers 'aA'; pellet core coated with layers 'aAB'; green pellet: pellet core coated with layers 'aABC' (coloured with 0.1% alcohol-soluble coloring agent (MaxColor Green) for visualisation), red pellet: pellet core coated with layers 'aABD' (0.1% alcohol-soluble food coloring (MaxColor Red) is applied for visualisation). **b.)** Pictures show the size increase of the initial cores with the added layers on top. From left to right: uncoated core; 'a'; 'aA'; 'aAB'; 'aABD' (*Keyence VHX 970 digital microscope*)

4.3 BICARBONATE RELEASE FROM PELLET PREPARATION

The pH-dependent gradual/pulsatile release of the active agent can be achieved by the simultaneous use of micropellets (MPs) having at least two types of multilayer coatings. The structures of two types of MPs form a layer-by-layer structure, where the first type of particles is provided with a multilayer polymer coating “aABC”. The average diameter of the coated particles is 0.90-2.0 mm. The layer starts to dissolve at lower pH ($\text{pH} > 3.0$), but dissolves completely at $\text{pH} > 4.5 \pm 0.5$. The second type of particle is provided with multilayer polymer coating “aABD”. The average diameter of the coated particle is 0.90-2.0 mm, and it dissolves at $\text{pH} > 5.5 \pm 0.5$.

The first coating layer contacting the bicarbonate (polymer layer “a”) comprises a cationic polymer insoluble at $\text{pH} > 5$. The function of this polymer is to protect the enterosolvent coatings from the active alkaline agent of the core. The insulation is due to the complex formation between the polymer’s amine groups and sodium bicarbonate, decreasing the possibility of the reaction between the following layer’s polymer and the active ingredient, resulting in the next layer’s reactive degrading effect and the loss of active ingredient.

The use of layer „A” (Eudragit® L) was proved to be necessary as it hinders the dissolution of the coating layers, thus the early release of the sodium bicarbonate, even during the following steps of coating.

The third coating, polymer layer “B” (Eudragit® NE) provides a pH-independent sustained release of the active agent.

In one of the particle types, the outermost, fourth coating of the particles is polymer layer “C”, a gastro-resistant coating dissolving at weakly acidic pH, which ensures the pH-dependent release of the active agent.

In the other particle type, the fourth coating (polymer layer “D”) is a gastro-resistant coating, which dissolves at $\text{pH} > 5.5$.

The optimal therapeutic goal can be achieved with a combination of pellets in a voluntary proportion. This patient-centricity is especially advantageous to overcome the high interpersonal varieties in gastric emptying and the intrapersonal varieties caused as a result of the different health issues or other medicines with a gastroparetic side effect. Thus, with the mixing of the two types of particles filled into gastrosolvent capsules, the

release and the pH-control rate of the API can be tuned according to the patients' needs. At the intake, the combination of layers of a different character successfully protects the API from the erosive effect of the gastric juice.

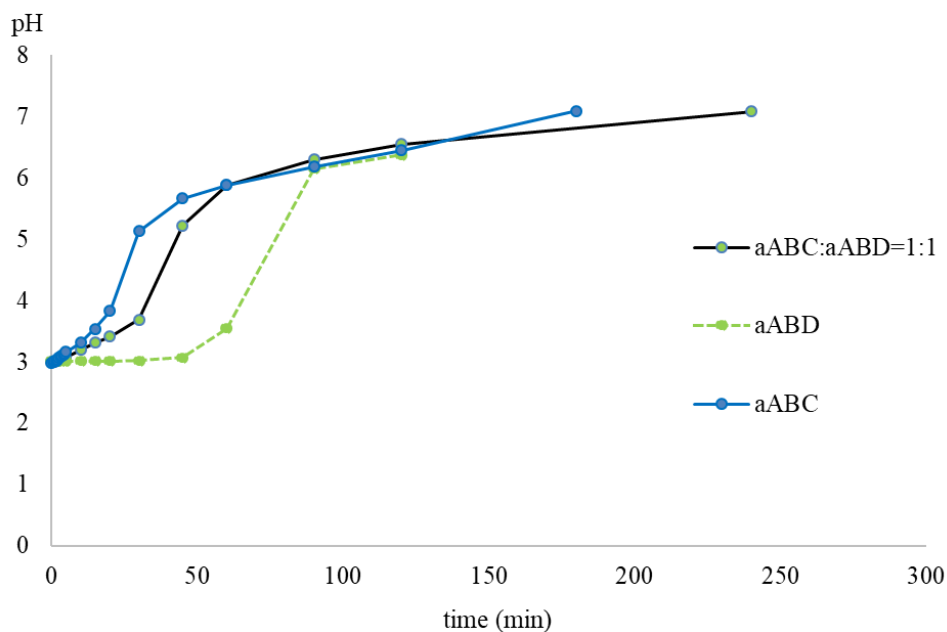


Figure 39. The pH changing ability of different polymer layers (aABC, aABD and their 1:1 mixture tested in pH 3.0 HCl medium) (SD<0.05)

The bicarbonate release starting at lower pH into the duodenal lumen contributes to alleviating the acid load and increasing the pH. When the duodenal environment reaches the second threshold value of pH 5.5, the second component of the pharmaceutical composition, i.e., aABD starts to release bicarbonate in a sustained manner. Thus, sodium bicarbonate released from aABD pellets augments the acid load moderating effect of aABC pellets and exerts a prolonged effect. It cooperates with the bicarbonate secreted into the duodenal lumen by the pancreas, the liver, and the intestinal mucosa; it favourably contributes to the alleviation of the acid load of the duodenal lumen, as they further increase the pH along with the physiologic process (Fig. 39).

In the medium having an initial pH of 4.5, the 2:1 mixture of particles with two types of coatings released bicarbonate within about 30 to 40 minutes, similarly to the 1:1 mixture. In the medium of pH 5.5, the sample of 2:1 mixture released sodium bicarbonate within 15 minutes, which was a little faster than in the case of the sample of 1:1 mixture.

Firstly, the above results clearly show that both types of coatings hinder the release of sodium bicarbonate in the acidic environment of the fasted stomach. This result is attained by the use of cationic protecting layer “a”. Secondly, both aABC and the mixtures of aABC and aABD pellets, that is, 1:1 and 2:1 mixtures provide adequate protection in the acidic environment of the stomach, but can decrease the hydrogen ion concentration at a higher pH value, which is of great importance given the residence time in the duodenum.

4.4 MISCIBILITY OF POLYMERS

The film-forming temperature of Eudragit[®] NE is low, and a few degrees above this temperature, the polymer becomes very sticky, which characteristics can be decreased by the addition of anti-tacking agents like talc. A sufficient amount of talc and a curing time (regularly 24 hours) leads to the formation of a proper layer with extended-release kinetics. However, during the further coating process, the neutral layer becomes soft and sticky again by adding the next layer, where the polymer’s film-forming temperature is very close to the film-forming temperature of Eudragit[®] NE.

To avoid this phenomenon, thus increasing the processability of the coating, simplifying the process by mixing the different coating polymer components is evident. However, due to their different solubility, some components are not miscible at the pH, where their solubility is highest.

The miscibility of the two polymers (Eudragit[®] NE and Eudragit[®] L30D55) has been tested. At the pH of the aqueous dispersions, NE and L30D55 (pH 7.12 and 5.4 respectively) the two polymers were miscible in a 1:1 ratio (Fig. 40).

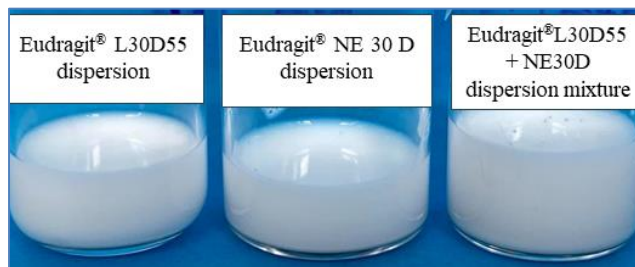


Figure 40. Miscibility of Eudragit[®] NE and Eudragit[®] L30D55 polymers in 1:1 ratio

The effect of mixing the two polymers was also checked by FT-IR. Cast films were

prepared on a flat silicone moulding form, that was placed on a heater, firstly from the mixed dispersion and secondly, in two steps: after having dried the first, Eudragit® NE layer, another layer of Eudragit® L30D55 was moulded on top. The temperature of drying was adjusted according to the temperature applied for the coating procedure (Table XIII). The FT-IR spectra showed no chemical interaction dependently on if the layers were casted separately or in a mixture (Fig. 41).

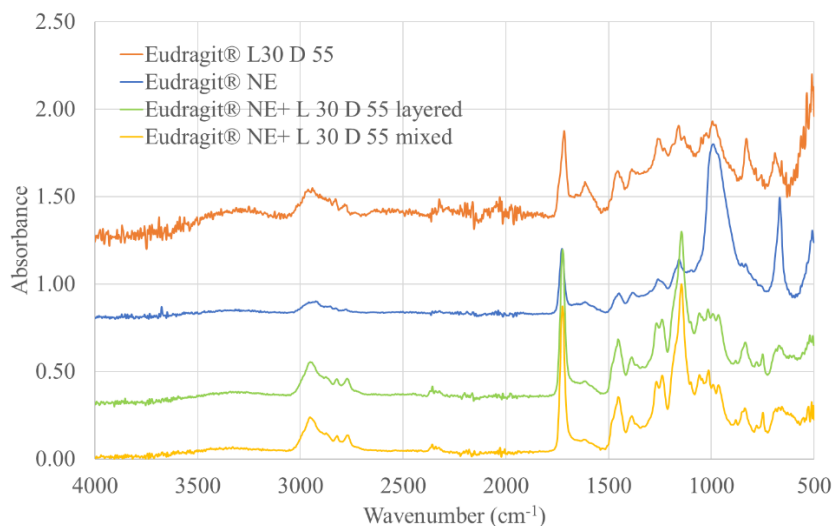


Figure 41. The FT-IR spectra of the free films of the applied coating dispersions. Eudragit® NE dispersion, Eudragit® L30D55, their mixture and the second layer moulded on top of first layer

5. DISCUSSION

The cross-linking effect of some important divalent and trivalent cations on the formation of alginate microspheres has been investigated. The shape memory of calcium alginate microspheres was tested concomitant to swelling in hyposmotic, and in hyperosmotic nonionic and ionic media. The particles showed a very rapid swelling and disintegration in the NaCl medium independently of its osmolality. The swelling was also effective in sugar solutions. The effect of isomalt as a freeze-drying excipient was also tested. The calcium alginate particles, where no isomalt was used showed a significant decrease in particle size when dried and the spherical character was lost, which can be an important feature in the further processing of dried or lyophilized particles. Isomalt caused the keeping of the sphericity of gel microcapsules during drying process.

Sodium bicarbonate was formulated as modified-release coated pellets. The considerable difficulty with coatings soluble at slightly acidic pH is that the polymer coating begins to swell at the acidic pH of the stomach. As soon as moisture reaches the particle core, the pH on the surface of the active alkaline agent may locally exceed the lowest pH value at which the polymer is soluble; consequently, the coating starts to erode from the inside, which leads to an early, uncontrolled release of the active agent. The coating layers need to resist both the acidic and alkaline media. The aim was to elaborate on the reproducible pharmaceutical composition corresponding to the double standard. The invention concerns a preparation composition that starts to release the active agent at pH 4.5 in a gradual, pH-dependent, and sustained manner while passing through the intestines together with the intestinal content. The above-outlined features are implemented by a composition containing microparticles having a core of high sodium hydrogen carbonate content with a multilayer coating. The function of the coating layers are: the exterior layer provides the pH-dependent dissolution, the next layer provides the sustained release of the active agent, and the innermost layer prevents the alkaline leaking, caused by the moisture that reaches the alkaline content of the particle core and deteriorates the pH-sensitive layered coating from inside. The gradual release can be achieved by blending particles having two types of coatings of pH-dependent solubility.

The enterosolvent coatings are generally soluble in near neutral or slightly alkaline conditions, the coatings described above, dissolve at weakly acidic pH values. It is usable

for increasing the pH in the duodenum and the further parts of the small intestine.

Due to the gastro-resistant polymer coatings, this preparation presumably does not release the active agent in the gastric lumen at pH 1.2, but moves together with the chymus into the duodenum and exerts their pharmacodynamic effect there, i.e., they neutralize the gastric acid or the chymus in the duodenum. The ratio of the components mentioned above can be adjusted according to the condition to be treated. The combination of microparticles with different characteristics, providing the pH-dependent sustained release of the active agent, enables individual treatment in the changing environment of the duodenum. The acid load caused by the acid or the acidic chymus emptying into the duodenum from the stomach and the amount of bicarbonate secreted by the pancreas, the liver, and the intestinal mucosa can vary with the health condition of the patients. Therefore, the amount of bicarbonate dissolved from the composition can favorably be varied by adjusting the ratio of the components according to individual needs in treating the absolute or relative bicarbonate deficit in the duodenal lumen.

5.1 PERSONALIZED, INDIVIDUAL COMPOSITION AND THERAPY

If the acid load of the duodenum is permanently high, higher ratios of aABC/aABD can be set; thus the composition can exert the acid load decreasing effect at more acidic environment, with a quicker onset of action. On the other hand, a higher of aABD/aABC ratio can be adjusted to avoid the delivery of the active agent content in the stomach, although the acid load of the duodenum/small intestine is not permanently high, however the amount of the bicarbonate secreted by the pancreas, the liver and the intestinal mucosa low in the duodenum for any reason.

When it is used orally, the pharmaceutical preparation delivers bicarbonate directly into the duodenal lumen and thus, it exerts its activity according to the physiologic processes in the duodenum/small intestine lumen, where the bicarbonate deficiency appears to supplement the bicarbonate need. The compositions can advantageously be used in clinical aspects, where the actual amount of the bicarbonate secreted in the lumen of the small intestine is too low, in order to decrease or neutralize the acidity of the gastric acid or the chymus entering the lumen of the small intestine. The composition can be used for the treatment of the acute or chronic bicarbonate deficiencies of various extent, where the types of the bicarbonate deficiencies are as follows:

-Real bicarbonate deficiency due to failure of secretion (exocrine)

-Relative bicarbonate deficiency with intact efferent system, physiologically proper bicarbonate secretion with improper neuro-hormonal regulation resulting in acute or permanent increased acid load.

The optimal alkalic pH is a prerequisite for the proper functioning of pancreatic digestive enzymes. When the neutralization of the chymus is incomplete due to the bicarbonate deficiency, and the luminal pH of the small intestine remains permanently lower, the activity of the pancreatic digestive enzymes decreases. In a worse scenario, these enzymes are present in the duodenum at a decreased level, performing a lower activity, which is further aggravated by low bicarbonate secretion. Bicarbonate supply can also be necessary in such cases.

The bicarbonate pellets must be packaged with moisture protection and stored at cool place to avoid the instability of the gastroresistant methacrylate polymers and the concomitant release of the sodium bicarbonate.

6. CONCLUSIONS

CONCLUSIONS REGARDING MICROSPHERES

1. The production of spherical calcium alginate microparticles was studied by using surface-active agents. The surface-active agent was found to be applicable both in the alginate or the coacervation medium in 0.25-1.00 w/w% Polysorbate 80 content in terms of preserving the spherical shape of the particles at optimal preparation conditions.
2. The freeze-drying process was applied with cryoprotectant isomalt to preserve the particles' spherical shape in a dried state.
3. The addition of isomalt was beneficial in the freeze-drying of calcium-alginate microspheres: it improved the roundness of the freeze-dried microspheres of low alginate concentration compared to microspheres produced without the addition of cryoprotectants. The increase in the sphericity leads to an increased flowability, thus the processability of the xerogel particles.
4. The internal 3-dimensional trabecular calcium-alginate structure can be evaluated by micro-CT.
5. Reconstitution of freeze-dried and air-dried samples was compared at various media (pH, osmolarity). Higher pH values and NaCl content influenced the swelling process.
6. Although the trabecular separation was different, the swelling behavior was not affected by the cryoprotectant additive. The optimal morphology of the dry microspheres can be advantageous when the particles need further technological processing, i. e., coating, or capsule filling, as it increases the flowability and diminishes the friability deriving from abrasion.
7. The role of different divalent and trivalent cations in the coacervation process of cation-alginate complex formation was compared in terms of gel strength and hardness in order to create a gel structure that is swellable and acceptably soft to be administered in an easy-to-swallow, for example, pediatric preparation.

CONCLUSIONS REGARDING MICROPELLET FORMULATION

8. Sodium bicarbonate-containing particles were prepared with alcohol as granulating liquid as well as with an aqueous method.
9. The pellet cores were coated with a multi-layer enteric solvent polymer coating overcoming the interaction of alkaline active ingredient and the enterosolvent polymers with an acid character. The coating proves a gradual sustained release: a cationic polymer coating contacting the core (for acid-protection), a pH-independent polymer coating (for extended-release), and a pH-dependent soluble anionic polymer coating (for optimal release start: at pH 4.5; 5.5).
10. The external layer provides the optimal drug release (pH 4.5 or 5.5), which can be fine-tuned by setting the proper ratio by mixing the first and second microparticles' types. The composition can be adjusted between 20/80 to 80/20 and filled in gastrosolvent capsules or packed in sachets.
11. Actual bicarbonate deficiency may appear along with the various extents of the partial defects of the pancreatic digestive juice, where simultaneous supplement of pancreatic digestive enzymes is required. Thus, the preparation may advantageously be used to meet the bicarbonate need in different clinical scenarios.

7. SUMMARY

Numerous microparticulate formulations gained therapeutical and diagnostic significance in the past few decades. To reach the required effect and regulate the release of active ingredients, a significant number of polymers have been tested, of which several have proved to be effective.

New methods have been developed to accomplish traditional coacervation (freeze-drying, spray drying, microfluidic flow-focusing). However, the traditional techniques offer substantial potential for fine-tuning drug release mechanisms and optimizing the pharmacokinetic profile.

The development work summarized in the thesis describes various methods for the production of spherical microparticles with the aid of different excipient systems for various use.

An investigation of alginate gel and xerogel microparticles in terms of the composition and process parameters was done in order to produce swellable and shape-retaining microparticles.

The thesis also introduces the formulation study of a sodium bicarbonate-containing multiparticulate preparation (105). The formula can gradually release the active ingredient, stepwise at weak acidic media (pH 3-4.5 and pH 5.5), while protecting it from the release in an acidic environment of the fasted stomach. The preparation offers a solution for the therapy of different gastrointestinal symptoms and illnesses where the controlled release of sodium bicarbonate is a critical parameter. The development and the formulation was patented by the Hungarian Patent Office in 2010 (P1000407) and the United States Patent Office in 2017 (US 9,839,607 B2) (106).

8. REFERENCES

- [1] Bale S, Khurana A, Reddy ASS, Singh M, Godugu C. Overview on Therapeutic Applications of Microparticulate Drug Delivery Systems. *Crit Rev Ther Drug Carr Syst.* 2016;33:309–361.
<https://doi.org/10.1615/CritRevTherDrugCarrierSyst.2016015798>
- [2] Newton JM. Gastric emptying of multi-particulate dosage forms. *Int J Pharm.* 2010;395:2–8. <https://doi.org/10.1016/j.ijpharm.2010.04.047>
- [3] Fonyó A. Az orvosi ételtan tankönyve. In: Chapter 2. Budapest: Medicina Könyvkiadó Zrt.; 2011. p. 466.
- [4] Davis SS, Hardy JG, Fara JW. Transit of pharmaceutical dosage forms through the small intestine. *Gut.* 1986;27:886–892.
- [5] Microencapsulation Market Published Date: Sep 2020 Report Code: FB 5546. [Internet] [cited 2021 Sep. 2]. [accessed: 29.09.2020.] Available from <https://www.marketsandmarkets.com/Market-Reports/microencapsulation-market-83597438.html>
- [6] Wang BH, Longquin HTJS. *Drug Delivery Principles and Applications* Wang. Drug Deliv. Hoboken NJ, USA: John Wiley and Sons Inc; 2016. p509.
- [7] Lengyel M, Kállai-Szabó N, Antal V, Laki AJ, Antal I. Microparticles, Microspheres, and Microcapsules for Advanced Drug Delivery. *Sci Pharm.* 2019;87:20. <https://doi.org/10.3390/scipharm87030020>
- [8] Ghosh SK. Functional Coatings and Microencapsulation: A General Perspective. In: *Functional Coatings*. Weinheim: Wiley-VCH Verlag & Co.; 2006. p. 1–28. <https://doi.org/10.1002/3527608478.ch1>
- [9] Lee JH, Garner J, Skidmore S. Fabrication of Drug-loaded Microparticles Using Hydrogel Technology and Recent Innovation in Automation. *Material Matters.* 2013 8(3):88. [Internet][cited 2021 Sept 02] Available from: <https://www.sigmaaldrich.com/technical-documents/articles/material-matters/fabrication-of-drug-loaded-microparticles.html>

- [10] Mema I, Wagner EC, van Ommen JR, Padding JT. Fluidization of spherical versus elongated particles - experimental investigation using X-ray tomography. *Chem Eng J.* 2020;397:125203.
<https://doi.org/10.1016/j.cej.2020.125203>
- [11] Ji S, Wang S, Zhou Z. Influence of particle shape on mixing rate in rotating drums based on super-quadric DEM simulations. *Adv Powder Technol.* 2020;31:3540–3550. <https://doi.org/10.1016/j.appt.2020.06.040>.
- [12] Davidson MR, Cooper-White JJ. Pendant drop formation of shear-thinning and yield stress fluids. *Appl Math Model.* 2006;30:1392–1405.
<https://doi.org/10.1016/j.apm.2006.03.016>
- [13] Chan ES, Lee BB, Ravindra P, Poncelet D. Prediction models for shape and size of ca-alginate macrobeads produced through extrusion-dripping method. *J Colloid Interface Sci.* 2009;338:63–72.
<https://doi.org/10.1016/j.jcis.2009.05.027>
- [14] Whelehan M, Marison IW. Microencapsulation using vibrating technology. *J Microencapsul.* 2011;28:669–688.
<https://doi.org/10.3109/02652048.2011.586068>
- [15] Serp D, Cantana E, Heinzen C, Von Stockar U, Marison IW. Characterization of an encapsulation device for the production of monodisperse alginate beads for cell immobilization. *Biotechnol Bioeng.* 2000;70:41–53.
[https://doi.org/10.1002/1097-0290\(20001005\)70:1<41::AID-BIT6>3.0.CO;2-U](https://doi.org/10.1002/1097-0290(20001005)70:1<41::AID-BIT6>3.0.CO;2-U)
- [16] Aizpurua-Olaizola O, Navarro P, Vallejo A, Olivares M, Etxebarria N, Usobiaga A. Microencapsulation and storage stability of polyphenols from *Vitis vinifera* grape wastes. *Food Chem.* 2016;190:614–621.
<https://doi.org/10.1016/j.foodchem.2015.05.117>
- [17] Kállai-Szabó N., Luhn O, Dredán J, Kovács K, Lengyel M, Antal I. Evaluation of drug release from coated pellets based on isomalt, sugar, and microcrystalline cellulose inert cores. *AAPS PharmSciTech.* 2010;11:383–391.
<https://doi.org/10.1208/s12249-010-9396-x>.

- [18] Market Intellica, Wheeling, Illinois, USA. [Internet] [cited 2020 Sep. 29]. Available from <https://www.marketintellica.com/report/MI51494-global-pharmaceutical-pellets-market-report-2019>.
- [19] Wurster DE. Air-Suspension Technique of Coating Drug Particles. *J Am Pharm Assoc.* 1959;XLVIII.:451–454.
- [20] Das SK, David SR, Rajabalaya R, Halder T. Microencapsulation techniques and its practices. *Int J Pharma Sci Tech.* 2011;6 (2):1-23.
- [21] McNaught AD, Wilkinson A. IUPAC. Compendium of Chemical Terminology, 2nd ed. (the “Gold Book”). In: Chalk SJ online 2019-, editor. Blackwell Scientific Publications. Oxford: Blackwell Scientific Publications; 1997. p. 1815. <https://doi.org/https://doi.org/10.1351/goldbook.S05598>
- [22] Batubara I, Rahayu D, Mohamad K, Prasetyaningtyas WE. Leydig Cells Encapsulation with Alginate-Chitosan: Optimization of Microcapsule Formation. *J Encapsulation Adsorpt Sci.* 2012;02:15–20. <https://doi.org/10.4236/jeas.2012.22003>
- [23] Capretto L, Mazzitelli S, Luca G, Nastruzzi C. Preparation and characterization of polysaccharidic microbeads by a microfluidic technique: Application to the encapsulation of Sertoli cells. *Acta Biomater.* 2010;6:429–435. <https://doi.org/10.1016/j.actbio.2009.08.023>
- [24] Shaddel R, Hesari J, Azadmard-Damirchi S, Hamishehkar H. Use of gelatin and gum arabic for encapsulation of black raspberry anthocyanins by complex coacervation. *Int J Biol Macromol.* 2017;107:1800–1810. <https://doi.org/10.1016/j.ijbiomac.2017.10.044>

- [25] Bhattacharya SS, Shukla S, Banerjee S, Chowdhury P, Chakraborty P, Ghosh A. Tailored IPN hydrogel bead of sodium carboxymethyl cellulose and sodium carboxymethyl xanthan gum for controlled delivery of diclofenac sodium. *Polym - Plast Technol Eng.* 2013;52:795–805.
<https://doi.org/10.1080/03602559.2013.763361>
- [26] Kaity S, Isaac J, Ghosh A. Interpenetrating polymer network of locust bean gum-poly (vinyl alcohol) for controlled release drug delivery. *Carbohydr Polym.* 2013;94:456–467. <https://doi.org/10.1016/j.carbpol.2013.01.070>.
- [27] Maciel VB V, Yoshida CMP, Pereira SMSS, Goycoolea FM, Franco TT. Nano- and Microparticles for Insulin Delivery. *Molecules.* 2017;22:1707. <https://doi.org/10.3390/molecules22101707>
- [28] Rocha-Selmi GA, Theodoro AC, Thomazini M, Bolini HMA, Favaro-Trindade CS. Double emulsion stage prior to complex coacervation process for microencapsulation of sweetener sucralose. *J Food Eng.* 2013;119:28–32. <https://doi.org/10.1016/j.jfoodeng.2013.05.002>
- [29] Rabani F, Aziz A, Jai J, Raslan R, Subuki I. Microencapsulation of citronella oil by complex coacervation using chitosan-gelatin (b) system : operating design , preparation and characterization. In: *MATEC Web of Conferences, ICCPE.* Vol 69. 2016. p. 04002. <https://doi.org/DOI: 10.1051/mateconf/2016 6904002>
- [30] Fioramonti SA, Stepanic EM, Tibaldo AM, Pavón YL, Santiago LG. Spray dried flaxseed oil powdered microcapsules obtained using milk whey proteins-alginate double layer emulsions. *Food Res Int.* 2019;119:931–940. <https://doi.org/10.1016/j.foodres.2018.10.079>
- [31] Alvarado Y, Muro C, Illescas J, Díaz MDC, Riera F. Encapsulation of Antihypertensive Peptides from Whey Proteins and Their Releasing in Gastrointestinal Conditions. *Biomolecules.* 2019;9 (5) 164.
<https://doi.org/10.3390/biom9050164>

- [32] Riaz T, Iqbal MW, Saeed M, Yasmin I, Hassanin HAM, Mahmood S, Rehman A. In vitro survival of *Bifidobacterium bifidum* microencapsulated in zein-coated alginate hydrogel microbeads. *J Microencapsul.* 2019;36:192–203.
<https://doi.org/10.1080/02652048.2019.1618403>
- [33] Farris E, Brown DM, Ramer-Tait AE, Pannier AK. Chitosan-zein nano-in-microparticles capable of mediating in vivo transgene expression following oral delivery. *J Control Release.* 2017;249:150–161.
<https://doi.org/10.1016/j.jconrel.2017.01.035>
- [34] Giovagnoli S, Blasi P, Luca G, Fallarino F, Calvitti M, Mancuso F, Ricci M, Basta G, Becchetti E, Rossi C, Calafiore R. Bioactive long-term release from biodegradable microspheres preserves implanted ALG-PLO-ALG microcapsules from in vivo response to purified alginate. *Pharm Res.* 2010;27:285–295. <https://doi.org/10.1007/s11095-009-0017-x>
- [35] Mooranian A, Negrulj R, Al-Salami H, Morahan G, Jamieson E. Designing anti-diabetic β -cells microcapsules using polystyrenic sulfonate, polyallylamine, and a tertiary bile acid: Morphology, bioenergetics, and cytokine analysis. *Biotechnol Prog.* 2016;32:501–509. <https://doi.org/10.1002/btpr.2223>
- [36] Wells LA, Sheardown H. Photosensitive controlled release with polyethylene glycol-anthracene modified alginate. *Eur J Pharm Biopharm.* 2011;79:304–313.
<https://doi.org/10.1016/j.ejpb.2011.03.023>
- [37] Mahou R, Meier RRH, Bühler LH, Wandrey C. Alginate-poly(ethylene glycol) hybrid microspheres for primary cell microencapsulation. *Materials (Basel).* 2014;7:275–286. <https://doi.org/10.3390/ma7010275>
- [38] Colinet I, Dulong V, Mocanu G, Picton L, Le Cerf D. New amphiphilic and pH-sensitive hydrogel for controlled release of a model poorly water-soluble drug. *Eur J Pharm Biopharm.* 2009.
<https://doi.org/10.1016/j.ejpb.2009.07.008>

- [39] Streubel A, Siepmann J, Bodmeier R. Floating microparticles based on low density foam powder. *Int J Pharm.* 2002;241:279–292.
- [40] Wu J, Kong T, Yeung KWK, Shum HC, Cheung KMC, Wang L, To MKT. Fabrication and characterization of monodisperse PLGA-alginate core-shell microspheres with monodisperse size and homogeneous shells for controlled drug release. *Acta Biomater.* 2013;9:7410–7419. <https://doi.org/10.1016/j.actbio.2013.03.022>
- [41] Kim J, Kang K, Drogemuller CJ, Wallace GG, Coates PT. Bioprinting an Artificial Pancreas for Type 1 Diabetes. *Curr Diab Rep.* 2019;19 (8):53. <https://doi.org/10.1007/s11892-019-1166-x>
- [42] Agüero L, Zaldivar-Silva D, Peña L, Dias M. Alginate microparticles as oral colon drug delivery device: A review. *Carbohydr Polym.* 2017;168:32–43. <https://doi.org/10.1016/j.carbpol.2017.03.033>
- [43] Wang W, Liu X, Xie Y, Zhang H, Yu W, Xiong Y, Xie W, Ma X. Microencapsulation using natural polysaccharides for drug delivery and cell implantation. *J Mater Chem.* 2006;16:3252–3267. <https://doi.org/10.1039/b603595g>
- [44] Zimmermann U, Mimietz S, Zimmermann H, Hillgartner M, Schneider H, Ludwig J, Hasse C, Haase A, Rothmund M, Fuhr G. Hydrogel-Based Non-Autologous Cell and Tissue Therapy. *Biotechniques.* 2000;29:564–581. <https://doi.org/10.2144/00293RV01>
- [45] Banerjee S, Singh S, Bhattacharya SS, Chattopadhyay P. Trivalent ion cross-linked pH sensitive alginate-methyl cellulose blend hydrogel beads from aqueous template. *Int J Biol Macromol.* 2013;57:297–307. <https://doi.org/10.1016/J.IJBIOMAC.2013.03.039>
- [46] Sun JY, Zhao X, Illeperuma WRK, Chaudhuri O, Oh KH, Mooney DJ, Vlassak JJ, Suo Z. Highly stretchable and tough hydrogels. 2021;489(7414):133-136. <https://doi.org/10.1038/nature11409>

- [47] Yang CH, Wang MX, Haider H, Yang JH, Sun JY, Chen YM, Zhou J, Suo Z. Strengthening alginate/polyacrylamide hydrogels using various multivalent cations. *ACS Appl Mater Interfaces*. 2013;5:10418–10422. <https://doi.org/10.1021/AM403966X>
- [48] Moebus K, Siepmann J, Bodmeier R. Novel preparation techniques for alginate-ploxamer microparticles controlling protein release on mucosal surfaces. *Eur J Pharm Sci*. 2012;45:358–366. <https://doi.org/10.1016/j.ejps.2011.12.004>
- [49] Möbus K, Siepmann J, Bodmeier R. Zinc–alginate microparticles for controlled pulmonary delivery of proteins prepared by spray-drying. *Eur J Pharm Biopharm*. 2012;81:121–130. <https://doi.org/10.1016/J.EJPB.2012.01.018>
- [50] Smirnova A, Loca D, Stipniece L, Locs J, Pura A. Encapsulation of strontium ranelate in poly(lactic acid) matrix. *Key Eng Mater*. 2017;721 KEM:208–212. <https://doi.org/10.4028/www.scientific.net/KEM.721.208>.
- [51] Neves N, Campos BB, Almeida IF, Costa PC, Cabral AT, Barbosa MA, Ribeiro CC. Strontium-rich injectable hybrid system for bone regeneration. *Mater Sci Eng C*. 2016;59:818–827. <https://doi.org/10.1016/j.msec.2015.10.038>
- [52] Howard M, Zern BJ, Anselmo AC, Shuvaev V V., Mitragotri S, Muzykantov V. Vascular targeting of nanocarriers: Perplexing aspects of the seemingly straightforward paradigm. *ACS Nano*. 2014;8:4100–4132. <https://doi.org/10.1021/nn500136z>
- [53] Decuzzi P, Pasqualini R, Arap W, Ferrari M. Intravascular delivery of particulate systems: Does geometry really matter? *Pharm Res*. 2009;26:235–243. <https://doi.org/10.1007/s11095-008-9697-x>
- [54] Champion JA, Walker A, Mitragotri S. Role of particle size in phagocytosis of polymeric microspheres. *Pharm Res*. 2008;25:1815–1821. <https://doi.org/10.1007/s11095-008-9562-y>

- [55] Ritger PL, Peppas NA. A simple equation for description of solute release II. Fickian and anomalous release from swellable devices. *J Control Release*. 1987;5:37–42. [https://doi.org/10.1016/0168-3659\(87\)90035-6](https://doi.org/10.1016/0168-3659(87)90035-6)
- [56] Ritger PL, Peppas NA. A simple equation for description of solute release I. Fickian and non-fickian release from non-swellable devices in the form of slabs, spheres, cylinders or discs. *J Control Release*. 1987;5:23–36. [https://doi.org/10.1016/0168-3659\(87\)90034-4](https://doi.org/10.1016/0168-3659(87)90034-4)
- [57] Costa P, Lobo JM. Modeling and comparison of dissolution profiles. *Eur J Pharm Sci*. 2001;13:123–133.
- [58] Lengyel M, Dredán J, Gal S, Klebovich I, Antal I. A kioldódási profil jelentősége a stabilitási vizsgálatokban. *Acta Pharm Hung*. 2007;77:132–141.
- [59] CFR - Code of Federal Regulations Title 21 Volume 6. [Internet] [cited 2021 Apr. 1]. Available from <https://www.accessdata.fda.gov/scripts/cdrh/cfdocs/cfcfr/CFRSearch.cfm?fr=582.1736>
- [60] Cho KJ, Keener TC, Khang SJ. A study on the conversion of trona to sodium bicarbonate. *Powder Technol*. 2008;184:58–63. <https://doi.org/10.1016/j.powtec.2007.08.005>
- [61] OGYÉI Gyógyszeradatbázis [Internet] [cited 2021 Feb. 14] Available from <https://ogyei.gov.hu/gyogyszeradatbазis>
- [62] *Formulae Normales*. Editio VII. Budapest: Melania Könyvkiadó; 2003.
- [63] *Formulae Normales Editio VIII*. [Internet] [cited 2021 Aug. 4]. Available from https://ogyei.gov.hu/formulae_normales
- [64] Carlson TL, Lock JY, Carrier RL. Engineering the Mucus Barrier. *Annu Rev Biomed Eng*. 2018;20:197–220. <https://doi.org/10.1146/annurev-bioeng-062117-121156>

- [65] Turssi CP, Messias DCF, Hara AT, Hughes N, Garcia-Godoy F. Brushing abrasion of dentin: Effect of diluent and dilution rate of toothpaste. *Am J Dent.* 2010;23:247–250.
- [66] Barnes CM. An In-depth Look at Air-polishing. *Dimens Dent Hyg.* 2010;8(3):34-36.
- [67] Corral L, Post L, Montville T. Antimicrobial Activity of Sodium Bicarbonate: A Research Note. *J Food Sci.* 1988;53:981–982. <https://doi.org/10.1111/j.1365-2621.1988.tb09005.x>
- [68] Newbrun E, Hoover CI, Ryder MI. Bactericidal Action of Bicarbonate Ion on Selected Periodontal Pathogenic Microorganisms. *J Periodontol.* 1984;55:658–667. <https://doi.org/10.1902/jop.1984.55.11.658>
- [69] Madeswaran S, Jayachandran S. Sodium bicarbonate: A review and its uses in dentistry. *Indian J Dent Res.* 2018;29:672–677. https://doi.org/10.4103/ijdr.IJDR_30_17
- [70] Takigawa S, Sugano N, Ochiai K, Arai N, Ota N, Ito K. Effects of sodium bicarbonate on butyric acid-induced epithelial cell damage in vitro. *J Oral Sci.* 2008;50:413–417. <https://doi.org/10.2334/josnusd.50.413>
- [71] Kim KN, Yang SW, Kim H, Kwak SS, Kim YS, Cho DY. Acid Inhibitory Effect of a Combination of Omeprazole and Sodium Bicarbonate (CDFR0209) Compared With Delayed-Release Omeprazole 40 mg Alone in Healthy Adult Male Subjects. *Clin Pharmacol Drug Dev.* 2018;7:53–58. <https://doi.org/10.1002/cpdd.331>
- [72] Fonyó A. Az orvosi élettan tankönyve. In: Chapter 17. Budapest: Medicina Könyvkiadó Zrt.; 2011. p. 426-437.
- [73] Szeto CC, Wong TYH, Chow KM, Leung CB, Li PKT. Oral sodium bicarbonate for the treatment of metabolic acidosis in peritoneal dialysis patients: A randomized placebo-control trial. *J Am Soc Nephrol.* 2003;14:2119–2126. <https://doi.org/10.1097/01.ASN.0000080316.37254.7A>

- [74] Krstrup P, Ermidis G, Mohr M. Sodium bicarbonate intake improves high-intensity intermittent exercise performance in trained young men. *J Int Soc Sports Nutr.* 2015;12:1–7. <https://doi.org/10.1186/s12970-015-0087-6>
- [75] McNaughton LR, Siegler J, Midgley A. Ergogenic effects of sodium bicarbonate. *Curr Sports Med Rep.* 2008;7:230–236. <https://doi.org/10.1249/JSR.0b013e31817ef530>
- [76] Yang M, Zhong X, Yuan Y. Does Baking Soda Function as a Magic Bullet for Patients With Cancer? A Mini Review. *Integr Cancer Ther.* 2020;19. <https://doi.org/10.1177/1534735420922579>
- [77] Forssell H. Gastric mucosal defence mechanisms: A brief review. *Scand J Gastroenterol.* 1988;23:23–28. <https://doi.org/10.3109/00365528809096277>
- [78] Allen A, Flemström G. Gastroduodenal mucus bicarbonate barrier: protection against acid and pepsin. *Am J Physiol Cell Physiol.* 2005;288:1–19. <https://doi.org/10.1152/ajpcell.00102.2004.-Secretion>
- [79] Kaunitz JD, Akiba Y. Duodenal carbonic anhydrase: mucosal protection, luminal chemosensing, and gastric acid disposal. *Keio J Med.* 2006;55:96–106. <https://doi.org/10.2302/KJM.55.96>
- [80] Shames B. *Anatomy and Physiology of the Duodenum.* 8th Ed. Elsevier Inc.; 2019. <https://doi.org/10.1016/b978-0-323-40232-3.00068-6>
- [81] Ori Y, Zingerman B, Bergman M, Bessler H, Salman H. The effect of sodium bicarbonate on cytokine secretion in CKD patients with metabolic acidosis. *Biomed Pharmacother.* 2015;71:98–101. <https://doi.org/10.1016/j.biopha.2015.02.012>
- [82] Mahajan A, Simoni J, Sheather SJ, Broglio KR, Rajab MH, Wesson DE. Daily oral sodium bicarbonate preserves glomerular filtration rate by slowing its decline in early hypertensive nephropathy. *Kidney Int.* 2010;78:303–309. <https://doi.org/10.1038/ki.2010.129>

- [83] Kraut JA, Madias NE. Metabolic Acidosis of CKD: An Update. *Am J Kidney Dis.* 2016;67:307–317. <https://doi.org/10.1053/j.ajkd.2015.08.028>
- [84] Turnberg LA, Fordtran JS, Carter NW, Rector FC. Mechanism of bicarbonate absorption and its relationship to sodium transport in the human jejunum. *J Clin Invest.* 1970;49:548–556. <https://doi.org/10.1172/JCI106265>
- [85] Vásquez A, Domínguez C, Perdomo CF. Spontaneous gastric rupture after Sodium Bicarbonate consumption: A case report. *Radiography.* 2017;23:e62–e64. <https://doi.org/10.1016/j.radi.2017.03.019>
- [86] Breitzkreutz J, Gan TG, Schneider B, Kalisch P. Enteric-coated solid dosage forms containing sodium bicarbonate as a drug substance: an exception from the rule? *J Pharm Pharmacol.* 2007;59:59–65. <https://doi.org/10.1211/jpp.59.1.0008>
- [87] Schmidt PC, Lang S. Pharmazeutische Hilfsstoffe. In: Eschborn: Govi-Verlag Pharmazeutischer Verlag GmbH; 2013. p. 104–121.
- [88] Meena A, Parikh T, Gupta SS, Serajuddin ATM. Investigation of thermal and viscoelastic properties of polymers relevant to hot melt extrusion - II: Cellulosic polymers. *J Excipients Food Chem.* 2014;5:46–55.
- [89] Haynes WM (ed. . *CRC Handbook of Chemistry and Physics.* In: *CRC Handbook of Chemistry and Physics.* 95th Editi. CRC Press LLC; p. 4–90.
- [90] Reade Advanced Materials - Mohs' Hardness (Typical) of Abrasives. [Internet] [cited 2021 Jun. 1]. Available from <https://www.reade.com/rea-de-resources/reference-educational/rea-de-reference-chart-particle-property-briefings/32-mohs-hardness-of-abrasives>
- [91] Lee BB, Ravindra P, Chan ES. Size and shape of calcium alginate beads produced by extrusion dripping. *Chem Eng Technol.* 2013;36:1627–1642. <https://doi.org/10.1002/ceat.201300230>
- [92] Smrdel P, Bogataj M, Mrhar A. The influence of selected parameters on the size and shape of alginate beads prepared by ionotropic gelation. *Sci Pharm.* 2008;76:77–89. <https://doi.org/10.3797/scipharm.0611-07>
- [93] Lee OS, Ha BJ, Park SN, Lee YS. Studies on the pH-dependent swelling properties and morphologies of chitosan/calcium-alginate complexed beads.

- Macromol Chem Phys. 1997;198:2971–2976.
<https://doi.org/10.1002/macp.1997.021980925>
- [94] Tuderman AK, Strachan CJ, Juppo AM. Isomalt and its diastereomer mixtures as stabilizing excipients with freeze-dried lactate dehydrogenase. *Int J Pharm.* 2018;538:287–295.
<https://doi.org/10.1016/j.ijpharm.2018.01.015>
- [95] Koskinen AK, Fraser-Miller SJ, Bøtker JP, Heljo VP, Barnsley JE, Gordon KC, Strachan CJ, Juppo AM. Physical Stability of Freeze-Dried Isomalt Diastereomer Mixtures. *Pharm Res.* 2016;33:1752–1768.
<https://doi.org/10.1007/s11095-016-1915-3>
- [96] Salmon P. *A Short Guide to Analysis of Bone by Micro-CT*. Aatselaar, Belgium: Skyscan NV; 2003.
- [97] Lee CSD, Moyer HR, Gittens I. RA, Williams JK, Boskey AL, Boyan BD, Schwartz Z. Regulating in vivo calcification of alginate microbeads. *Biomaterials.* 2010;31:4926–4934.
<https://doi.org/10.1016/j.biomaterials.2010.03.001>
- [98] Lengyel M, Balogh E, Szerőczei D, Dobó-Nagy C, Pápay Z, Stömmer V, Klebovich I, Antal I. Study on process parameters and optimization of microencapsulation based on phase separation. *Eur J Pharm Sci.* 2018;122:273–278. <https://doi.org/10.1016/j.ejps.2018.07.015>
- [99] Gupta P, Vermani K, Garg S. Hydrogels: From controlled release to pH-responsive drug delivery. *Drug Discov Today.* 2002;7:569–579.
[https://doi.org/10.1016/S1359-6446\(02\)02255-9](https://doi.org/10.1016/S1359-6446(02)02255-9)

- [100] Silva KMMN, de Carvalho DÉL, Valente VMM, Campos Rubio JC, Faria PE, Silva-Caldeira PP. Concomitant and controlled release of furazolidone and bismuth(III) incorporated in a cross-linked sodium alginate-carboxymethyl cellulose hydrogel. *Int J Biol Macromol.* 2019;126:359–366. <https://doi.org/10.1016/J.IJBIOMAC.2018.12.136>
- [101] Dávid ÁZ, Lengyel M, Marton S, Klebovich I, Antal I. Example for a new alternative application of NIR spectroscopy in the parallel determination of active ingredients and an excipient in powders and tablets. *Acta Pharm Hung.* 2005;75:141–145.
- [102] Larsen CC, Sonnergaard JM, Bertelsen P, Holm P. Validation of an image analysis method for estimating coating thickness on pellets. *Eur J Pharm Sci.* 2003;18:191–196. [https://doi.org/10.1016/S0928-0987\(02\)00260-9](https://doi.org/10.1016/S0928-0987(02)00260-9)
- [103] Galata DL, Mészáros LA, Kállai-Szabó N, Szabó E, Pataki H, Marosi G, Nagy ZK. Applications of machine vision in pharmaceutical technology: A review. *Eur J Pharm Sci.* 2021;159:105717 <https://doi.org/10.1016/j.ejps.2021.105717>
- [104] Farkas D, Madarász L, Nagy ZK, Antal I, Kállai-Szabó N. Image analysis: A versatile tool in the manufacturing and quality control of pharmaceutical dosage forms. *Pharmaceutics.* 2021;13(5):685. <https://doi.org/10.3390/PHARMACEUTICS13050685>
- [105] Hajnal P, Szegő P, Antal I, Dredán J, Klebovich I, Lengyel M . pH-függő szakaszos és nyújtott hatóanyag-leadású gyógyszerkészítmény P 10 00407. Szellemi Tulajdon Nemzeti Hivatala. 2016;A61K 9/58.
- [106] Hajnal P, Szegő P, Antal I, Dredán J, Klebovich I, Lengyel M. pH-dependent Gradual Release Pharmaceutical Composition- United States Patent US 9,839,607 B2 Dec. 12, 2017. April.

9. BIBLIOGRAPHY OF THE CANDIDATE'S PUBLICATIONS

9.1 PUBLICATIONS CLOSELY RELATED TO THE THESIS

1. **Lengyel M**, Kállai-Szabó N, Antal V, Laki AJ, Antal I. Microparticles, Microspheres, and Microcapsules for Advanced Drug Delivery. *Sci. Pharm.* 2019; 87(3) p. 30. <https://doi.org/10.3390/scipharm87030020>. *Q2 Cited: Independent ref.: 169.*
(<https://m2.mtmt.hu/gui2/?type=authors&mode=browse&sel=10020628> accessed: 10.08.2022.)
2. **Lengyel M**, Balogh E, Szeroczei D, Dobo-Nagy Cs, Papay Zs, Stommer V, Klebovich I, Antal I. Study on Process Parameters and Optimization of Microencapsulation Based on Phase Separation. *Eur. J. Pharm. Sci.* 2018;122:273–280. <https://doi:10.1016/j.ejps.2018.07.015>. *Q1 IF: 3.532*
3. Hajnal P, Szegő P, Antal I, Dredán J, Klebovich I, **Lengyel M**. pH-függő szakaszos módosított hatóanyagleadású gyógyszerkészítmény. **Magyar szabadalom** Lajstromszám: 230 560, Szabadalmi bejelentés: 2010.07.30, Ügyszám: P1000407, Benyújtás országa: Magyarország
4. Hajnal P, Szegő P, Antal I, Dredán J, Klebovich I, **Lengyel M**. pH-dependent Gradual Release Pharmaceutical Composition- **United States Patent Dec. 12, 2017. 9,839,607 B2.**
5. **Lengyel M**, Dredan J, Shafir G, Klebovich I, Antal I. A kioldódási profil jelentősége a stabilitási vizsgálatokban *Acta Pharm. Hung.* 2007;77/2(10):132-141, *Q3*

PRESENTATIONS RELATED TO THE THESIS

PUBLISHED OR DOCUMENTED IN SCIENTIFIC PAPERS

1. **Lengyel M**, Süvegh K, Antal V, Zelkó R, Antal I, Kállai-Szabó N. Hydrocolloid Gel-formers and Polyvalent Coations in the Formation of Microparticles. DDRS International Conference on Advances in Pharmaceutical Drug Development, Quality Control and Regulatory Science, Budapest, 2021 Nov 15-17. P-50.
2. **Lengyel M**, Süvegh K, Kállai-Szabó N, Antal V, Zelkó R, Antal I. Hidrokolloid gélképző segédanyagot tartalmazó mikrogömbök összehasonlító vizsgálata. Gyógyszertechnológiai és Ipari Gyógyszerészeti Konferencia, Siófok, 2019 Sept 26-28., P-016
3. **Lengyel M**, Balogh E, Szerőcsei D, Dobó-Nagy Cs, Antal I. Study on the effect of multivalent cations and matrix formers applied for microencapsulation. Proceeding of the 12th Central European Symposium on Pharmaceutical Technology and Regulatory Affairs, (CESPT) 2018 September 20-22. Szeged, Hungary
4. **Lengyel M**, Stömmer V, Szerőcsei D., Bertalanné Balogh E, Klebovich I., Antal I. Study on the effect of surfactants and optimization of process parameters of the microencapsulation based on phase separation Proceeding of the 7th BBBB International Conference on Pharmaceutical Sciences 2017 Oct 5-7 Balatonfüred, Hungary in Acta Pharm Hung. 2017; 87 (3–4): 155–156. P1D11
5. **Lengyel M**, Zelko R, Nagy ZsK, Dredan J, Stiedl B, Klebovich I, Antal I. Study on Dissolution Profile Stability of Pellets Coated with Ethyl Acrylate Methyl Methacrylate Copolymers. 7th Central European Symposium on Pharmaceutical Technology and Biodelivery Systems, 2008 Sept 18-20 Ljubljana, Slovenia, in Farmaceutski Vestnik 2008;59(Spec.Issue):224–226.

9.2 PUBLICATIONS RELATED TO OTHER WORKS

1. Kállai-Szabó N, **Lengyel M**, Farkas D, Barna ÁT, Fleck C, Basa B, Antal I. Review on Starter Pellets: Inert and Functional Cores. *Pharmaceutics*. 2022;14:1299. [http://doi: 10.3390/pharmaceutics14061299](http://doi.org/10.3390/pharmaceutics14061299) *IF:6.525*
2. Farkas D, Kállai-Szabó N, Sárádi-Kesztyűs Á, **Lengyel M**, Magramane S, Kiss É, Antal I. Investigation of propellant-free aqueous foams as pharmaceutical carrier systems. *Pharm Dev Techn.* 2021; 26(3),253–261. <http://doi.org/10.1080/10837450.2020.1863426> *IF: 3.133*
3. Niczinger N, Kállai-Szabó B, **Lengyel M**, Gordon P, Klebovich I, Antal I. Physicochemical analysis in the evaluation of reconstituted dry emulsion tablets. *J Pharm Biomed Anal.* 2017;134,86–93. <http://doi.org/10.1016/j.jpba.2016.11.031> *IF:0.919*
4. Kallai N, Luhn O, Dredan J, Kovacs K, **Lengyel M**, Antal I. Evaluation of drug release from coated pellets based on isomalt, sugar, and microcrystalline cellulose inert cores. *AAPS Pharm Sci Tech.* 2010;11(1),383–391. <http://doi.org/10.1208/s12249-010-9396-x> *IF:1.445*
5. Tost H, Hably Cs, **Lengyel M**, Gogl A, Lendvai A, Bartha J. Effect of nitric oxide synthase inhibition on renal circulation and excretory function in anaesthetized rats. *Exp Physiol.* 2000; 85(6), 791–800. <https://doi.org/10.1017/S0958067000020856> *IF: 1.062*
6. Antal I, Dredán J, Fekete P, **Lengyel M**, Balogh E, Marton S, Klebovich I. Középzemmi gyógyszer technológiai műveletek és gyógyszerkészítési eljárások. Budapest: Semmelweis Kiadó és Multimédia Stúdió 2007. egyetemi jegyzet
7. Balogh E, Kallai N, Dredan J, **Lengyel M**, Klebovich I, Antal I. Számítógépes képanalízis alkalmazása gyógyszeres pelletek jellemzésére. *Acta Pharm Hung.* 2007; 77(2), 123–131.

9.3 PRESENTATIONS, PROCEEDINGS OF CONFERENCES

1. Szerőcsei D, Fülöp V, Jakab G, **Lengyel M**, Balogh E, Antal I. Evaluation of biocompatible polymer gels before and after freeze-drying. Proceeding of the 7th BBBB International Conference on Pharmaceutical Sciences 2017 Oct 5-7 Balatonfüred, Hungary Acta Pharm. Hung., 87(3-4), 199. P2D6
2. Dredán J, **Lengyel M**, Kállai N, Klebovich I, Antal I. Bevonó polimerek és lágyítók interakcióinak vizsgálata. Gyógyszer az ezredfordulón VII: Továbbképző Konferencia, Sopron, 2008 Sept 25-27, P-15.
3. Antal I, Kállai N, Balogh E, Dredán J, **Lengyel M**, Klebovich I. Rétegzett pelletek előállítási folyamatának elemzése és ellenőrzése. Gyógyszerkutatási Szimpózium, 2007 Nov 9-10., Szeged, Hungary. E-2.
4. Balogh E, Kállai N, Dredán J, **Lengyel M**, Klebovich I, Antal I. Neutrális pelletmagok és rétegzett gyógyszeres pelletjeik vízadszorpciójának vizsgálata. Gyógyszerkutatási Szimpózium, 2007 Nov 9-10., Szeged, Hungary. P-3.
5. Kállai N, Balogh E, Dredán J, **Lengyel M**, Klebovich I, Antal I. (2007). Neutrális pelletmagok vizsgálata bevont multipartikuláris gyógyszerhordozó rendszer előállítására. PhD Tudományos Napok, Budapest, 2007 Apr 12-13, P-II/14.
6. Dredán J, **Lengyel M**, Klebovich I, Antal I. Bevont multipartikuláris rendszerek összehasonlító vizsgálata. Congressus Pharmaceuticus Hungaricus XIII. 2006 Mai 25-27. Budapest, Hungary in Gyógyszerészet, 50, 275. P-50.
7. **Lengyel M**, Dredán J, Klebovich I., Antal I. Polimer bevonóanyag-rendszerek stabilitás vizsgálata. Congressus Pharmaceuticus Hungaricus XIII. 2006 Mai 25-27 Budapest, Hungary in Gyógyszerészet, 50, 275. P-60.
8. Plachy J, Gyenei Z, **Lengyel M**, Antal I, Klebovich I. Kalcium-terápiában alkalmazható kalciumpótló hatóanyagok felszívódásának modellezése dializáló membránokkal. Congressus Pharmaceuticus Hungaricus XIII. 2006 Mai 25-27 Budapest, Hungary in Gyógyszerészet, 50, 275. P-68.
9. Antal I, Dredán J, **Lengyel M**, Dávid ÁZ, Pál Sz, Klebovich I, Dévay A. Prediction of dissolution profile stability based on diffuse reflectance spectra and solvent adsorption kinetics of coated pellets. 5th World Meeting on Pharmaceutics Biopharmaceutics and Pharmaceutical Technology, 2006 March 27-30 Geneva, Switzerland L-22

10. Dredán J, Odri S, **Lengyel M**, Klebovich I, Antal I. Optimization study of comminution process in planetary ball mill. 11th European Symposium on Comminution, 2006 Oct 9-12, Budapest, Hungary
11. Dávid ÁZ, **Lengyel M**, Marton S, Klebovich I, Antal I. Példa a NIR spektroszkópia alternatív alkalmazhatóságára: porkeverékek és tabletták komponenseinek egyidejű meghatározása. *Acta Pharm Hung.* 2005; 75(3):141–145.
12. Dávid ÁZ, Kelen Á, **Lengyel M**, Klebovich I, Antal I Microwave drying and drying-kinetic study of solid pharmaceutical compounds. Proceeding of 6th Central European Symposium on Pharmaceutical Technology and Biotechnology. 2005 May 25–27. Siófok, Hungary in *Eur J Pharm Sci.* 2005;25(Suppl. 1), P-24.
<https://doi.org/10.1016/j.ejps.2005.04.007>
13. Dávid ÁZ, **Lengyel M**, Marton S, Klebovich I, Antal I. The quantitative determination of active ingredients and an excipient in powders and tablets with a new alternative NIR spectroscopic application. Proceeding of 6th Central European Symposium on Pharmaceutical Technology and Biotechnology. 2005 May 25–27. Siófok, Hungary in *Eur J Pharm Sci.* 2005;25(Suppl. 1),S150–S151.
<https://doi.org/10.1016/j.ejps.2005.04.007> P-25.
14. Dredán J, **Lengyel M**, Szepesi I, Antal, Klebovich I. Spectrophotometric and tenziometric characterization of polyethylene glycols applied in pharmaceutical technology. Proceeding of 6th Central European Symposium on Pharmaceutical Technology and Biotechnology. 2005 May 25–27. Siófok, Hungary in *Eur J Pharm Sci.* 2005;25(Suppl. 1),S150–S151.
<https://doi.org/10.1016/j.ejps.2005.04.007> P-32.
15. **Lengyel M**, Dávid ÁZ, Dredán J, Klebovich I, Antal I. Dissolution profile and solvent-uptake stability of theophylline containing pellets coated by methacrylate copolymers. Proceeding of 6th Central European Symposium on Pharmaceutical Technology and Biotechnology. 2005 May 25–27. Siófok, Hungary in *Eur J Pharm Sci.* 2005;25(Suppl. 1),S150–S151.
<https://doi.org/10.1016/j.ejps.2005.04.007> P-64.

16. Antal I, Dredán J, Dávid ÁZ, **Lengyel M**, Zsigmond Zs, Fekete P, Dévay A. Concanetations of dissolution profile comparison performed by calculating similarity factor and parameters of the Weibull distribution simultaneously. International Meeting on Pharm, Biopharm and Pharmac Techn., 2004 March 15-18. Nuremberg, Germany. P169-170
17. Plachy J, Rác I, Antal I, **Lengyel M**, Marton S. A gyomor-béltraktusban helyileg ható gyógyszerek hatékonyságának vizsgálata *in vitro* biofarmáciai módszerekkel. Gyógyszerészet, 2003;47:85.
18. Antal I, Dredán J, Balogh E, **Lengyel M**, Rác I, Marton S. Modifying drug release from coated pellets by pore forming agents. XIV Országos Gyógyszertechnológiai Konferencia 2002 Nov 8-11. Hévíz, Hungary.
19. Dávid Á, **Lengyel M**, Antal I, Marton S. Többkomponensű rendszerek vizsgálata NIR spektroszkópiával preformulációs vizsgálatok során. XIV Országos Gyógyszertechnológiai Konferencia 2002 Nov 8-11. Hévíz, Hungary.
20. **Lengyel M**, Plachy J, Rác I, Marton S. Kölcsönhatás-vizsgálatok cukorészterek és antioxidánsok között szilárd, folyékony és olvadék fázisban. XIV Országos Gyógyszertechnológiai Konferencia 2002 Nov 8-11. Hévíz, Hungary.
21. **Lengyel, M**. Természetes eredetű antioxidáns oldódásának elősegítése cukorészterekkel. XIV Országos Gyógyszertechnológiai Konferencia 2002 Nov 8-11. Hévíz, Hungary.
22. **Lengyel, M**. A NOS blokkolás hatása a veseműködésre 60 ml/kg Ringer-oldattal volumenexpandált patkányban. 1999 Febr 10-12. Semmelweis Medical University Scientific Students' Conference Budapest, Hungary.
23. **Lengyel M**. A NOS blokkolás hatása a veseműködésre 60 ml/kg Ringer-oldattal volumenexpandált patkányban. 1999 March 26-28. Scientific Students' Conference. Marosvásárhely, Romania.
24. Tost H, **Lengyel M**, Bartha J. A nitrogén-monoxid szintézis blokkolás hatása a veseműködésre altatott, volumen expandált patkányban. Hypertonia és Nephrologia, 1998;S2(3)

10. ACKNOWLEDGEMENTS

First of all, I am incredibly grateful to my supervisor, *Prof. István Antal* for the continuous indispensable guidance, brilliant ideas, steady support and encouragement throughout my work, keeping me on the right track and providing the opportunity to acquire a significant number of skills both on the field of pharmaceutical technology research and education of students in the Department of Pharmaceutics.

I'm very grateful for *Prof. Imre Klebovich* for his constant support, enthusiasm for work and positive feedback in the past years that serves as an example.

I am also very grateful for *Dr. Nikolett Kállai-Szabó* and *Dr. Barnabás Kállai-Szabó* for their great ideas, constant support, fruitful discussions and observations that sometimes broke the deadlocks with the projects.

I thank to my colleagues, the excellent team of the Semmelweis University Department of Pharmaceutics that I could always turn to them for advice in my projects: *Dr. Mária Hajdú, Dr. Dóra Farkas, Dr. Krisztina Ludányi, Dr. Borbála Kiss-Dalmadiné, Dr. Zsófia Pápay, Dr. Emese Bertalanné Balogh, Dr. Livia Budai, Dr. Dávid Virág, Dr. Márton Király, Dr. Konrád Sántha, Dr. Bálint Basa, Dr. Andrea Kovács*. I am also very grateful for *Katalin Jakab, Ágnes Sárádi-Kesztyűs, Gabriella Biczók, Enikő Hetényi, Katalin Döme, Valéria Berki, Ilona Soros, and Zsuzsanna Ábrám* who were and are always enthusiastically eager to help me.

I thank to *Dr. Károly Süvegh, Prof. Romána Zelkó, Dr. Adrienn Kazsoki, Prof. Csaba Dobó-Nagy, Dr. Krisztián Csomó and Dr. Bence Szabó* for their support and the opportunities for research cooperations. I'm grateful for *Péter Hajnal* for the initiation and support of the formulation work, *Dr. Péter Szegő*, who realized the importance of the gradual intake of sodium bicarbonate. I gratefully think back to two of my teachers, *Dr. Judit Dredán*, who played an important role in the formulation work and *Dr. György Stampf*, who shared his love of education. I would like to thank all the co-authors for their support in my works.

The most excellent acknowledgement is tributed to my great and loving family. My Mom, my Dad, *Fruzsina and Noémi*, the best daughters ever and *Attila*, my great husband for their help, love and their inexhaustible patience for me during the past years.